University of Naples Federico II
Polytechnic and Basic Sciences School

Department of Chemical Sciences

Ph.D. in Chemical Sciences

Recalcitrant COD: characterization and abatement in the wastewater derived from the tanning industry.

Maria Toscanesi

Advisor:
prof. Marco Trifuoggi

Examiner:
prof. Riccardo Tesser

XXXIV Cycle 2018 – 2021
Coordinator: prof. Angelina Lombardi

A te che vegli su di me

CONTENTS

ABSTRACT

The wastewater from the tanning industry represents a serious environmental problem, as it has high concentrations of organic and inorganic contaminants. Some of these compounds are not degraded by the wastewater treatments and, for this reason, are called recalcitrant. The nature of these contaminants is not always known, and the research project focuses on their characterization. The first results showed the presence of COD values higher than the limits set by the legislation and strongly correlated with the TOC values, denoting an exclusively organic origin; furthermore, the low values of the BOD/COD ratios confirm that these compounds are not very biodegradable. The result of chemical analyses for the research of organic compounds showed, in particular, the absence of persistent organic pollutants such as polycyclic aromatic hydrocarbons and pesticides, the presence of organic substances of various kinds such as fatty acids, alcohols, alkyl-benzenes, phthalates, and terpenes. Among the recalcitrant organic compounds that arouse greater interest in the tanning sector are polyphenolic compounds, alkylphenols and their ethoxylated derivatives. The analyses, carried out by gas chromatography technique coupled with mass spectrometry, confirmed the presence of organic compounds belonging to the class of alkylphenols and ethoxylated alkylphenols in relatively low concentrations, while the analyses carried out by MALDI-TOF/TOF, showed the presence of residues of polyphenolic molecules. A method based on the UNI EN ISO 18857 standard was developed for the quantification of alkylphenols and their

derivatives; the method was also validated as described by the UNI EN ISO 17025: 2015 standards. In this case, the method involved solid phase extraction (SPE), followed by instrumental analysis in gas chromatography coupled with mass spectrometry (GC-MS); in the validation phase, the detection limit (LOD) and the quantification limit (LOQ), the repeatability uncertainty, the calibration uncertainty, the extended uncertainty, as well as the recovery values of the method were determined. Finally, the last part of the project focused on the characterization of some of the synthetic and natural tannins, present on the market and used in the tanning industry, during different stages of the tanning process. The chemical characterization of these compounds was carried out by MALDI-TOF/TOF analysis, which provided innumerable information about the main molecules of which both synthetic and vegetable tannins are made, but also the degree of polymerization. These compounds are not very biodegradable, as demonstrated by the chemical analyzes and the literature, it turned out that these compounds cannot be eliminated by the classic methods of biological oxidation. In this contest, the project focused on the study of advanced oxidation processes that can be used for the abatement of vegetable and synthetic tannins and therefore for the abatement of recalcitrant COD. The processes studied are heterogeneous photodegradation and adsorption. Both processes were carried out in batches and using TiO_2 Aeroxide P-25 both as a catalyst and as an adsorbent material. The various experiments were conducted to verify the influence of temperature, the amount of catalyst and the amount of initial COD concentration, on the recalcitrant COD reduction resulting from the presence of natural

and synthetic tannins in the wastewaters. TiO_2 Areoxide P-25 was used as catalyst, irradiated with UV light, which proved to be an effective catalyst for COD abatement with a maximum value of 60%. From the collected evidence, an activation energy of E_a = 28 KJ/mol was obtained comparable with the literature values obtained for persistent organic molecules. In every experiment, COD reached a *plateau* value, independent of the temperature value but linearly dependent with both the catalyst loading and the initial COD value. This effect was already observed in the literature, where Jouali et al. attributed the phenomenon to the shield effect due to the tanning residual content. Higher is the catalyst load, more efficient is the photodegradation process, while using high values of COD_0 could lead to non-optimal reaction conditions as it inhibits the reaction itself, suggesting a surface mechanism. In preliminary study of adsorption, different experiment was conducted to verify the influence of the temperature and the quantity of adsorbent. The influence of the reaction temperature was investigated. It was observed that as the temperature increases, a reduction in the adsorbed quantity of contaminant was observed. The effect of COD concentration was evaluated by varying its value from 50 mg/L to 200 mg/L. The results showed a degradation efficiency of about 60% for COD concentrations of 50 mg / L, while for concentrations above 100 mg/L, the efficiency decreases up to a maximum value of 40%.

In the equilibrium analysis the experimental data were fitted with classical isotherm Freundlich equations.

Part A – Characterization of wastewaters from the tanning industry

Chapter 1 – Tanning industries: general aspects

1. Introduction

The habit of transforming raw hides for slaughter into leather has traveled throughout thousands of years of traditions. In fact, leather has always been one of the most commonly used materials by human-kind in order to manufacture footwear, clothing and also different kind of objects to use on a daily basis, being fabricated into several different types and qualities. The primitives were probably the first ones using the skins of the animals they hunted for cover and protection.

Figure 1.1 Making of leather goods (adapted from Acron - The Olde Hide House (http://www.leathertown.com).

The first evidence hails from the Egyptian civilization as engravings, papyrus, mural, objects found in the tombs and, furthermore, in other areas on earth, more proofs of the use of leather in olden times have been brought to light: suffice is to think of the Romans and the Greeks population who used leather for the realization of numerous objects including sandals (Figure 1.1). Ancestors hunted animals mainly for food but, once they consumed their flesh, they used their cleaned of bones carcasses to cover their selves. However, they soon learned that their clean skin did not last over time as due to deteriorate. Over the centuries, they understood that the deterioration process of the skins could have been slowed down if they exposed the skins to the sun, drying them off even if stiff. Well later they realized they were able to obtain a better, long lasting and less unyielding product, by dipping the skin in tanks with some bark, leaves or fruit.

The modern tanning as we know it today was born between the end of the 19th century and the beginning of the 20th century, with the advent of the industrial revolution and with the technological development, in fact in 1910 the chrome tanning was patented (Figure 1.2) [1].

Figure 1.2. Tanning industry at the beginning of the 19th century.

Italy is considered to be a world leader in the tanning sector [2] due to the high technological and qualitative development which, as highlighted by the data collected by the National Union of Tanning Industry (UNIC), led to production od several volumes at the end of 2017 (129 million meters paintings of finished leathers; 11 thousand tons of sole leather) which amount to a value of about 5 billion euros. The Italian tanning industries are organized in specialized districts, mainly concentrated in the localities of: Valle del Chiampo (VI), Santa Croce sull'Arno (PI) and Solofra (AV) (Figure 1.3). These production poles have developed and changed their peculiar characteristics in terms of product and process, due to the need to adapt to the market:

- In Veneto the Chiampo Valley is the first tanning center for turnover and employment (over 50% of the total of Nation). It is represented by the simultaneous presence of medium-small companies and large industrial groups at the forefront in the automation and standardization of the process phases, while on the production level the main specialization is medium-large cowhides for upholstered furniture, footwear, and leather goods.
- Tuscany is the second largest tanning center (28.5% of total production) and it includes important districts such as that of S. Croce sull'Arno, specialized mainly in bovine and calf leathers destined for fashion, characterized by a high degree of craftsmanship and flexibility.
- Campania is a national landmark for processing sheep and goat leathers for clothing, footwear and leather goods, with a production value equal to 10% of the national total.

Regardless of the peculiarities of the sector, the tanning process consists of an alternation of chemical and mechanical operations aimed at eliminating the epidermis and the subcutaneous tissue from the remaining dermis, which is the only section of animal skin of real interest in terms of tanning. Raw leather goes from a putrescible state, with little resistance and irregular shape, to a state where it assumes an almost constant thickness, gaining characteristics such as rot-proof, good flexibility, high resistance to traction

and abrasion and good aesthetic finishing [3].

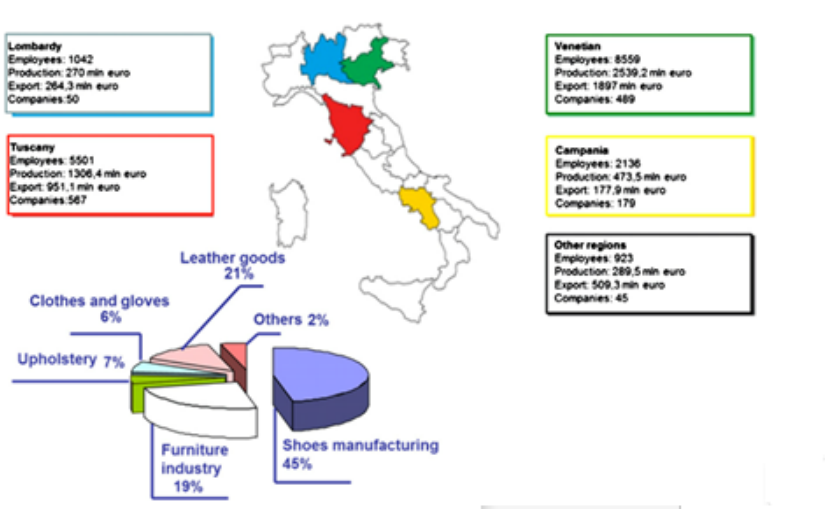

Figure 1.3. Distribution of the Italian tanning industries.

2. Tanning process

The tanning process involves a series of wet and dry phases which are outlined in Figure 1.4. The wet phases are the so-called ground work (desalination, soaking, calcination, deliming-maceration operations), the real ones of tanning and re-tanning, dyeing and fattening. All these operations, which require the use of a large amount of water, are generally carried out in reactors called drums, which basically consist of wooden cylinders where the hides are introduced together with the water and the necessary chemicals that can penetrate through the fibrous structures of the skin by rotation around its axis.

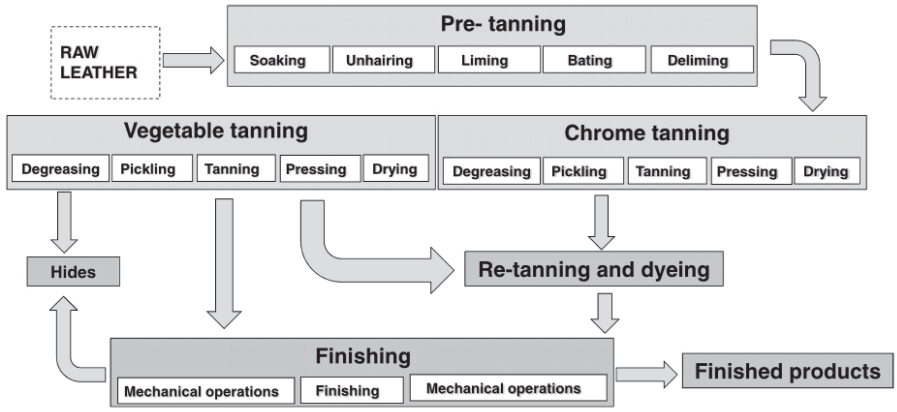

Figure 1.4. Typical flow of a tanning process

The dry phases, on the other hand, mainly concern some mechanical processes (hollowing and splitting) and finally the finishing process.

The tanning technological cycle is long and articulated so it is useful to describe all the operations that are carried out starting from the raw material.

2.1 Skin and its components

The skins of mammals all have the same histological constitution, which in the cross section can be divided into three main layers: epidermis, dermis and subcutaneous layer.

- The epidermis represents the outermost part of the skin, the barrier between the animal and its environment, and is the main site of horny (hair, scales, nails, horns, etc.) and glandular (sebaceous and sweat) productions of some animals. During the transformation into leather this part of the leather, except for the processing of fur skins, is eliminated in the liming with all its parts (hairs, follicles, sebaceous and sweat glands). The dermis, or corium, represents ca. 85% of the thickness of the skin and it is therefore the most interesting part from

a tanning point of view, since this is essentially the one that will be converted into leather. In turn, the dermis is divided into two layers: the flower (or papillary) layer and the flesh (or reticular) layer. Both are made up of collagen fibers, which are thinner and predominantly arranged horizontally in the flower layer, a structure that gives it higher level of compactness than the underlying papillary layer, where these fibers are thicker and arranged in all directions.

- The subcutaneous tissue, or adipose layer, is located below the dermis and it has the task of fixing the skin to the underlying tissues. It consists largely of fat and collagen fibers arranged parallel to the surface of the skin, so it has a much looser structure than the overlying connective tissue. Not affecting the tanning operations, it is eliminated in the fleshing operation. The fleshing residue is called fleshing and it is intended for the grease industry to obtain emulsifiers.

Finally, among the parts described above, the dermis is the one that has the most commercial value. Its quality varies according to three fundamental factors: the compactness or density of the fibrous tissue (on which the strength and elasticity depend on); the thickness; the uniformity and finally the appearance of the grain.

In particular, the thickness of the skin varies according to the area of the animal body it covers. The most used subdivision divides the skin into three parts:

- the rump is the most valuable part because it is thicker, with a more uniform fibrous structure and with a very large surface (45-55%).
- the sides have a looser fibrous structure and a smaller thickness.
- the shoulders have the same thickness as the rump but a looser fibrous structure.

In the tannery, different types of raw hides are processed. The most used are bovine, ovine, caprine, porcine, equine and buffalo hides as they are also the most available sources in nature. Sometimes, special leathers such as kangaroo, reptile, deer and fish can also be tanned. The most processed raw hides are the bovine ones, which are the most suitable for the production of various types of leather [4–6].

2.2 Stages of the tanning process

The tanning cycle can be divided into four macro-phases: riviera, tanning, dyeing and finishing. Despite the above subdivision, however, the work cycles of each phase can change between different companies, and, more importantly, they change according to the histology of the processed leather and the type of product to be obtained.

Conservation

The leathers need special conservation treatments to prevent from rotting. In fact, the processes of degradation of the tissues begin straight after the death of the animal, causing serious damage to the skin in terms of quality and value from a tanning point of view as they deteriorate rapidly. Furthermore, since tanneries are almost always not located sufficiently close to the places of production of the hides, the time between skinning and the start of the tanning process would be too long and the hides would risk being rotten. It is therefore necessary to stop the ruining processes for the enough amount of time needed to transport them to the tannery. Using these following treatments, inside the skin, conditions are created that make it impossible for bacteria and microorganisms to

proliferate and to produce the enzymes of putrefaction as they multiply in environments of water and humidity. The two generally most used methods for this purpose are preservation by salting and preservation by drying. Preservation by salting consists in saturating the skin with common salt (sodium chloride, NaCl), which penetrates the skin very quickly and produces a partial elimination of water by osmotic effect. Salting is carried out in two ways: either by sprinkling the skins with salt or treating the skins in drum with a saturated aqueous solution. Preservation by drying is, on the other hand, the method most used in the warmest and driest countries, where the moisture level of the skins is around 10-15%, inhibiting bacterial activity. However, drying is a process suitable for thin skins only, as the migration of water from the inner layers is faster. Consequently, it is the most suitable preservation system for sheep and goat skins and is not used for cowhides.

Soaking

This operation restores the skin to the conditions in which it was just skinned, removing the salt used in storage, cleansing it from dirt, leading it to reabsorb the water lost following the storage treatment. It is carried out with the use of large quantities of water with the addition of surfactants, alkalis (such as sodium carbonate, sodium hydroxide), sodium chloride (used only for unsalted skin, as an anti-swelling), bactericides and proteolytic enzymes, to accelerate the rehydration process and to begin eliminating some substances contained in the skin

that are harmful for tanning purposes, such as water-soluble fats and proteins.

Unhairing- Liming

Although they have different purposes, these two operations are carried out at the same time as they involve the use of the same chemical products. Unhairing aims to remove the hair and epidermis. The calcination has the purpose of increasing its reactivity and the absorption capacity of the tanning products and moreover a part of the subcutaneous adipose layer is eliminated by partial saponification. Generally, the chemicals used are: sodium sulphide, depilating agents capable of reducing the disulfide bridges of keratins; and calcium hydroxide, which stabilizes the pH of the hair removal bath around 12.5, optimal for the reducing action of the sulphide. Following liming, the skins are swollen and turgid and therefore have a considerably increased thickness.

Deliming

The purpose is to remove most of the lime used in the previous calcination operation. The depilated and calcined skin is swollen, turgid and strongly alkaline and in this state, it could not be subject to subsequent chemical operations. In this phase the pH is lowered up to values of about 8-9 in order to obtain the proteolytic activity of the enzymes used in the bating phase, in addition of a considerable deflation of the dermis. Deliming is carried out with acid substances: strong acids (sulfuric, hydrochloric), weak acids (formic, acetic, boric etc.), or with acid dissociation salts, such as ammonium sulphate, commonly used for bovine skins. Deliming can also be carried out by introducing gaseous

carbon dioxide into the drum; however, the diffusion inside the skin is quite slow, therefore the use of normal deliming agents is preferred.

Bating

This operation, which aims to complete the action of calcination, causes further relaxation of the collagen fibrous structure. In this way, the residues of other non-useful interfibrillar substances are eliminated, thus obtaining a softer and softer leather. It consists in treating the skin in warm environment with deliming chemicals and organic substances containing proteolytic enzymes that come from animal plants or from microbiological origin to eliminate lime and remove non-collagenic protein substances from the fibrous tissue of the dermis.

Degreasing

Solvent-based and / or surfactant-based treatment reduces excesses of fatty substances present in the skin that could cause difficulties in the absorption and fixation of chemicals and different types of defects on the finished leather.

Tanning

In the tanning phase, stable transverse bonds are formed between the polypeptide chains of collagen and a consequent consolidation that preserves the dermal substance from degradation processes, giving the tanned leather mechanical resistance, humidity, temperature, and chemical agents.

Obviously, since there are different types of binding sites on collagen, it will be possible to carry out different types of tanning with different

tanning materials. We can divide the tanning substances according to the bond they can develop with collagen:

1. **Coordination bond**: chromium, zirconium, iron, titanium, aluminum.
2. **Covalent bond**: formaldehyde, glutaraldehyde, (aldehydes in general).
3. **Hydrogen and dipolar bond**: vegetable tannins, synthetic tannins

It must therefore be considered that the stability of the skin depends mainly on factors such as the number of cross links and the intensity of the bond.

Whatever the type of reagent used, tanning consists of two important phases: the penetration of the tanning agent and its fixation. This is because the fixation of the tanning agent in the leather tends to hinder diffusion; thus, in order to achieve a homogeneous distribution of the tanning agent throughout the thickness of the hide, it is initially necessary to operate in conditions of minimum fixation.

For example, in tanning with coordination bonds, the fixation site is constituted by the carboxy functions present on the collagen side chains, therefore in an acid environment and, being protonated, they have a low affinity for the binding metal, which therefore manages to penetrate deeply into the dermis. On the other hand, in case of vegetal tanning using tannins, taking advantage of hydrogen bonds, much milder acidity conditions are set up and much diluted baths are used to avoid agglomeration of tannins. Once the conditions of homogeneity of the tanning agent within the skin have been reached, it is possible to move onto fixation by varying the pH; in the case of tanning with mineral salts,

the pH will increase, leading to deprotonation of the carboxylic groups present on the collagen side chains, obtaining an increase in affinity towards the metals present between the polypeptide chains; while during vegetal tanning, it will be necessary to increase the concentration of the tanning agent and a reduction of pH, it is possible to carry out a vegetal tanning by passing the hides from one tank to the next one, so that they have higher concentrations of tanning agent. The two most common types of tanning are chromium and vegetal tanning, but numerous other substances such as aluminum, zirconium, aldehydes, and fats can be used as tanning agents.

Chrome Tanning

Chrome tanning is definitely the most common type of tanning, as it is a relatively simple process to perform as cheap, fast and sufficiently versatile.

The tanning agent used is basic chromium sulphate ($CrOH(SO_4)$), where the ability of trivalent chromium (Cr^{3+}) to form complexes with the carboxyl groups of collagen is exploited. However, the leather must be prepared before treating it with tanning agents. This preparation operation, called pickling, consists in treating the leather with an acid solution (usually a mixture of sulfuric acid and formic acid) to facilitate the penetration of the tanning agent into the leather. After the process of calcination and decalcination, the leather has an isoelectric point of about 4 and, at its neutral pH, the collagen has a clearly negative charge. In these conditions, the positively charged trivalent chromium would have a strong tendency to react, preferential by electrostatic attraction and it would quickly fix itself only in the outermost layers of the skin, leaving the innermost layers untanned. Furthermore, at pH higher than 4-4.5 Cr^{3+}

forms insoluble hydroxide and it could no longer act as a tanning agent. It is thus necessary to reduce the pH of the bath to avoid the precipitation of chromium hydroxide and to bring the skin below to its isoelectric point. In these conditions, the skin assumes a predominantly positive charge and Cr3 + no longer has a reactive capacity towards it. Therefore, chromium can easily diffuse into the innermost layers of the skin (diffusion is greatly accelerated by movements in the drum). When complete penetration of the skin has been achieved, however, it is necessary to restore the skin-chromium reactivity, and this is achieved with basification, consisting of slowly raising the pH of the bath up to values around 4. In this way the leather recuperates a slightly negative charge and the coordinated leather-chromium bond can be established producing the tanning. The increase in pH also favors the breakdown of chromium, i.e., the formation of bonds between chromium atoms which lead to the formation of chains of chromium atoms of various lengths, with a consequent increase in the possibility of intra and inter-molecular bonds with carboxyl groups of collagens. However, the pH must not be too high to avoid chromium precipitation (the OH^- ion is a stronger complexing agent than collagen and would detach the chromium from the complex with the leather to form hydroxide).

At the end of the tanning, the tanned leather is green-blue. In this state, in fact, the tanned leather is called "wet-blue" with reference to the fact that it is wet and has a color in the blue field. The wet-blue, being now stable over time, can also be marketed.

Vegetal Tanning

The oldest tanning system is the vegetable one as it involves the use of tannins, complex phenolic substances contained in all plants, as tanning agents. They are in fact extracted from the bark of the wood of various plants as they take their name (e.g., chestnut, sumac, mimosa, oak tannins) but they are also found in fruits and in many varieties of tree leaves. Originally, the process was carried out by placing the hides in large pits and leaving them to soak with oak bark or other tannins. These were very long processes where the hides were left immersed even for several months to allow the complete transformation of the hides into leather, at the end of which a fat liquoring was enough. Nowadays tannic extracts and/or synthetic tannins are used such as sulphonic acids of phenols, naphthols and cresols.

The binding mechanism of the tanning agent in this case is completely different from the chromium one. It is in fact a hydrogen bond that is established between the phenolic groups of the tannin and the peptide groups of the collagen. To have binding capacity, it is thus necessary that the phenolic group of the tannin is electrically discharged with an acid pH. It follows that the pH variations are from the opposite sign compared to chromium in order to benefit the penetration and fixation of the tanning agent in the innermost layers of the leather. At first, a not too acidic pH (between 5 and 6) is used in such a way that the phenolic groups of the tannins are mainly dissociated, therefore unable to form hydrogen bonds. Once the penetration has been achieved, the binding capacity is restored by lowering the pH with acids so that the phenolic groups of the tannins return undissociated, consequently able to form hydrogen bonds.

The quantities of tannins used are considerably higher than those indicated for chrome tanning, ranging from 15-20% for small leathers intended for lining or small leather goods, to 40-50% for heavy soles. The duration of the tanning is also considerably longer and varies according to the method adopted:

• In the “slow tank” tanning, the hides are immersed in tanks containing tannin solutions at progressively increasing concentrations. The so-called "counter-current" technique is usually used because the leathers are moved from a less concentrated tub to a more concentrated tub as the bath follows the reverse path. The tanning in the vat lasts about 30 days and it is used to produce a very full and not very flexible sole leather.

• In “rapid barrel” tanning, the drum is used and, due to the rotation movement, a more flexible leather is obtained, suitable for the sole of women's shoes or for leather goods. In any case, barrel tanning lasts 36-48 hours, much longer than chrome tanning.

Other types of conce

Tanning can be done with many other tanning agents.

In the field of mineral tanning there are aluminum, zirconium, and titanium tanning. The process is very similar to the one of chrome tanning, but the characteristics of the leather obtained are quite different. The main difference is in the hardness of the leather, which is harder and more compact than chromium. Furthermore, the hydrothermal stability is lower: with these tans the leather contracts (denatures) at about 75…85 ° C, temperatures much lower than the chrome-tanned one, which makes them unsuitable for the realization of some products.

There are also many tanneries defined as organic tanneries, which use mainly synthetic organic substances as tanning agents. Among these ones, we find aldehyde tanning and oil tanning.

The first uses simple or complex aldehydes. Formaldehyde was in past used (prohibited then by recent regulations), to be then replaced by glutaraldehyde which gives the leather a yellowish color.

Very common in the past, oil tanning uses fish oils with a high content of polyunsaturated fatty acids or synthetic oils substituting those from fish as a tanning substance; soft leathers and suede leathers are obtained from this type of tanning.

Post-tanning operations

At the end of the tanning operations, the leather does not yet have the characteristics suitable for marketing: it is in fact a wet material which, even if dried, would give rise to a rather rigid product with the typical color of the tanning as firstly it was obtained. To transform it into a useful material for manufacturing products, it must then be subject to further chemical treatments, such as re-tanning, dyeing, fat liquoring and finishing processes.

Re-tanning

Re-tanning is a treatment where leather absorbs further tanning substance, often different from the ones used for the main tanning, in order to modify the product characteristics in the desired sense. For example, following a chrome tanning, vegetal tannins can be used as re-tanning agents, to obtain a less flexible leather than a pure chrome leather. Conversely, if you want to produce a more flexible and soft leather from a pure vegetal leather, a chrome re-tanning must be carried

out. Often aluminum, zirconium or titanium tanning agents are used as re-tanning agents to obtain a more reactive leather towards dyes therefore with more intense and brilliant colors.

Dyeing

The dye gives the leather the desired color. The dyes used are mainly organic compounds soluble in water, capable of anchoring themselves to the collagen fibers through ionic bonds, whose polarization strictly depends on the type of tanning carried out. Generally, the dyeing is carried out in drums at 50…60°C, where concentrated solutions of dye are added to the water and, subsequently, of an acid (usually formic), which contributes to the exhaustion of the bath and to fix the dye onto the leather, not only on the surface but also throughout the section.

Fat liquoring

It is carried out to lubricate the dermal fibers to avoid sticking and to give fullness and softness to the finished product. In addition, the fat liquor affects the permeability of water, thus determining the absorbency which is a very important feature for the subsequent finishing.

The operation is often carried out simultaneously with the dyeing with fattening products, generally consisting of both natural and synthetic origin fats and oils; they are normally made soluble in water before adding them to the drum, mixing them with products with an emulsifying action. Surfactants are also generally used.

Finishing

This operation consists of numerous mechanical and chemical processes, designed to improve the surface layer of the skin, not only from an

aesthetic point of view, but also from a functional point of view, increasing its resistance to external agents. On the surface of the leather different types of chemical substances are applied (polymeric resins, caseins, waxes, pigments and dyes), which, once dried, form a more or less transparent, elastic or hard surface film depending on the type of finish used and on the intended use of the finished product. There are different finishing application technologies (veil, roller, transfer, spray etc.), but the most frequently used is spraying with compressed air. In this mode, the hides receive the products by means of guns mounted on a rotating carousel and subsequently enter a drying tunnel where the products are permanently fixed [4–6].

3. Environmental aspects

Despite being one of the most innovative sectors and representing an excellence of the Italian economy, the tanning sector is one of the industrial sectors with the greatest environmental impact. It is estimated that 25 to 80 m^3 of water are used for every ton of raw material processed; from 9.3 to 42 GJ of electricity and about 350…400 Kg of chemical products. Some of the substances are almost completely absorbed by the skin, but they most remain into the wastewater in their original state as the fixation yields almost never exceed 50…70% [2,7]. Air, water, and soil pollution have therefore always represented a huge problem and cost for companies in the sector. In the past, the districts have played an active role in promoting common solutions to the most urgent and serious environmental problems, fostering cooperation between companies and maximizing the use of human, technical and financial resources.

The emissions into the atmosphere of the tanning industry hail mainly from the effluents of the calcination process releasing ammonia and from the encounter between liming effluents and water, deriving from processes in which acid solutions are used and, also, from subsequent tanning operations that can cause acid hydrogen sulphide stripping gaseous with diffusion of the smell of rotten eggs.

Other sources of emissions derive from generic operations, related to dermal powders of mechanical operations and the use of shaving machines. The emissions related to the auxiliary service phase mainly concern emissions of carbon dioxide, unburnt hydrocarbons, nitrogen and sulfur oxides, carbon monoxide, coming from pre-treatment plants and thermal plants. Finally, we have the emissions attributable to the finishing phase. During finishing, the use of large quantities of volatile solvents is the main source of toxic gases that are hazardous to health. The main compounds monitored are benzene, toluene, xylenes, ethylbenzene, butyl acetate, isobutanol and methoxy-2-propanol.

Another aspect of the tanning process is the production of a large quantity of dangerous waste, ie industrial. Solid tanning waste is about 35% of the total waste produced. The main solid wastes from leather production are tanned leather scraps containing chromium, fleshings and lime fragments and sludge produced by on-site effluent treatment, containing chromium.

The biggest polluting contribution although is represented by tanning wastewater with a high polluting load, as a large part of the production cycle is carried out using a large quantity of water. For this reason, the wastewater from the tanning industry is a serious environmental problem, as it has high concentrations of organic and inorganic pollutants. In the different stages of tanning many compounds are used such as acids, alkalis, chromium salts, tannins, solvents, dyes, oils, resins, synthetic tannins, but

they aren't completely fixed onto the leather, thus remaining in the water. Then high values of chemical oxygen demand (COD), biochemical oxygen demand (BOD), sulphate, chloride, heavy metals and various organic substances characterize the discharged wastewater [8–10].

We know that COD represents the amount of oxygen required to oxidize oxidizable organic and inorganic substances, therefore it provides an index of the degree of water pollution by oxidizable substances, mainly organic. The suspended solids, on the other hand, refer to the quantity of substances present in suspension that can be separated by energetic mechanical means such as filtration. It is possible to notice how the content of COD and how suspended solids has been strongly increasing over the last few years, both out of the production process and out of the wastewater treatment plant. This could be explained by the increase in persistent organic substances, such as organochlorine pesticides, solvents, and polychlorinated biphenyls, but a large number of emerging pollutants of both synthetic and natural origins are increasing and that these latter are not degraded with classic mechanical treatments and chemicals which the waters are subject to before their introduction into surface waters [11].

3.1 Italian legislation

The requirements of the Community directives on environmental matters that are reported in the Legislative Decree 152/2006, which replaces the Legislative Decree 152/99 which it has taken all the articles from, organized them in a single text with all other environmental regulations, the discipline for the protection and management of the water resource and the introduction of measures for the improvement of the quality of water bodies, in order to achieve the objectives of environmental quality and for specific destination of the waters. Specifically, the interventions for the

protection and rehabilitation of surface and underground water bodies and the sustainable use of water are all reported, identifying the integrated measures for wastewater treatment plants for the qualitative and quantitative protection of the water resource, which they also contribute to guaranteeing the natural self-purification of water bodies, as well as their ability to support large and well-diversified animal and plant communities. Purification plants with a potential exceeding 10,000 A.E. (equivalent inhabitant, or specific organic load) are required to comply with the limits indicated in Annex 5 to the third part of Legislative Decree 152/06 (Table 1.1 and 1.2) [16]. The legislation therefore describes an adequate "discipline of discharges", requiring the application of emission limit values also defined in relation to the characteristics of the receiving water bodies and the related quality objective. The numerous purification treatments, which the wastewater is subject, have the aim of verifying compliance with these emission limits, which makes a distinction for the discharge in superficial water or in in sewerage network.

Parameter	Effluent discharge standards D.lgs 152/2006 Attached 5- Part III	
	Discharge in superficial water	Discharge in sewerage network
Color	-	-
pH	5,5-9,5	5,5-9,5
Conductivity (µS cm^{-1})	-	-
BOD_5	≤40	≤250
COD	≤160	≤500
TOC	-	-
BOD_5 /COD	-	-
Total Phosphorus	≤10	≤10
Ammonium	≤15	≤30
Nitrous nitrogen	≤0,6	≤0,6
Chromium (VI)	≤0,02	≤0,20
Total Surfactants	≤2	≤4
Sulphate	≤1000	≤1000
Chloride	≤1200	≤1200
Fluoride	≤6	≤12
Nitric Nitrogen	≤20	≤30
Al	≤1	≤2
As	≤0,5	≤0,5
Ba	≤20	-
B	≤2	≤4
Cd	≤0,02	≤0,02
Cr	≤2	≤4
Fe	≤2	≤4
Mn	≤2	≤4
Hg	≤0,005	≤0,005
Ni	≤2	≤4
Pb	≤0,2	≤0,3
Cu	≤0,1	≤0,4
Se	≤0,03	≤0,03
Sn	≤10	-
Zn	≤0,5	≤1,0

Table 1.1. Limits of the main chemical-physical parameters.

Parameter	Effluent discharge standards D.lgs 152/2006 Attached 5- Part III	
	Discharge in superficial water	Discharge in sewerage network
Animal and vegetable fats and oils	≤20	≤40
Total Hydrocarbon	≤5	≤10
Aromatic organic solvents	≤0,2	≤0,4
Chlorinated solvents	≤1	≤2
Total Pesticides	≤0,05	≤0,05
Aldrin	≤0,01	≤0,01
Dieldrin	≤0,01	≤0,01
Endrin	≤0,002	≤0,002
Isodrin	≤0,002	≤0,002

Table 2. Limit of the organic pollutants.

3.2 Traditional treatment plant of wastewaters

Based on local economic conditions and their territorial location, the treatment of wastewater by the tanneries can be carried out on site, then discharging the treated waste directly into the sewer. At the end of the treatments it is necessary that the wastewater reaches the limits imposed by current legislation [12]. The purification phases act on two distinct lines, the water line and the sludge line and they can be described as follows:

Mechanical pre-treatments: these operations are dedicated to the removal of part of the sedimentable organic substances contained in the wastewater. These treatments include coarse screening, sandblasting, oil removal and primary sedimentation.

Chemical-physical or primary treatments: with these treatments we intend to remove most of the organic substances, of the sulphide (from the wastewater following the riviera processes) and chromium (from the wastewater following the tanning and post-tanning operations) and other inorganic compounds. These operations are carried out by oxidation, precipitation, sedimentation, flotation, compensation flows and neutralization.

Oxidative-biological or biological treatment (with activated sludge): includes a series of biodegradation processes by aerobic microorganisms, present in the muddy solution, converting the organic compounds present in the wastewater into simpler inorganic substances such as CO_2, H_2O, NH_4^+, NO_2^-, NO_3^{2-}.

Tertiary treatments, such as secondary sedimentation, where separation of the activated sludge from the effluent leaving the oxidation tank takes place and chemical treatments for the removal of other substances such as stripping and redox process.

Sludge line: the sludge coming out of the primary and secondary sedimentation and the sludge from the oxidation tanks that can no longer be reused are collected and they are subject to stabilization in special tanks, with the aim of eliminating the high quantity of water contained, removing the residual organic material and to destroy the pathogenic organisms present, in such a way to make the final disposal less expensive and less harmful to the environment. Following these treatments, through mechanical equipment the sludge, through mechanical equipment, is subject to high pressures to remove residual water and is often followed by a drying process. Before dewatering, thickeners (polyelectrolytes) can be used to make the sludge denser. The final treated effluent or clarified

wastewater is conveyed to a pipeline named emissary, with final delivery to the surface waters (streams, sea, etc.), incisions or the surface layer of the soil (e.g., Drainage trenches). If it has some defined characteristics, the final effluent can also be used for irrigation or in industry [13-15].

4. References

1. Saran, S.; Chib, S.; Saxena, R.K. Biotechnology of Leather: An Alternative to Conventional Leather Processing. In *High Value Fermentation Products*; John Wiley & Sons, Ltd, **2019**; pp. 23–47 ISBN 978-1-119-55538-4.
2. Mannucci, A.; Munz, G.; Mori, G.; Lubello, C. Anaerobic Treatment of Vegetable Tannery Wastewaters: A Review. *Desalination* **2010**, *264*, 1–8, doi:10.1016/j.desal.2010.07.021.
3. L'Industria Conciaria Italiana Available online: https://www.unic.it/conceria-italiana/industria-conciaria-italiana.
4. Bienkiewicz, K.J. Physical Chemistry of Leather Making. *Krieger Publishing Co. Inc.* **1983**, ISBN 0-8987-4304-4
5. Covington, A.D. Modern Tanning Chemistry. *Chem. Soc. Rev.* **1997**, *26*, 111–126, doi:10.1039/CS9972600111.
6. Covington, A.D., Tanning chemistry: the science of leather. Royal Society of Chemistry, **2009**.
7. Lofrano, G.; Aydin, E.; Russo, F.; Guida, M.; Belgiorno, V.; Meric, S. Characterization, Fluxes and Toxicity of Leather Tanning Bath Chemicals in a Large Tanning District Area (IT). *Water Air Soil Pollut: Focus* **2008**, *8*, 529–542, doi:10.1007/s11267-008-9177-7.
8. Bharagava, R.N.; Saxena, G.; Mulla, S.I.; Patel, D.K. Characterization and Identification of Recalcitrant Organic Pollutants (ROPs) in Tannery Wastewater and Its Phytotoxicity Evaluation for Environmental Safety. *Arch Environ Contam Toxicol* **2018**, *75*, 259–272, doi:10.1007/s00244-017-0490-x.
9. Lofrano, G.; Meriç, S.; Zengin, G.E.; Orhon, D. Chemical and Biological Treatment Technologies for Leather Tannery Chemicals and Wastewaters: A Review. *Science of The Total Environment* **2013**, *461–462*, 265–281, doi:10.1016/j.scitotenv.2013.05.004.
10. Tünay, O.; Kabdasli, I.; Orhon, D.; Ates, E. Characterization and Pollution Profile of Leather Tanning Industry in Turkey. *Water Science and Technology* **1995**, *32*, 1–9, doi:10.1016/0273-1223(96)00132-1.
11. Ikehata, K.; Gamal El-Din, M.; Snyder, S.A. Ozonation and Advanced Oxidation Treatment of Emerging Organic Pollutants in Water and Wastewater. *Ozone: Science & Engineering* **2008**, *30*, 21–26, doi:10.1080/01919510701728970.
12. Cassano, A.; Molinari, R.; Romano, M.; Drioli, E. Treatment of Aqueous Effluents of the Leather Industry by Membrane Processes: A Review. *Journal of Membrane Science* **2001**, *181*, 111–126, doi:10.1016/S0376-7388(00)00399-9.

13. L. Del Pezzo, G. De Simone, M. Tomaselli, G. Ummarino, Proposta di un 'modello' schematico per impianti di depurazione di acque di scarico conciarie, *Cuoio, Pelli, Mat.Concianti* 56 (1) (**1980**) 17.
14. U. Peila, Impianto di depurazione acque reflue da trattamento di concia delle pelli, AES 3 (10) (**1981**) 61.
15. Metcalf & Eddy, Inc. Wastewater Engineering, Treatment and Reuse. McGraw-Hill, **2006**.

16. Decreto Legislativo 3 aprile **2006**, n.152, *testo unico ambientale*.

Chapter 2 – Chemical characterization of wastewaters from the tanning industry

1. Introduction

The tanning process can be divided into four phases: beamhouse operation, tannage operation, re-tanning and finishing.

During the Beamhouse phase, the leather is prepared for the following tanning process (soaking, unhairing, and liming, bating and deliming, degreasing, and pickling). During the tanning operation, the leather is treated using different chemicals such as chromium salts, vegetable substances, aldehydes, oils, etc. Subsequently they undergo re-tanning and finishing processes to give the leather the desired characteristics for marketing.

In the different stages of tanning many compounds are used such as acids, alkalis, chromium salts, tannins, solvents, dyes, oils, resins, synthetic tannins, but they aren't completely fixed onto the leather remaining in the water. Then high values of chemical oxygen demand (COD), biochemical oxygen demand (BOD), sulfate, chloride, heavy metals and different organic substances characterize the discharged wastewaters. The first phase provides the characterization of the wastewater deriving from the tanning industry according to D. Lgs 152/2006 (Attached 5- Part III) [1].

COD is one of the main parameters used to evaluate the quality of wastewaters; in particular, it can provide indications on the content of organic matter. We can distinguish two fractions for the COD: the biodegradable one, represented by all those compounds that are removed from urban or industrial wastewater through traditional purification processes, and the not-biodegradable fraction, represented by all those

substances defined as "recalcitrant", which they persist after the common treatments and providing also characterization of the organic substances that contribute to recalcitrant COD [2–5]. In the tanning scene, substances such as alkylphenols, ethoxylated alkylphenols and chlorophenols are used for various purposes. Alkylphenols are characterized by a phenolic group bonded to one or more variable alkyl groups. They can be natural or synthetic and the main exponents of these compounds are nonylphenols and octyl-phenols.

Alkyl phenols and ethoxylated alkyl phenols have multiple uses in the tanning industry. They are used as emulsifiers, dispersants, wetting agents and disinfectants. Alkylphenols are characterized by a phenolic group bonded to one or more variable alkyl groups. They can be natural or synthetic and the main exponents of these compounds are nonylphenols (Figure 1) and octylphenols. The most common synthetic homologs are ethoxylated nonylphenols (NPE) (Figure 2) and ethoxylated octylphenol (OPE).

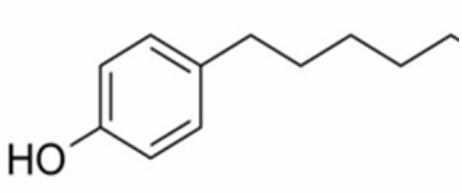

Figure 1. Structure of nonylphenol

These substances are found in significant concentrations in fabrics because they are used in the washing and dyeing of fabrics. They are very active molecules at a physiological level and they are responsible for dermatitis and allergies. They are persistent in the environment and

they do not degrade and can accumulate in living organisms up to humans through contamination of the food chain, and in plant organisms due to their acute and chronic toxicity and impairment of hormonal activity. In fact, the similarity with natural estrogen hormones interferes with the sexual development of many organisms. In fish they cause feminization.

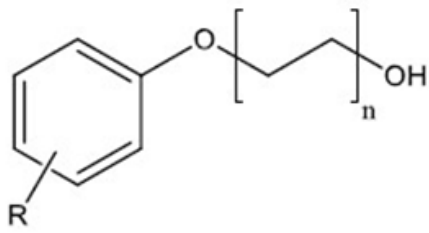

Figure 2. Structure of nonylphenol ethoxylate (NPE)

Chlorophenols, on the other hand, are used by the tanning industry for their biocidal and fungal activity. Their toxicity is due to the tendency of these compounds to accumulate in the fat of animals and humans, affecting the endocrine system. Many chlorophenols have carcinogenic properties: they cause liver tumors and leukemia, and they exhibit immunosuppressive properties.

In organisms, and in mammals, the toxicity of chlorophenols increases linearly with the number of chlorine atoms present in the molecule while for an isomer it increases in relation to its acidity. The damage caused by chlorophenols is found in the liver, spleen and immune system. Pentachlorophenol produces severe liver damage and the onset of tumors. In addition, some dioxins (whose toxic aspects are known) are also produced in its synthesis [6]. Another group of substances widely

used are the polyphenolic compounds used in vegetal tanning or in the re-tanning process. Most of the used compounds are of natural origin and they derive mainly from leaves, wood, and bark of some plants such as mimosa, mangrove, chestnut and oak. The compounds mentioned above appear to be poorly biodegradable and they contribute to increase the concentration of COD [7–9].

2. Materials and methods

In this first part of the project, different samples of wastewater deriving from various companies (for confidentiality reasons the names are omitted) present in the various districts of the tanning sector on the Italian territory were analyzed. The samples were taken out of the treatment plants.

The collected samples were stored at 4° C and they were used for the analysis of chemical-physical parameters, characterization, and identification of recalcitrant organic pollutants. The samples were analyzed for the main chemical-physical parameters according to the methods provided by "Standard Methods for Examination of Water and Wastewater" (APHA, 2020), APAT CNR IRSA Methods (Man.29, 2003) and UNI EN ISO Methods.

2.1 Chemical-physical parameters

For determination of pH and conductivity was used potentiometric methods (Mod 856/867, Metrohm, Switzerland).

The organic substance was evaluated with COD, BOD_5 and TOC. The determination of COD involves the oxidative acid digestion of 2 mL of sample at 170 ° C for 20 min using an oxidizing agent such as potassium

dichromate in the presence of sulfuric acid and silver sulfate. The concentration of the organic substance is proportional to the quantity of dichromate consumed. The quantification is performed with a colorimetric method at a wavelength of 440 nm (Hach, DR 3900, Germany) [10-].

The respirometric method is based on the ascertainment of dissolved oxygen in the sample before and after an incubation of 5 days in the dark at a temperature of 20 ° C. The sample is placed in a hermetically sealed container equipped with a differential pressure gauge to avoid oxygen exchanges. During the biological decay of the organic content, oxygen is consumed and this generates a vacuum in the gas, measured by the manometer. The BOD_5 value of the sample under examination, expressed in mg/L of oxygen.

Moreover, the ratio between BOD and COD can assume values higher or less high than 0.5. Values which are equal or greater than 0.5 indicate that the organic substance present can either be suitable for biological treatment or they can be biodegradable; values below 0.1 indicate low biodegradability [11].

The TOC, together with the COD and the BOD_5, provides information on the organic load. The principle supporting the method for determination of organic carbon is based on combustion; an aliquot of the sample under examination, suitably homogenized and diluted, if necessary, is injected into a reaction chamber heated to a high temperature (680 ° C), where there is a platinum-based oxidative catalyst. The water sample is vaporized, and the total carbon is oxidized to CO_2 and H_2O. The CO_2 resulting from the oxidation of organic and / or inorganic carbon is transported using a flow of carrier gas and measured by a non-dispersive infrared analyzer (NDIR).

An aliquot of the sample to be analyzed, suitably diluted, if necessary, is transferred to a flask and it is placed in one of the autosampler stations; the sample is inserted in the appropriate line of the software in the analysis session. Organic carbon is set by the difference of total carbon (TC) and inorganic carbon (IC) according to TOC = TC - IC. All operations are performed automatically by the tool. The software provides the concentration of the total organic carbon content (TOC) for the sample under examination by linear interpolation of the measured area, for the parameter TC and IC, on the calibration curve and the result is expressed in mg/L (TOC-V – Shimadzu, Japan) [12].

The main parameters such as total phosphorus, ammonium, nitrous nitrogen, chromium (VI) and total surfactants were determined by spectrophotometric methods (Cary 50 UV/Vis, Varian, US). For determination of nitrous nitrogen, the method provides that at pH 2.0-2.5 the sulfonamide is diazotized by nitrous acid and the resulting diazo compound is coupled with N-(1-naphthyl) - ethylenediamine; a colored azo-compound is thus obtained and its absorbance is measured at 543 nm. To get ammonium, 10 ml of sample are derived with phenol and hypochlorite which leads to the formation of an indo phenolic complex which, in an alkaline environment and in the presence of sodium nitroprusside, acting as a catalyst, takes on a blue color that can be measured spectrophotometrically at the wavelength of 640 nm. In aqueous solution, phosphorus is present as orthophosphates, polyphosphates and organic phosphates, but orthophosphates (PO_4^{3-}, HPO_4^{2-}, $H_2PO_4^-$) represent the readily available form for biological metabolism. In any case, in order to determine the total phosphorus, whatever the species in which it is found, the phosphorus must first be transformed into orthophosphate. This transformation is carried out with

an oxidizing attack for organic compounds and for those with an oxidation number below +5 and with acid hydrolysis for polyphosphates. Subsequently, the orthophosphate ions react with ammonium molybdate and potassium antimonyl tartrate, in an acid medium, forming a heteropolyacid which is reduced with ascorbic acid to molybdenum blue, intensely colored, whose absorbance is measured at the wavelength of 880 nm.

Chromium is used in tanning processes, and it requires the use of basic chromium sulfate ($Cr_2(OH)_2(SO_4)_2$). The oxidation of trivalent chromium to hexavalent involves the fattening substances, used by industry with unsaturations in the hydrocarbon chains. The method for the establishment is based on the development of color following the reaction between hexavalent chromium and diphenylcarbazide. It is hypothesized that the mechanism of this reaction concerns a reduction of chromium (VI) to chromium (III) and a simultaneous oxidation of diphenylcarbazide to diphenylcarbazone with consequent formation of a red-violet colored compound. Following this reaction, the absorbance is read at the wavelength at 540 nm.

The main anions and cations such as chloride, sulfate, nitric nitrogen and fluoride were gained by ionic exchange chromatography with conductivity detectors. The analytes were separated by a Metrosep C4 250/4.0 column using 3.0 mM HNO_3 as eluent and a flow rate of 0.9 mL/min, whereas anions by a Metrosep A supp7 250/40 column using 3.6 mM Na_2CO_3 as eluent at a flow rate of 0.7 mL/min (IC 856, Metrohm, Switzerland).

For heavy metal (Al, As, Ba, B, Cd, Cr, Fe, Mn, Hg, Ni, Pb, Cu, Se, Sn, Zn) analyses, 45 mL sample were digested with 5 mL HNO_3 and assisted

by microwave (Mars-CEM, US), the mineralized samples were analyzed by ICP-MS (Aurora M90 Bruker, US).

To establish animal and vegetable fats and oils, samples (0.250 L) were extracted by liquid-liquid extraction method with n-hexane (30 mL); the extract was then concentrated to 1 mL by a rotavapor at $T \leq 40°C$. The final extracts obtained were purified on florisil and then analyzed by GC-FID (GC6890-Agilent, US). Then, chlorinated organic solvents were analyzed by GC-ECD (GC7890, Agilent, US) preceded by headspace static extraction (HS 7698, Agilent, US).

2.2 Determination of organic pollutants

For the research of organic contaminants such as polycyclic aromatic hydrocarbons and pesticides, samples were treated by solid-phase extraction (SPE); 0.5 L of sample was filtered and then concentrated on a C18 disk (ENVI, -18 DSK SPE Disk, diam. 47 mm). Before starting the extraction process, samples were spiked with 25 µL of decachlorobiphenyl (100 μgL^{-1} standard solution). The disks were pre-conditioned with methanol and then with distilled water. The analytes were eluted with a solution of 1:1 dichloromethane and n-hexane. The extract was then concentrated by an automatic evaporator under nitrogen flow (Multivap, LabTech, Italy) and then recovered with 1 ml, a solution of 1:1 n-hexane and acetone. The internal standard was added to the extract (mixture of deuterated PAHs) and it was injected to a GC-MS in SIM mode (MS-TQ8030-Shimadzu, Japan). The chromatographic separation was performed on a DB-5 (60 m, id 0.25 mm, 0.25 µm, Agilent) fused silica capillary column coated with 5% phenyl

polycarborane-siloxane. The oven temperature program is shown in Table 1 and Table 2.

Temperature (°C)	Gradient (°C/min)	Hold Time (minutes)
60	-	2.0
200	25	0.0
270	10	6.0
310	25	10

Table 1 Gas-chromatographic conditions for PAHs analysis.

Temperature (°C)	Gradient (°C/min)	Hold Time (minutes)
50	-	1.0
120	25	0.0
285	8.4	4.0

Table 2 Gas-chromatographic conditions for pesticides analysis.

The accuracy, precision and recovery for all the analytes were evaluated using certified reference materials based on the participation in inter-laboratory circuits (Proficiency testing) on wastewater and similar matrices.

2.3 Determination of emerging organic pollutants

For the first characterization of emerging organic pollutants that contribute the recalcitrant COD, the samples were analyzed to confirm the presence of compounds like phenols, chlorophenols, Bisphenol A, alkylphenol and alkylphenol ethoxylates. The methods UNI-EN-ISO 17070 and UNI-EN-ISO 18857 were applied and also validated.

2.3.1. Method validation

The method validation for the identification and quantification of chlorophenols, Bisphenol A, alkylphenol and alkylphenol ethoxylates was performed according to the Eurachem guidelines and EN ISO/IEC 17025 standards and it was accredited by the Italian Accreditation Body Accredia. [13]. [10]

The limit of detection (LOD) and the limit of quantification (LOQ) are important tools for the analytic methods to identify the lower concentration limit which the sample cannot go below (LOD) or quantified (LOQ) with sufficient probability statistics.

The criterion of the calculation of LOD and LOQ used is that of the variability of the blanks or of a standard close to this limit, that is as follows

$$LOD = 3*s'_0$$

$$LOQ = 10*s'_0$$

Where s_0 is the standard deviation Where s0 is the standard deviation calculated as indicated in Figure 3.

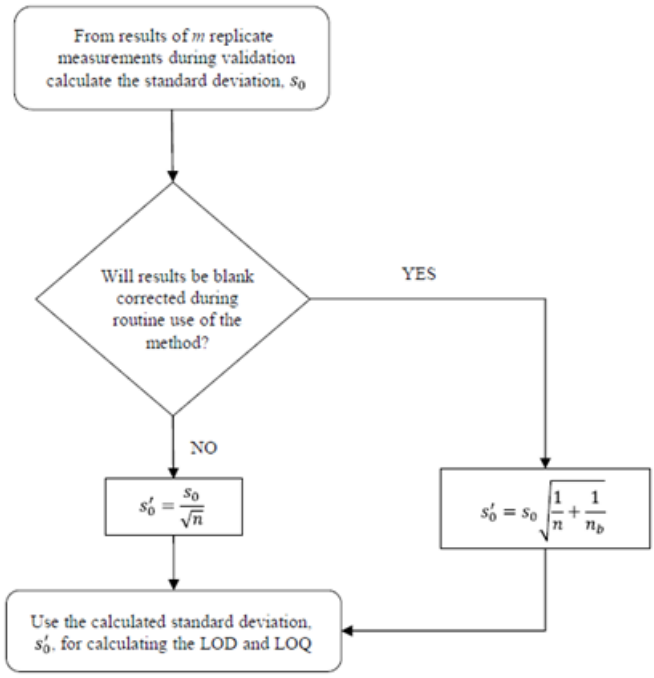

Figure 3. Flow chart for the determination of LOD and LOQ. Where: s'_0 is the standard deviation of the blank; n is the average number of replicates used to obtain the final result of the measurement, where each replica is obtained following the entire measurement process and n_b is the number of replicates performed for the reagent blank when the blank correction is performed according to the measurement procedure. [13] [10].

Another parameter to determine the validation of a method is the calculation of the measurement uncertainty. The uncertainty associated with a measure basically depends on three types of errors: gross, random or systematic. The three types of errors are independent from each other; therefore they can occur simultaneously, individually and with different weights. The gross error is the simplest to identify since it derives, as its name itself indicates, from an obvious error that misreports the analytical result in an unreal measurement, making the need to repeat the

establishment necessary. Random error is an ever-present error, its weight determines the repeatability and reproducibility of a method, or rather its accuracy; the smaller the random error, the more precise the determination will be. Finally, the systematic error shifts the set of determinations with respect to the true value, worsening the accuracy of the method. This type of error can only be identified if certified samples are analyzed or if you participate in interlaboratory circuits where the measurement is compared with data obtained from other laboratories. In general, as we have already stated previously, the result of a measurement is only an approximation or an estimate of the value of the measurement and consequently it will only be completed when accompanied by a declaration of the uncertainty from that estimate. The uncertainties can be determined through two evaluation categories, marked with the letters A and B. It is emphasized that all uncertainties have the same nature, so the distinction based on the evaluation categories (A and B) concerns only the way which uncertainties are estimated. The uncertainty of category A can be assessed directly by the laboratory through the repetition of a measurement process, under controlled conditions, and they can relate to the uncertainty of repeatability, recovery, and calibration line. Uncertainties of type B derive from information relating to the instrumentation or reference materials (for example tolerance of the glassware, calibration of a balance, etc.) which can be evaluated through information or estimates of internal origin (calibration uncertainty) or external. To estimate the uncertainty of measurement, the GUM (bottom-up) approach was used based on the identification and quantification of individual contributions to uncertainty and also on the combination of weighted variances. The GUM approach, or Metrological Approach, defines all the possible

sources of uncertainty that are relevant considering them separately in the contribution to the calculation of the total uncertainty. The uncertainty about the result can derive from many possible sources, each of which is called the "uncertainty component". When a component of the uncertainty is expressed as a standard deviation, it is called "standard uncertainty". The first step in calculating the uncertainty is to fill a full list of possible significant sources of uncertainty. In drawing up the list of sources, it is usually advisable to start from the basic equation used to calculate the measurement from the intermediate values. All the parameters in this equation may have an uncertainty associated with their value and they may therefore represent potential sources of uncertainty. Furthermore, there may be other parameters that do not appear explicitly in the equation used to calculate the value of the measurement, but they might nevertheless influence the measurement results, i.e. the extraction time or temperature. These parameters are also potential sources of uncertainty. All these different sources should be included in the list. All contributions to uncertainty, before being combined, must be expressed as standard uncertainties, that is, as standard deviations. If a component of the uncertainty has been experimentally evaluated by the dispersion of repeated measurement values, it can be expressed directly as a standard deviation. For the contribution to uncertainty in single measurements, the standard uncertainty is simply the observed standard deviation; for results that need to be averaged, the experimental standard deviation of the mean is used. If the uncertainty estimate derives from previous results or data, it should already be expressed as a standard deviation. However, when a confidence interval with a confidence level is given (in the form ± a, for a given level of p in%), then the standard deviation is calculated by

dividing the value of ‘a’ by the percentile of the normal distribution corresponding to the level of confidence used. If the limits ± a are not accompanied by a confidence interval, but it can be assumed that the extreme values are likely to be, a rectangular distribution can be assumed, with a standard deviation a / √3. If the limits ± a are not accompanied by a confidence interval, but it can be assumed that the extreme values are unlikely, a triangular distribution can be assumed, with a standard deviation a / √6. Once estimation is completed together with the individual components of the uncertainty, or groups of components and, after expressing them as standard uncertainties, the compound relative uncertainty is calculated according to the following formula:

$$u_r(y) = \sqrt{\sum_i \left[\left(\frac{\partial y}{\partial x_i}\right)^2 * u^2(\bar{x}_i)\right]}$$

The use of this expression is correct only if all the quantities considered to derive the result y of the process or test are mutually unrelated and independent.

In cases when to calculate the result y the formulas are of the type:

$$y = (b * c * d)/f$$

the above formula can be simplified as follows:

$$u_r(y) = \sqrt{\sum_i u_i^2}$$

The compound uncertainty is:

$$U_c = u_r(y) * \bar{x}$$

The composite standard uncertainty is then multiplied by a coverage factor k, in order to obtain the extended uncertainty.

$$U = ku_r$$

Many aspects must be considered when choosing the value for the coverage factor k, including:

- level of confidence required.
- available information on underlying distributions,
- any information on the number of values used to estimate random effects.

In most of the cases the recommended value for k is equal to 2. However, this value of k may be insufficient if the composite uncertainty is based on statistical observations with a relatively small number of degrees of freedom (less than six). If the composite standard uncertainty is dominated by a single contribution with several degrees of freedom less than six, it is recommended that k corresponds to the tabulated value of student's t in the bilateral case for the number of degrees of freedom associated with that contribution and for the level of confidence required. The expanded uncertainty, associated with the measurement, provides a presumable interval including the interval of the distribution of values that can reasonably be attributed to the measurement with the required level of confidence [13] [10].

2.3.2. Determination of free phenol, chlorophenols, alkylphenols and ethoxylated alkylphenols

The methods UNI-EN-ISO 17070 and UNI-EN-ISO 18857 were used respectively to determine chlorophenols, ethoxylated alkylphenols and alkylphenols [14-15].

In particular, the samples were treated by solid-phase extraction (SPE); 100 mL of sample were filtered and then concentrated on a polystyrene-divinylbenzene cartridge (CHROMABOND® HRP- 200 mg) [16] [11]. To determine phenol and chlorophenols the cartridge was pre-conditioned with 3 mL of methanol and then with 3 mL of distilled water. The cartridge was washed with 3 mL a solution of water whit 2%v/v of methanol. The analytes were eluted with 3 mL of acetone. The extract was then concentrated by an automatic evaporator under nitrogen flow (Multivap, LabTech, Italy) down to a volume of 1 mL.

To determine ethoxylated alkylphenols and alkylphenols the cartridge was pre-conditioned with 10 mL of acetone and then with 10 mL of distilled water. The cartridge was washed with 10 mL of water at pH 2.0. The analytes were eluted with 5 ml of acetone. The extract was then concentrated by an automatic evaporator under nitrogen flow (Multivap, LabTech, Italy) down to a volume of 1 mL. The extract was derivatized with MSTFA (N-Methyl-N-(trimethylsilyl) trifluoroacetamide) and subsequently added the internal standard (mixture of deuterated PAHs) and it was injected to a gas chromatograph (Shimadzu 2010 plus, Japan) coupled with a mass spectrometer (MS-TQ8030-Shimadzu, Japan) and a fused silica HP5-MS capillary column (30m x 0.25mm i.d.) with film thickness of 0.25 μm (Agilent Technologies, US). High purity helium (99.9 %) was used as a carrier gas at a flow rate of 1.0 mL min^{-1}. The

chromatograph gas was operated in split mode (1:20), and the separation conditions are shown in Table 3 and Table 4. The mass spectrometer was operated in SIM mode.

Temperature (°C)	Gradient (°C/min)	Hold Time (minutes)
50	-	2.0
300	15	5.0

Table 3 Gas-chromatographic conditions for phenol and chlorophenols analysis.

Temperature (°C)	Gradient (°C/min)	Hold Time (minutes)
60	-	1.0
280	10	5.0

Table 4 Gas-chromatographic conditions for and ethoxylated alkylphenols and alkylphenols analysis.

The qualitative analysis was performed using the retention time and the mass ions characteristic of each compound (Table 4 and Table 5).

Compounds	R.T. (min)	Quantification Ion	Confirmation Ions
Phenol	5,93	94	65, 66
2-Chlorophenol	6,08	128	64, 130
m-Cresol	6,91	108	107, 77, 79
o,p-Cresol	7,15	107	108, 77, 79, 90
2,4-Dichlorophenol	8,31	162	164, 98
4-Chlorophenol	8,55	128	65, 130
2,4,6-Trichlorophenol	10,19	196	198, 200

Table 4. Retention time, quantification ion and confirmation ion for GC–MS in SIM mode for phenols and chlorophenols.

Compounds	R.T. (min)	Quantification Ion	Confirmation Ions
4-tert-octylphenol	15,4	135	107, 136
Nonylphenol (Technical Mixture)	16,5…17,5	207	221, 193
4-Nonylphenol	18,5	107	220, 251
4-nonylphenol ethoxylate (Mixture of isomers)	20,3…20.8	251	265, 279, 307
4-nonylphenol diethoxylate (Mixture of isomers)	22.9…23.3	295	309, 323,351
Bisphenol A	21,5	213	228…107

Table 5. Retention time, quantification ion and confirmation ion for GC–MS in SIM mode for ethoxylated alkylphenols and alkylphenols.

The quantification of each compound was performed by the internal standard method. The calibration curves were constructed in the range 10…200 µg/L and 50…500 µg/L, respectively for phenols and chlorophenols, phenol alcohols and ethoxylated alkylphenols. All calibration curves are reported in APPENDIX I.

2.3.3. Screening analysis for the determination of polyphenols compounds

To determine polyphenols, the screening analysis was carried out on a 5800 MALDI-time of flight (TOF)/TOF AB SCIEX equipped with a nitrogen laser (337 nm) (AB SCIEX. Milan. Italy). The lyophilized sample was mixed (1:1. v/v) with a solution of 20 mg/mL 2.5-dihydroxybenzoic acid (DHB. Sigma Aldrich. Milan. Italy) in acetonitrile:water (50:50) solution.

To identify the different compounds. MS and tandem MS (MS/MS) spectra were acquired n positive reflection mode. by using a mass (m/z) range of 100…4000 Da.

3. Results and discussion

The results of the main chemical-physical parameters are shown in Table 6 and Table 7. The results showed that the samples have high conductivity values (8010…10150 µS cm^{-1}), compatible with the high concentrations of chlorides and sulphates, which are 1022…2489 mg/l and 903…1571 mg/l, respectively. All samples have chloride values above the limit imposed by the Italian legislation, except samples n° 8 and (Figure 4). Also, for sulphates many exceedances of the legal limit are observed, except for samples 2,3,6 and 7 (Figure 5). The concentrations of heavy metals were all very low and in any case below the limits set by the regulations, with the exception of sample n ° 1 where there were higher concentrations of total Cr equal to 8 mg/l and Cr(VI) equal to 0.88 mg/L. This result is compatible with the values in the wastewater of the tanning industries that only practice chrome tanning.

Parameter	N°1	N°2	N°3	N°4	N°5	N°6	N°7	N°8	N°9
pH	7.95	7.17	7.66	7.96	7.84	9.85	7.22	8.34	7.89
Conductivity (µS cm^{-1})	10150	10109	9151	8810	8310	9151	8522	5860	8010
BOD_5	**90**	40	26	56	**82**	**79**	**79**	45	53
COD	**786**	**228**	**167**	**1540**	**505**	150	**276**	151	**178**
TOC	151	72	64	384	140	70	75	56	50
BOD_5 /COD	0.10	0.20	0.20	0.04	0.16	0.53	0.29	0.29	0.30
Total Phosphorus	< LOQ	< LOQ	< LOQ	< LOQ	< LOQ	< LOQ	< LOQ	< LOQ	< LOQ
Ammonium	13	9	4	61	1	1	1	< LOQ	< LOQ
Nitrite	0.1	0.05	0.09	0.07	0.23	0.54	0.18	0.06	0.02
Chromium (VI)	**0.88**	< LOQ	< LOQ	0.17	0.22	0.02	0.1	0.03	0.01
Total Surfactants	3	2	1	10	15	6	9	1	6.8
Sulphate	**1306**	1083	1036	**1571**	**1374**	903	1064	**1134**	**1564**
Chloride	**1922**	**2489**	**2170**	**1815**	**1974**	**2053**	**2293**	1022	**1747**
Fluoride	< LOQ	< LOQ	< LOQ	< LOQ	< LOQ	< LOQ	< LOQ	< LOQ	< LOQ
Nitrate	< 1	< 1	19	< 1	< 1	< 1	11	**25**	15

Table 6. Results (mg/L) of the main chemical-physical parameters.
The LOQ values are shown in Table 16, Appendix I

Parameter	N°1	N°2	N°3	N°4	N°5	N°6	N°7	N°8	N°9
Al	2	0.04	0.03	0.107	0.528	0.014	0.059	0.54	0.06
As	0.003	0.003	0.001	0.004	0.004	0.005	0.005	0.004	0.007
Ba	0.008	0.02	0.08	< LOQ	0.017	0.01	0.113	0.02	0.05
B	0.5	0.3	0.9	0.6	2.0	0.5	2.0	0.1	0.4
Cd	< LOQ	< LOQ	< LOQ	< LOQ	< LOQ	< LOQ	< LOQ	< LOQ	< LOQ
Cr	**8**	0.07	0.1	2.4	3.3	0.16	0.21	0.8	0.8
Fe	3	0.1	2	0.8	1.3	0.6	**20**	0.1	0.3
Mn	0.06	0.003	0.4	0.02	0.0191	0.0106	0.561	0.1	0.01
Hg	0.0007	0.0003	< LOQ	< LOQ	0.0017	< LOQ	< LOQ	< LOQ	< LOQ
Ni	0.02	0.06	0.09	0.1	0.0463	0.0691	0.593	0.02	0.02
Pb	0.001	0.002	0.001	< LOQ	< LOQ	< LOQ	< LOQ	0.003	< LOQ
Cu	0.02	0.04	0.03	0.03	0.03	0.02	0.06	0.01	0.02
Se	0.006	0.003	0.002	0.002	0.02	0.02	0.02	0.004	0.006
Sn	< LOQ	< LOQ	< LOQ	< LOQ	< LOQ	< LOQ	< LOQ	< LOQ	< LOQ
Zn	0.05	0.04	0.04	0.02	0.07	0.01	0.1	0.02	0.03

Table 7. Results (mg/L) of the main metals. The LOQ values are shown in Table 16, Appendix I

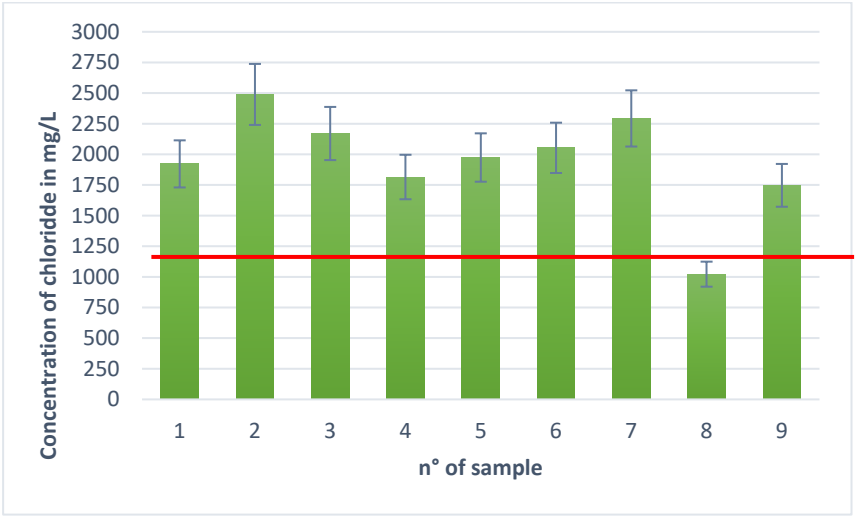

Figure 4. Concentration of chloride in the sample. The red line represents the limit value imposed by the legislation, equal to 1200 mg/L.

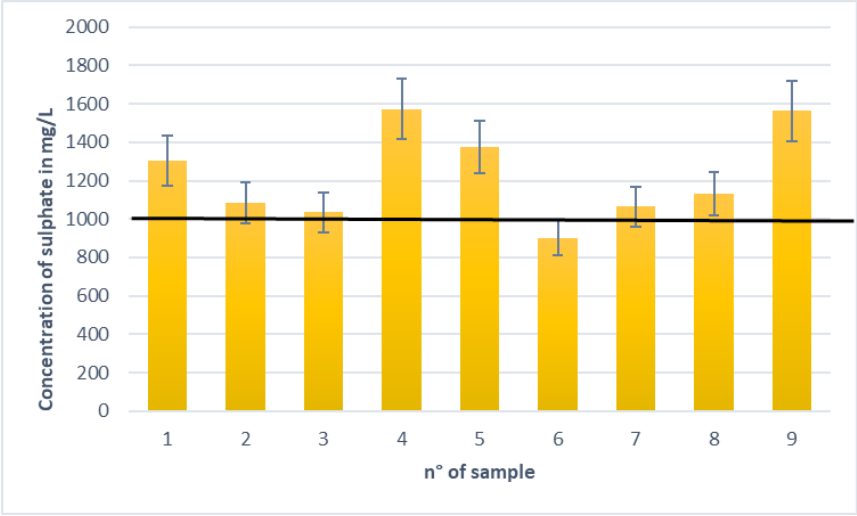

Figure 5. Concentration of sulphate in the sample. The black line represents the limit value imposed by the legislation, equal to 1000 mg/L.

All samples show a high organic matter content, as shown by the high COD above the limit value, except the sample 6 and 8. The samples n°5 has the highest COD content equal to 1540 mg/L and the sample n° 6 and 8 have the lowest COD content of 150 mg/L. Also, for the TOC parameter high values are recorded, the highest value (384 mg/L) is observed in sample n°5 and the lowest value (50mg/L) in sample n°9. These parameters were compared using Pearson's correlation at the $p < 0.05$ significance level. The results indicated that the COD and TOC have very strong correlation with $r = 0.98$ and $p < 0.05$ (Fig. 6); this suggests that the high values of COD depend only on the presence of organic compounds. Furthermore, the ratio between BOD_5 and COD (always less than 0.5) suggests that these compounds are not biodegradable.

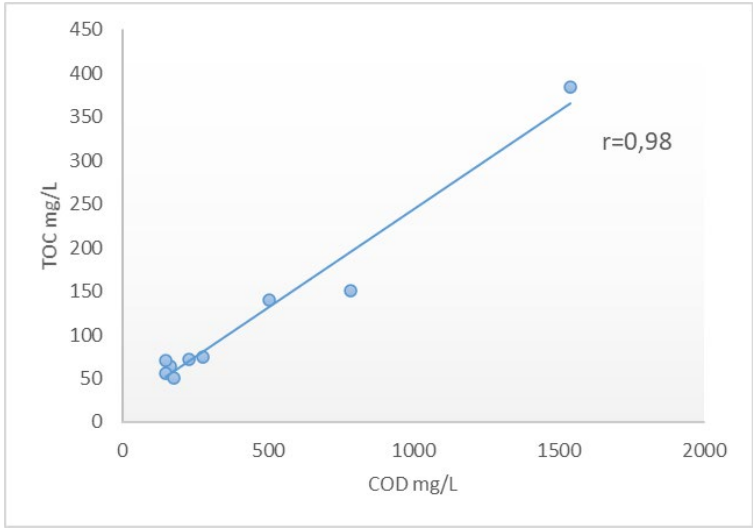

Fig 6. Pearson correlation diagram, with values of r=0.98 and $p < 0.05$.

The research for persistent organic pollutants, required by Italian legislation, showed the absence at the detection limit of the method of these compounds as shown in Table 8.

Parameter	N°1	N°2	N°3	N°4	N°5	N°6	N°7	N°8	N°9
Animal and vegetable fats and olis	1	1	2	< LOQ	2	< LOQ	< LOQ	< LOQ	< LOQ
Hydrocarbon	< LOQ	< LOQ	< LOQ	< LOQ	< LOQ	< LOQ	< LOQ	< LOQ	< LOQ
Aromatic Solvent	< LOQ	< LOQ	< LOQ	< LOQ	< LOQ	< LOQ	< LOQ	< LOQ	< LOQ
Chlorinated solvents	< LOQ	< LOQ	< LOQ	< LOQ	< LOQ	< LOQ	< LOQ	< LOQ	< LOQ
T. Pesticides	< LOQ	< LOQ	< LOQ	< LOQ	< LOQ	< LOQ	< LOQ	< LOQ	< LOQ
aldrin	< LOQ	< LOQ	< LOQ	< LOQ	< LOQ	< LOQ	< LOQ	< LOQ	< LOQ
dieldrin	< LOQ	< LOQ	< LOQ	< LOQ	< LOQ	< LOQ	< LOQ	< LOQ	< LOQ
endrin	< LOQ	< LOQ	< LOQ	< LOQ	< LOQ	< LOQ	< LOQ	< LOQ	< LOQ
isodrin	< LOQ	< LOQ	< LOQ	< LOQ	< LOQ	< LOQ	< LOQ	< LOQ	< LOQ
NAP	< LOQ	< LOQ	< LOQ	< LOQ	< LOQ	< LOQ	< LOQ	< LOQ	< LOQ
ACE	< LOQ	< LOQ	< LOQ	< LOQ	< LOQ	< LOQ	< LOQ	< LOQ	< LOQ
ACY	< LOQ	< LOQ	< LOQ	< LOQ	< LOQ	< LOQ	< LOQ	< LOQ	< LOQ
FLR	< LOQ	< LOQ	< LOQ	< LOQ	< LOQ	< LOQ	< LOQ	< LOQ	< LOQ
PHE	< LOQ	< LOQ	< LOQ	< LOQ	< LOQ	< LOQ	< LOQ	< LOQ	< LOQ
ANT	< LOQ	< LOQ	< LOQ	< LOQ	< LOQ	< LOQ	< LOQ	< LOQ	< LOQ
FLT	< LOQ	< LOQ	< LOQ	< LOQ	< LOQ	< LOQ	< LOQ	< LOQ	< LOQ
PYR	< LOQ	< LOQ	< LOQ	< LOQ	< LOQ	< LOQ	< LOQ	< LOQ	< LOQ
BaA	< LOQ	< LOQ	< LOQ	< LOQ	< LOQ	< LOQ	< LOQ	< LOQ	< LOQ
CHR	< LOQ	< LOQ	< LOQ	< LOQ	< LOQ	< LOQ	< LOQ	< LOQ	< LOQ
BkF	< LOQ	< LOQ	< LOQ	< LOQ	< LOQ	< LOQ	< LOQ	< LOQ	< LOQ
BbF	< LOQ	< LOQ	< LOQ	< LOQ	< LOQ	< LOQ	< LOQ	< LOQ	< LOQ
BaP	< LOQ	< LOQ	< LOQ	< LOQ	< LOQ	< LOQ	< LOQ	< LOQ	< LOQ
DhA	< LOQ	< LOQ	< LOQ	< LOQ	< LOQ	< LOQ	< LOQ	< LOQ	< LOQ
IND	< LOQ	< LOQ	< LOQ	< LOQ	< LOQ	< LOQ	< LOQ	< LOQ	< LOQ
BgP	< LOQ	< LOQ	< LOQ	< LOQ	< LOQ	< LOQ	< LOQ	< LOQ	< LOQ

Table 8. Results (mg/L) of the organic pollutants. The LOQ values are shown in Table 17, Appendix I

The determination of some recalcitrant organic compounds which phenols, chlorophenols, alkylphenols, alkylphenols ethoxylate and diethoxylate and bisphenols showed the presence of nonylphenol, nonylphenol ethoxylate and diethoxylate, but the concentrations are low and close to the limit of quantification. The data are reported in Table 9 and the validation data are reported in APPENDIX I.

Parameter	N.1	N.2	N.3	N.4	N.5	N.6	N.7	N.8	N.9
Bysphenol A	< 0.5	< 0.5	< 0.5	< 0.5	< 0.5	< 0.5	< 0.5	< 0.5	< 0.5
4-Nonylphenol	< 0.5	< 0.5	< 0.5	< 0.5	< 0.5	< 0.5	< 0.5	< 0.5	< 0.5
Nonylphenol (Technical Mixture)	< 0.5	< 0.5	< 0.5	< 0.5	< 0.5	< 0.5	< 0.5	< 0.5	< 0.5
4-tert-octylphenol	< 0.5	< 0.5	< 0.5	< 0.5	< 0.5	< 0.5	< 0.5	< 0.5	< 0.5
4-nonylphenol ethoxylate	< 0.5	< 0.5	< 0.5	< 0.5	< 0.5	< 0.5	**0.5**	< 0.5	< 0.5
4-nonylphenol diethoxylate	**0.7**	< 0.5	< 0.5	**1.3**	**1.2**	< 0.5	**1.0**	< 0.5	< 0.5

Table 9. Results (µg/L) of the analysis for the determination of main alkylphenols.

The results of the determination of phenol and chlorophenols are shown in Table 10. The data show the presence of phenol alone in concentrations just above the limit of quantification only in some samples and in the range 5.2… 10.2 µg / L.

Parameter	N.1	N.2	N.3	N.4	N.5	N.6	N.7	N.8	N.9
Phenol	**6.0**	**5.2**	**6.0**	< 0.1	**10.2**	< 0.1	< 0.1	< 0.1	< 0.1
4-Chlorophenol	< 0.1	< 0.1	< 0.1	< 0.1	< 0.1	< 0.1	< 0.1	< 0.1	< 0.1
m-Chresol	< 0.1	< 0.1	< 0.1	< 0.1	< 0.1	< 0.1	< 0.1	< 0.1	< 0.1
o,p- Chresol	< 0.1	< 0.1	< 0.1	< 0.1	< 0.1	< 0.1	< 0.1	< 0.1	< 0.1
2,4-dichlorophenol	< 0.1	< 0.1	< 0.1	< 0.1	< 0.1	< 0.1	< 0.1	< 0.1	< 0.1
4-chlorophenol	< 0.1	< 0.1	< 0.1	< 0.1	< 0.1	< 0.1	< 0.1	< 0.1	< 0.1
2,4,6-trichlorophenol	< 0.1	< 0.1	< 0.1	< 0.1	< 0.1	< 0.1	< 0.1	< 0.1	< 0.1

Table 10. Results (μg/L) of the analysis for the determination of phenol and chlorophenols.

This presence might be attributable to the use of synthetic tannins, which are widely used in the tanning industry as tanning agents in vegetal tanning, as re-tanning agents in chrome tanning and as auxiliaries in dyeing. It is hypothesized that the biological oxidation of these synthetic tannins produces an increase in the simpler phenolic substances. The presence of phenolic compounds acts as inhibitors for the development and growth of bacterial flora, thus causing an increase in global COD [16-17].

The concentrations of the alkylphenols and ethoxylated alkylphenols, such as phenol and chlorophenols are extremely low, such as not to justify the high COD values. Therefore, these values are probably to be attributed to the presence of polyphenolic substances.

To verify this hypothesis a real matrix was reconstructed. starting from a wastewater of domestic origin which different volumes of a known concentration solution containing tannic acid, pyrogallic acid, coumaric acid, vanillic acid and caffeic acid were added to. After each addition, the COD and TOC were determined. The results show an increase in the concentration of COD and TOC as the total concentration of polyphenol compounds increases (Table 11).

Volume (ml)	Total Polyphenols	COD	TOC
0.05	0.125	30.9	1.3
0.1	0.25	31.6	1.9
0.25	0.625	34.2	2.7
0.5	1.25	39.8	2.8
1	2.5	39.9	2.9
2	5	44.8	3.2
5	12.5	48.5	3.8
10	25	70.9	4.7
15	37.5	161	10.6
20	50	178	13.2
40	100	254	17.1
50	125	370	19.3
100	250	537	20.3

Table 11. Results (mg/l) of COD and TOC at different concentrations of total polyphenols.

These parameters were compared using Pearson's correlation at the $p < 0.05$ significance level. The results indicated that the COD and Total

polyphenols concentration were in correlation with r ≃1.00 and $p < 0.05$ (Fig. 7).

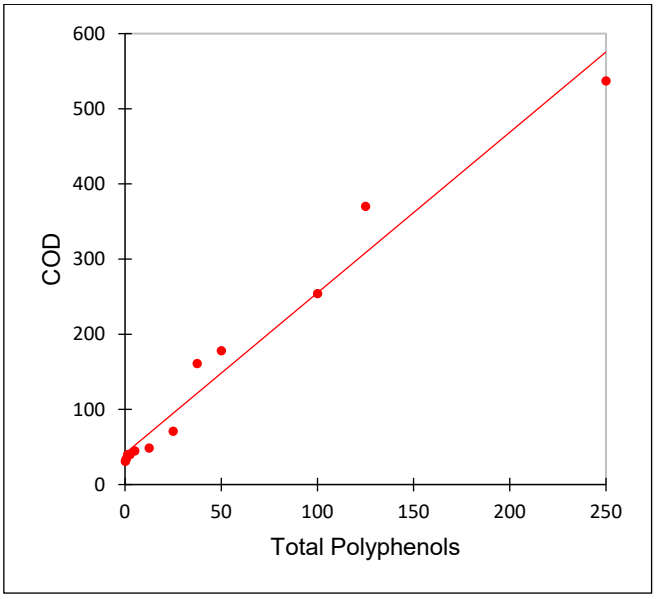

Figure 7. Pearson correlation diagram, with values of r≃1,00 and $p < 0.05$.

The screening analysis conducted by MALDI-TOF/TOF of the first 5 samples only, showed the presence of polyphenolic substances.

The MALDI spectra of all samples except sample n°3 show the abundance of the same peaks.

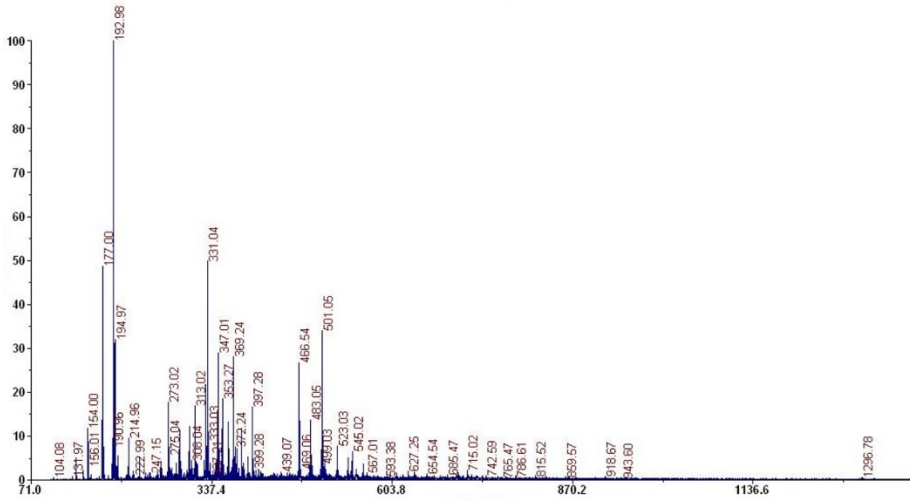

Figure 8. MALDI TOF/TOF mass spectrum of sample n°1,2,4, and 5. Details of 70-1500 m/z.

Figure 8 shows the presence of peaks attributable to the presence of tannic compounds, in particular the mass peaks at 177 m/z and 215 m/z. In fact, the mass peaks at 177 m/z, 253m/z, 329m/z, 359 m/z and 391 m/z, are typical for phenol–formaldehyde oligomers, while the mass 215 m/z, 245 m/z, 407 m/z indicates urea–formaldehyde oligomers [19,20]. In the MALDI mass spectrum of sample n°3 (Figure 9) there are not evident peaks attributable to the presence of polyphenolic substances.

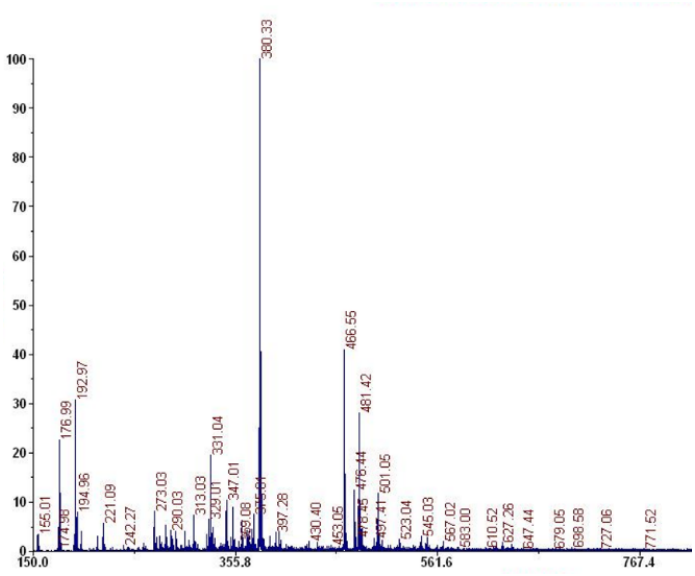

Figure 9. MALDI TOF/TOF mass spectrum of sample n°3. Details of 70-780 m/z.

4. Conclusion

The result of the chemical analyzes carried out on wastewater, by several companies after the treatment plants, have shown limit values above the law for the parameters, such as chlorides, sulphates, and COD. The analysis of emerging organic contaminants, such as phenols, chlorophenols, alkylphenols and ethoxylated alkylphenols, showed the presence in low concentrations, between 5...10 ug/L of phenol in most of the samples, and the presence of only 4-nonylphenol diethoxylate in concentrations just above the limit of quantification of 0.5 ug/L. These concentrations cannot justify the high COD values. From the reconstruction of a real matrix containing polyphenols, the results

indicated that the COD and total polyphenols concentration were correlation with $r \simeq 1.00$ and $p < 0.05$ Therefore these values are probably to be attributed to the presence of polyphenolic substances. From a first initial study of 5 samples by MALDI TOF / TOF analysis they showed the presence of 177 m / z, 215 m / z mass peaks which could be attributable to the use of synthetic tannins based on phenol, formaldehyde, and urea. Further analyzes are needed, with different techniques, for more insights.

5. References

1. Decreto Legislativo 3 aprile **2006**, n.152, *testo unico ambientale.*
2. Lofrano, G.; Meriç, S.; Zengin, G.E.; Orhon, D. Chemical and Biological Treatment Technologies for Leather Tannery Chemicals and Wastewaters: A Review. Science of The Total Environment **2013**, 461–462, 265–281, doi:10.1016/j.scitotenv.2013.05.004.
3. Archibald, F.; Roy-Arcand, L.; Méthot, M.; Valeanu, L. Recalcitrant Organic Compounds (Chemical Oxygen Demand Sources) in Biologically Treated Pulp and Paper Mill Effluents: Their Fate and Environmental Impact in Receiving Waters. Water Environment Research **1998**, 70, 1314–1326.
4. Bharagava, R.N.; Saxena, G.; Mulla, S.I.; Patel, D.K. Characterization and Identification of Recalcitrant Organic Pollutants (ROPs) in Tannery Wastewater and Its Phytotoxicity Evaluation for Environmental Safety. Arch Environ Contam Toxicol **2018**, 75, 259–272, doi:10.1007/s00244-017-0490-x.
5. Bardi, A.; Yuan, Q.; Tigini, V.; Spina, F.; Varese, G.C.; Spennati, F.; Becarelli, S.; Di Gregorio, S.; Petroni, G.; Munz, G. Recalcitrant Compounds Removal in Raw Leachate and Synthetic Effluents Using the White-Rot Fungus Bjerkandera Adusta. Water **2017**, 9, 824, doi:10.3390/w9110824.
6. Padilla-Sánchez, J.A.; Plaza-Bolaños, P.; Romero-González, R.; Barco-Bonilla, N.; Martínez-Vidal, J.L.; Garrido-Frenich, A. Simultaneous Analysis of Chlorophenols, Alkylphenols, Nitrophenols and Cresols in Wastewater Effluents, Using Solid Phase Extraction and Further

Determination by Gas Chromatography–Tandem Mass Spectrometry. Talanta **2011**, 85, 2397–2404, doi:10.1016/j.talanta.2011.07.081.

7. He, Q.; Yao, K.; Sun, D.; Shi, B. Biodegradability of Tannin-Containing Wastewater from Leather Industry. Biodegradation **2007**, 18, 465–472, doi:10.1007/s10532-006-9079-1.
8. Kalyanaraman, C.; Kameswari, K.S.B.; Rao, J.R. Studies on Enhancing the Biodegradation of Tannins by Ozonation and Fenton's Oxidation Process. Journal of Industrial and Engineering Chemistry 2015, 25, 329–337, doi:10.1016/j.jiec.2014.11.012.
9. Spier, F.; Gutterres, M. BIODEGRADATION OF ACACIA AND CHESTNUT TANNINS BY NATIVE ISOLATES OF THE GENUS Penicillium AND Aspergillus. Braz. J. Chem. Eng. **2019**, 36, 753–761, doi:10.1590/0104-6632.20190362s20180340.
10. APAT, IRSA CNR Manuali e Linee Guide n°29 del **2003**.
11. Bressi G., Signoroni F. "Caratteristiche e trattamento del percolato" in "Scarico controllato" a cura di Cossu R., de Fraia Frangipane E., C.I.P.A. Editore, **1995**, pp.139-187.
12. Shimadzu, User's Manual TOC-V Analyzer, **2014**.
13. The Fitness for Purpose of Analytical Methods: A Laboratory Guide to Method Validation and Related Topics; **2014**; ISBN 978-91-87461-59-0.
14. UNI-EN-ISO 17070 Determinazione del contenuto di tetraclorofenolo, triclorofenolo, diclorofenolo, isomeri di monoclorofenolo e di pentaclorofenolo, **2015**
15. UNI-EN-ISO 18857 Determinazione di alchilfenoli selezionati - Parte 2: Determinazione gascromatografica- spettrometria di massa di alchilfenoli, dei loro etossilati e bisfenolo A in campioni non filtrati e seguente estrazione in fase solida e derivatizzazione, **2002**

16. Ummarino G., Iacomino P. (**1985**), Biodegradabilità dei tannini di sintesi, Cuoio Pelli Materie Concianti – Napoli, 10793.
17. Ummarino G., Russo A. (**1984**), Biodegradabilità di tannini naturali e sintetici, Cuoio Pelli Materie Concianti – Napoli, 9742.
18. Puig, D.; Barceló, D. Comparison of Different Sorbent Materials for On-Line Liquid-Solid Extraction Followed by Liquid Chromatographic Determination of Priority Phenolic Compounds in Environmental Waters. Journal of Chromatography A **1996**, 733, 371–381, doi:10.1016/0021-9673(95)01136-6.
19. Schrod, M.; Rode, K.; Braun, D.; Pasch, H. Matrix-Assisted Laser Desorption/Ionization Mass Spectrometry of Synthetic Polymers. VI. Analysis of Phenol–Urea–Formaldehyde Cocondensates. Journal of Applied Polymer Science **2003**, 90, 2540–2548, doi:10.1002/app.12989.
20. Du, G.; Lei, H.; Pizzi, A.; Pasch, H. Synthesis–Structure–Performance Relationship of Cocondensed Phenol–Urea–Formaldehyde Resins by MALDI-ToF and 13C NMR. Journal of Applied Polymer Science **2008**, 110, 1182–1194, doi:10.1002/app.28735.

Chapter 3 – Characterization of the vegetal and synthetic tannins

1. Introduction

Vegetal tanning is the oldest type of tanning; indeed, it exploits natural substances and extracts present in the bark of different plants and also fruits or leaves also. In olden times, tanning was carried out by immersing the hides into solutions containing bark or leaves for several months but, in the modern tanning industry, both natural and synthetic extracts are used, allowing a much faster penetration into the leather. The quantities of tannins used are considerably higher than those used for chrome tanning, about 10% in weight than the leather, and they can also be used up to 50% in mass on the tanned leather or on most of used re-tanning agents (about 80%).

1.1. Vegetal tannins

Vegetal tannins originate from some parts of plants such as, for example, the bark (mimosa), the leaves (sumac), the branches (chestnut) and even the fruits (myrobalan). The extraction of these natural substances takes place very easily by treating the chopped parts of the plant with simple water and by leaching them counter current. Afterwards, an "atomization" of the tannic extracts is carried out in order to transform them into powders which can be traded more easily. The substances thus

obtained can generally be defined as polyphenols although these extracts have a high complexity as vegetal tannins are made up using a large quantity of chemical compounds, about 1000, whether they are tanning agents or not. In fact, the extracts contain chemicals called "non-tannins" and they consist of organic salts, weak organic acids and sugars, which do not react directly with collagen, but their presence markedly influences the tanning action of tannins. The extracts obtained from the extraction of vegetal tannins show a brown color, which indicates a partial oxidation of the phenolic nuclei into Quinone nuclei and this event seems to benefit the tanning process, exposing the extracts to air and light showing a gelatin precipitation, index to be higher than those ones of the same liqueurs left in dark conditions and in nitrogen current. The precipitation index is in close correlation with the molecular size of the tannins and, therefore, an increase in the size of the tanning molecules emerges.

From a chemical point of view, natural tannins are classified into two categories:

• Hydrolyzable tannins, the benzene nuclei are joined together through ester bonds

• Condensed tannins in which benzene rings are linked by C-C atoms

Hydrolyzable tannins are molecules that are easily hydrolyzed by acids, bases, enzymes, and heat. The hydrolysable tannins are divided into: gallotannins (figure 1); which by hydrolysis form gallic acid and sugars, and ellagitannins (figure 2) which by hydrolysis release ellagic acid, monosaccharides, and phenolic compounds.

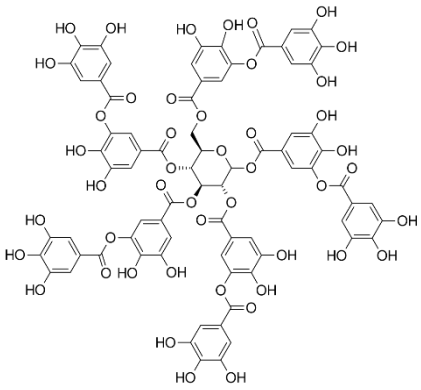

Figure 1. Example of a gallotannin: tannic acid.

Only gallotannins exhibit tanning properties they own at least three galloyl residues per glucose molecule. Compounds of the flavonoid type, coumarins, stilbenes and esters are present in the extracts of hydrolysable tannins. Although these substances do not have tanning properties, they improve the quality of the skin as they tend to increase the solubility of high molecular weight tannins and to reduce the reactivity of collagen by binding weakly to it; in effect, they initially help the tanning process by facilitating the penetration of the tanning agent by limiting cross-linking.

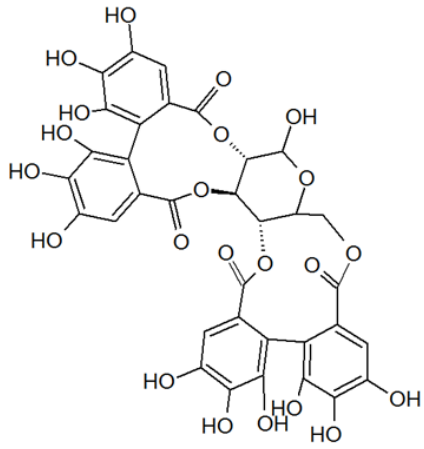

Figure 2. Example of ellagitannin: peduncolagina found in oak extracts.

The condensed tannins are made up of monomers connected by carbon-carbon bonds which in the presence of acids do not hydrolyze as, in contrast, they tend to polymerize leading to the formation of large aggregates: phlobaphenes. Condensed tannins have a much more complex structure than the hydrolysable tannin ones and, for this reason, they are much less known and studied.

The condensed tannins can be divided into two classes: the catechenic tannins and the stilbenic tannins. The best-known condensed tannins are quebracho, mimosa, mangrove, gambier and catechu [1,2].

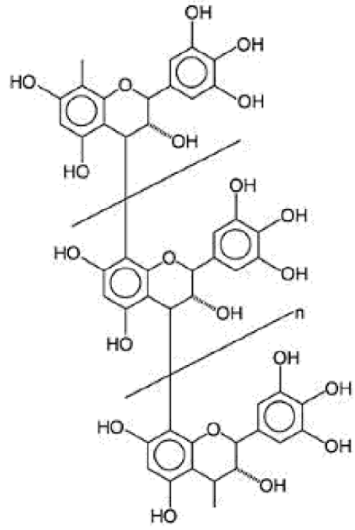

Figure 3. Example of condensed tannin of mimosa bark.

1.2. Synthetic tannins

Synthetic tannins or syntanes are organic compounds obtained from the condensation of aromatic substances such as phenol, naphthol, catechol, using formaldehyde, appositely sulphonated. The sulfonation process can take place before or after the condensation one. Figure 4 A and B shows a typical condensation process. Although the structure of these molecules is quite different from natural tannins, they have an evident reactivity towards collagen and therefore they can be used in the tanning and re-tanning process.

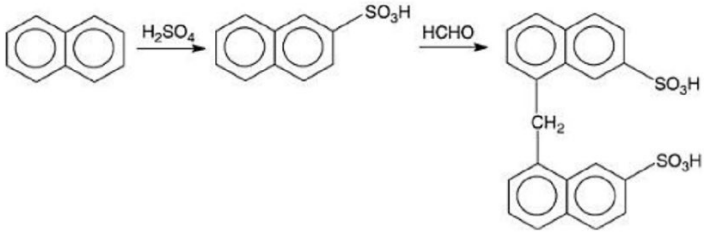

Figure 4 A. Nerodol Synthesis: sulfonation, then polymerisation.

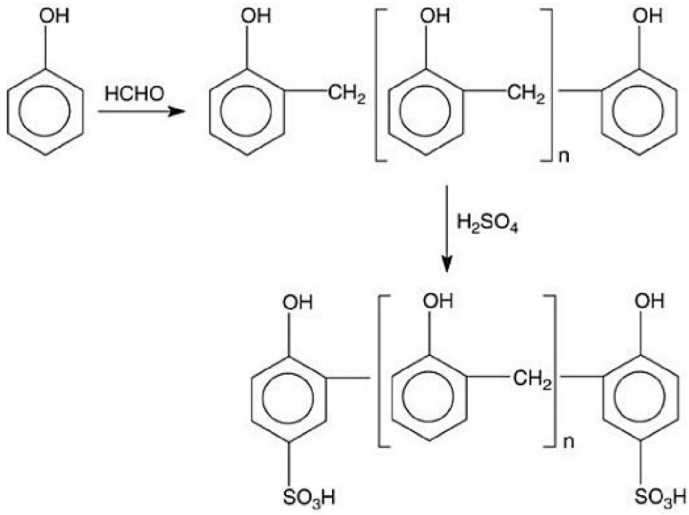

Figure 4 B. Novolak Synthesis: polymerisation, then sulfonation

The syntanes can be divided into two classes according to their actual qualities: auxiliary and substitution tannins.

The auxiliary syntanes consist mainly of sulphonated naphthalene nuclei, condensed with formaldehyde. Their main property is to act as dispersants; in fact, they are used together with other particularly astringent vegetal tannins such as oak or quebracho, in order to improve their qualities leading to an

excellent dissolution of molecules with a higher molecular weight (such as phlobaphenes), thus helping the dispersion in the dermis that precedes the fixation phase. The tannins for substitution have characteristics more similar to those from natural tannins having phenolic structures condensed with formaldehyde. They are called in this way because they are needed to replace vegetable tannins, although used only in the re-tanning and pre-tanning phases of the leathers. They are mainly utilized because they provide a white leather, which however tends to yellow over time.

2. Materials and methods

Chemical characterization by MALDI-TOF/TOF and LC-MS/MS analysis was performed on three extracts of mimosa, chestnut and tara (Soft Retan Ta extra) vegetal tannins; three synthetic tannins, two of these based on 4,4' dihydroxyphenylsulfone (Whitan RSD, Whitan White Conc) and the third one represents a condensation product of uric acid, formaldehyde and phenol (Syncotan CBN). All the analyzed tannins are commercial products mostly used in the tanning process and they were supplied by the company BiagioSiani, Italy.

About 10 mg of sample were dissolved in 5 ml of methanol and placed in an ultrasonic bath.

For MALDI TOF/TOF analysis, experiments were performed on a 5800 MALDI-time of flight (TOF)/TOF AB SCIEX equipped with a nitrogen laser (337 nm) (AB SCIEX, Milan, Italy). The tannins were solubilized in MeOH with a solution

of 20 mg/ml 2,5-dihydroxybenzoic acid (DHB, Sigma Aldrich, Milan, Italy). For identification, MS and tandem MS (MS/MS) spectra were acquired in positive reflection mode, by using a mass range of 100–4000 m/z.

LC-MS/MS analysis was performed using using a LC Eksigent with a column Halo C18 (2.7 μm 90A 1 × 50 mm) at a temperature of 38°C. Eluent A was H2O and 0.1% CH3COOH, whereas eluent B was a solution on 50% ACN, 50% isopropanol, and 0.1% CH3COOH. Gradient conditions were as follows: time 0 min, 20% eluent B; time 4 min 90% eluent B; time 4.5 min 20% eluent B; time 5 min 20% eluent B. The injection volume was 5 μl, and the flow rate was fixed to 40 μl/min. The mass spectrometer used is a 4000 QTRAP® of AB SCIEX; this system includes a hybrid triple-quadrupole linear ion trap (LIT) designed for qualitative analyzes. The study was carried out in MRM mode, typical "scan type," with an electrospray ionization (ESI) source. Precursor ions were scanned in negative mode

3. Results and discussion

3.1 Synthetic Tannins

The MALDI spectrum of synthetic tannins (Figure 5.) showed a series of peaks at m/z 535, m/z 797 and m/z 1059, corresponding at the sodiated forms of dimer, trimer and tetramer of the polycondensation reaction of 4,4' dihydroxyphenylsulfone with formaldehyde. However smaller

mass peaks are also observed at m/z 1321 and m/z 1583, which correspond to pentamer and hexamer [3].

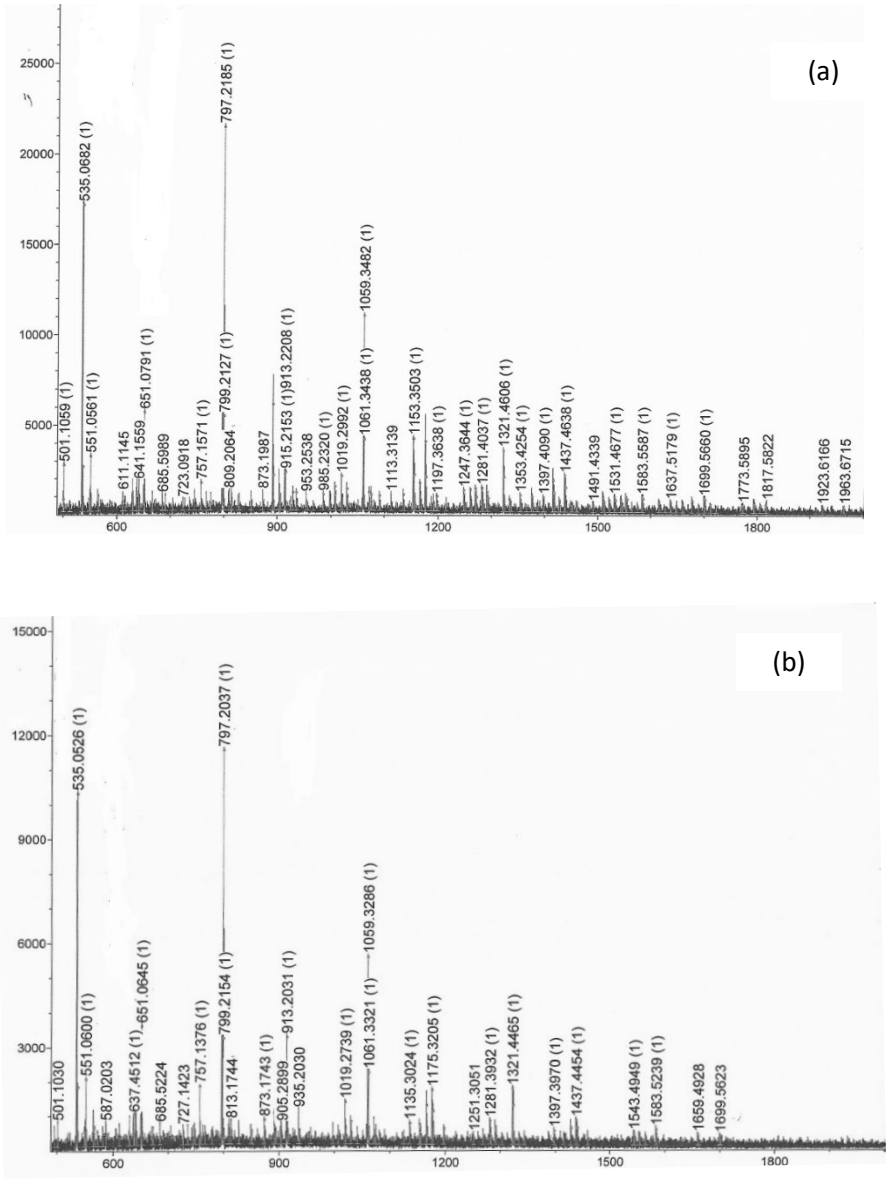

Figure 5. MALDI TOF/TOF mass spectrum of Whitan RSD (a) and Whitan White Conc (b). Details of 500-2000 m/z.

The Syncotan CBN is a resin formulated through the condensation of formaldehyde (F) urea (U) and phenol (P). The mass spectrum (Figure 6) showed the presence of three types of oligomers, urea–formaldehyde (UF) species, phenol–formaldehyde (PF) species, and mixed co-condensed phenol–urea–formaldehyde (PUF) species. These oligomers have different chemical compositions and different degrees of polymerization.

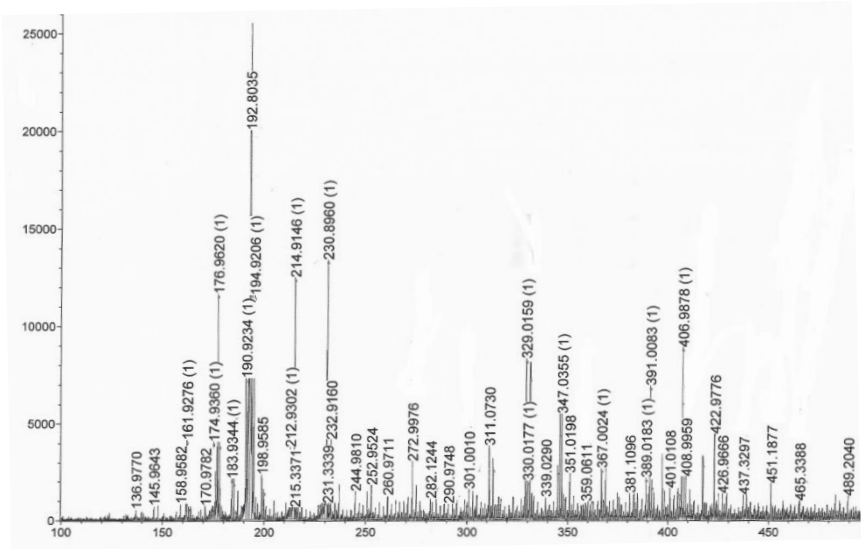

Figure 6. MALDI- TOF/TOF mass spectrum of Syncotan CBN. Details of 100-500 m/z.

The mass peaks at m/z 177, m/z 253, m/z 329, m/z 359 and m/z 391, are typical for phenol–formaldehyde oligomers, while the mass m/z 215, m/z 245, m/z 407 indicate urea–formaldehyde oligomers. Finally, the mass peaks at m/z 261, m/z 291 and m/z 351 correspond to different condensation oligomers between phenol, urea and formaldehyde [4,5]. The

complete assignment of all oligomer peaks in the spectrum is given in Table 1.

Peak	P_x	U_y	F_z
177	1	-	2
253	2	-	2
329	3	-	2
359	3	-	3
391	3	-	4
215	-	2	3
245	-	2	4
407	-	3	8
261	1	2	2
291	1	2	3
351	1	2	5

Table 1. Assignment of the peaks $[M+Na]^+$ in the MALDI - TOF/TOF for Phenol-Formaldehyde (P_xF_z), Urea – Formaldehyde (U_yF_z) and cocondensates Phenol-Urea-Formaldehyde ($P_xU_yF_z$). X, Y and Z indicate molecules of phenol, urea and formaldehyde in the respective oligomers.

3.2 Vegetal Tannins

Soft Retan Ta Extra tannins (tara tannins) are extracted from the tare and the MALDI spectrum shown in the figure 7.

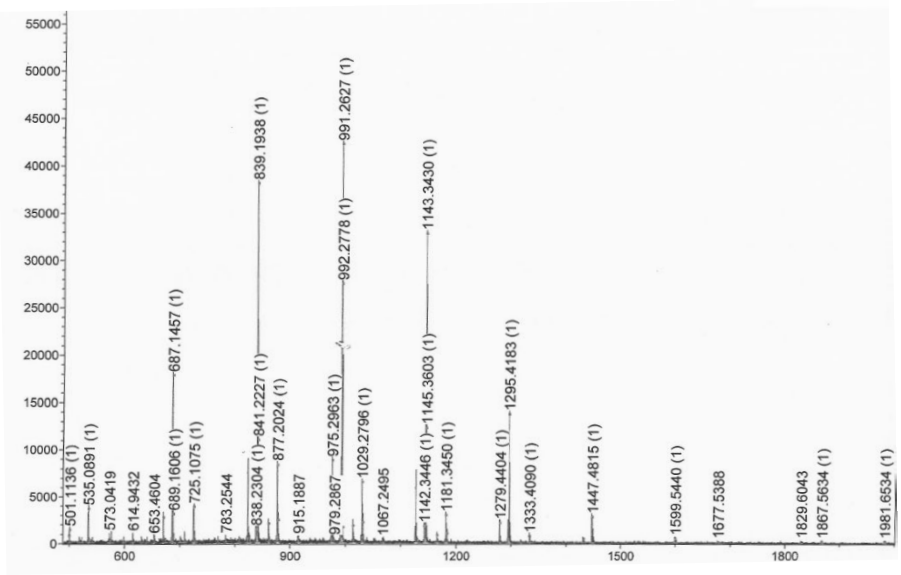

Figure 7. MALDI- TOF/TOF mass spectrum of Soft Retan Ta Extra. Details of 500-2000 m/z.

MALDI analysis revealed the presence of polymers formed by glucose units combined with gallic acid units. Mass peaks m/z 687, m/z 839, m/z 991, m/z 1143, m/z 1295, m/z 1447, m/z 1599 were found which differ from each other by exactly m/z 152, corresponding to a monomer unit of gallic acid (AcGAL). The proposed structure for the ion of mass m/z 839 is depicted in the Figure 8 [6].

The masses of peaks formed by two units of glucose (GLC) joined to monomers of gallic acid were recognized. The complete assignment is shown in Table 2.

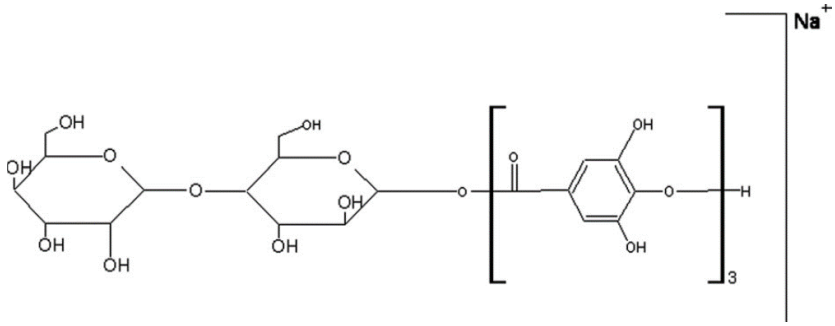

Figure 8. Proposed structure for the trimer at m/z 839.

Peak	Description M+Na$^+$
687	GCL_2 + $AcGAL_2$
839	GCL_2 + $AcGAL_3$
991	GCL_2 + $AcGAL_4$
1143	GCL_2 + $AcGAL_5$
1295	GCL_2 + $AcGAL_6$
1447	GCL_2 + $AcGAL_7$
1599	GCL_2 + $AcGAL_8$

Table 2. Assignment of the peaks [M+Na]$^+$ in the MALDI - TOF/TOF for Glucose-Gallic Acid (GCL_xAcGAL_y),. X, and Y indicates molecules of glucose and gallic acid in the respective oligomers.

The most interesting result of the chestnut tannins is the spectrum obtained by MALDI TOF/TOF showed in Figure 9 (a), (b) and (c). Different patterns are present. In Figure 9 (a) there are two known peaks which are that at m/z 302 and m/z

483, which correspond respectively either to an ellagic acid residue or to a digallic acid residue but, furthermore, they could also correspond to a residue of ellagic acid or digallic acid linked to a glucose [7].

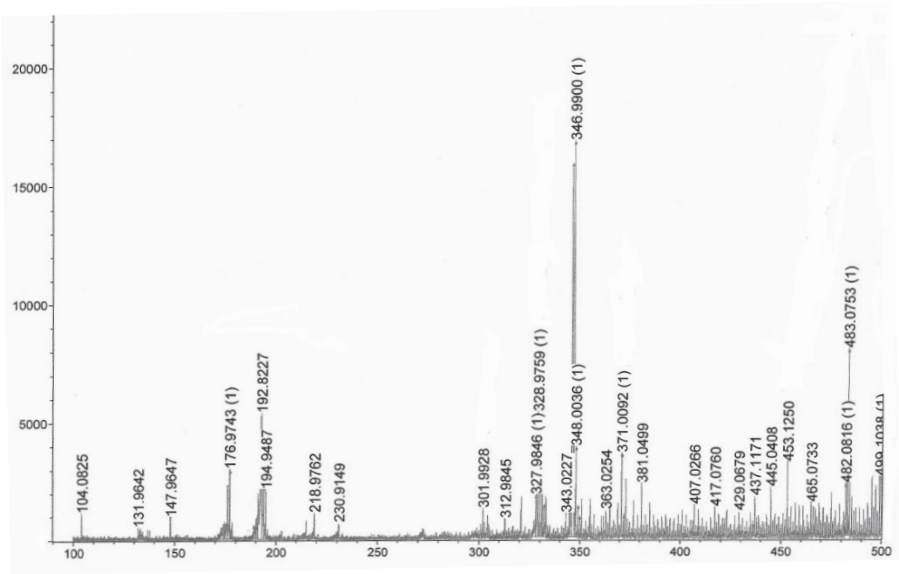

Figure 9a. MALDI- TOF/TOF mass spectrum of Chestnut tannins. Details of 100-500 m/z.

Figure 9(b) shows the presence of m/z 655 and m/z 671 peaks, obtained from the m/z 958 and m/z 973, through a loss of an ellagic acid structure (-302). The major peaks at m/z 957 and m/z 973 are, respectively, the m/z 935 castalagin or pentagalloylglucose, which a C-O-C grouping has been added to (the structure proposed by Pasch is represented in Figure 10), and a m/z 935 to which (m/z 973), again, a C-O-C remains attached and an –OH has been subtracted (957 m/z). The peak

at m/z 1125 corresponds at peak m/z 973 which a molecule of gallic acid is attached to. [8].

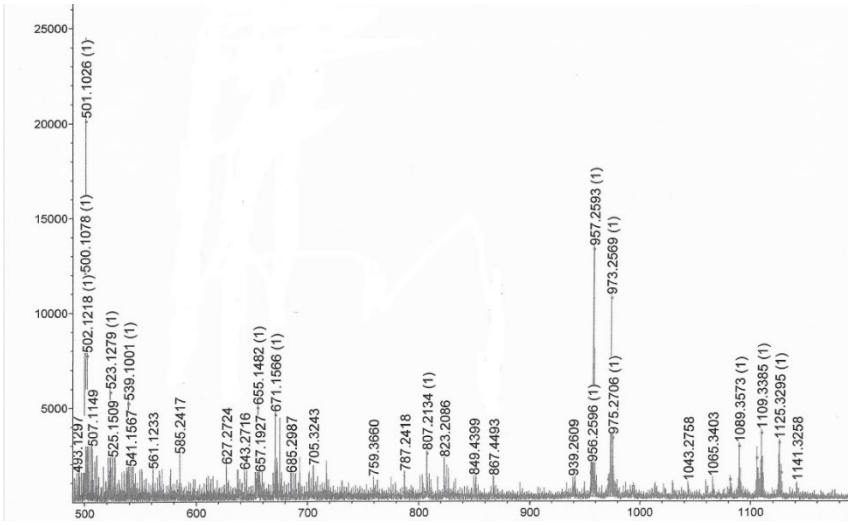

Figure 9b. MALDI- TOF/TOF mass spectrum of Chestnut tannins. Details of 500-1200 m/z.

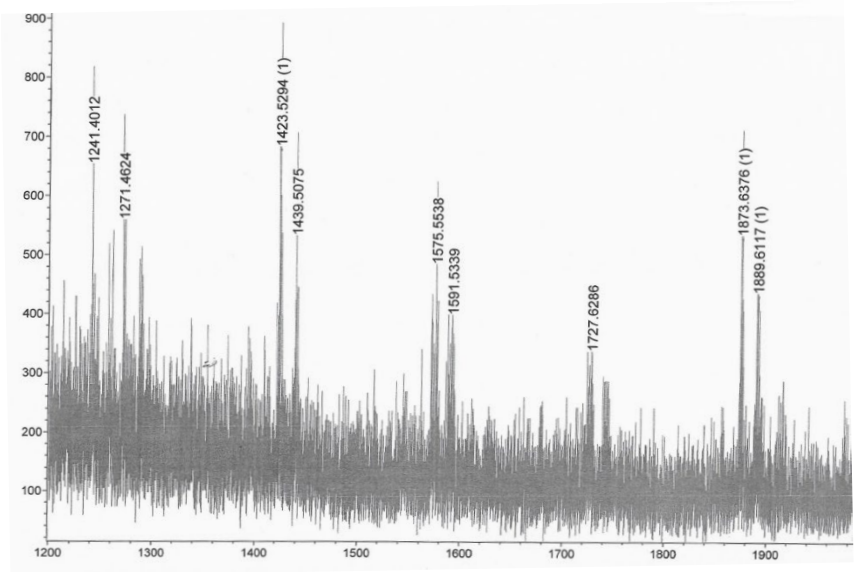

Figure 9c. MALDI- TOF/TOF mass spectrum of Chestnut tannins. Details of 1200-2000 m/z.

In figure 9(c) shows the precence of the other pattern. The peak at m/z 1439 corresponds to castalagin bound, linked to nonahydroxytriphenic through a single ester bond. The series continue with the peak at m/z 1592, which have a mass increment of m/z 152, indicating galloyl units [6].

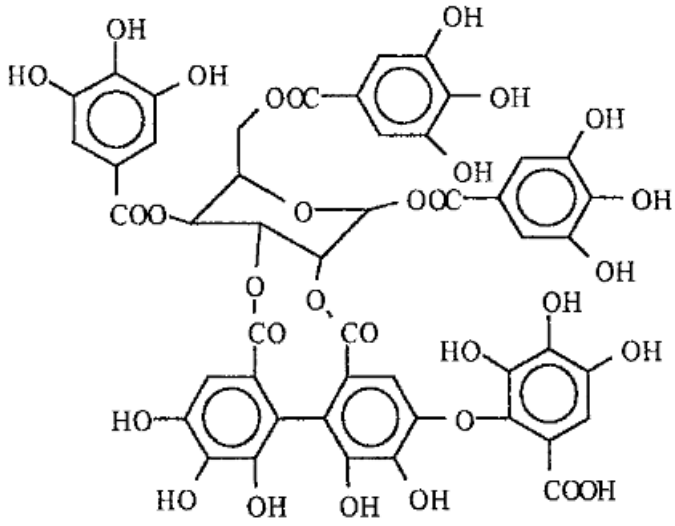

Figure 10. Structure proposed for 974 m/z peak.

Mimosa spectra (Figure 11) shows the degree of polymeritazion of the building units and oligomers series with masses of the repeat unit of m/z 288 and m/z 304. For each oligomer, there is a substructure with mass increment of m/z 16, indicating different combination of different substructure.

Mimosa is mainly based on combination of three different type unit, at different masses which we call A (m/z 272), B (m/z 288) and C (m/z 304) respectively and they are represented in Figure 12. The complete assignment of the peaks is shown in the Table 3 [9,10].

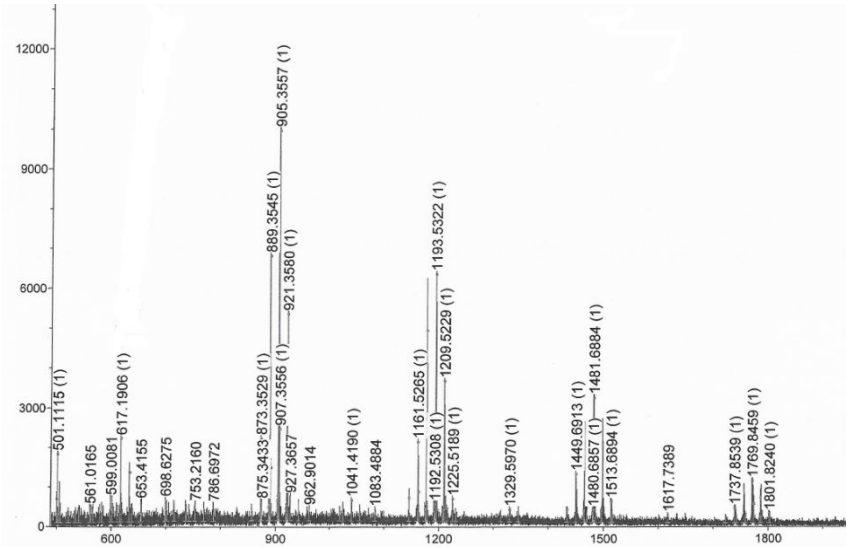

Figure 11. MALDI- TOF/TOF mass spectrum of Mimosa tannins. Details of 500-2000 m/z.

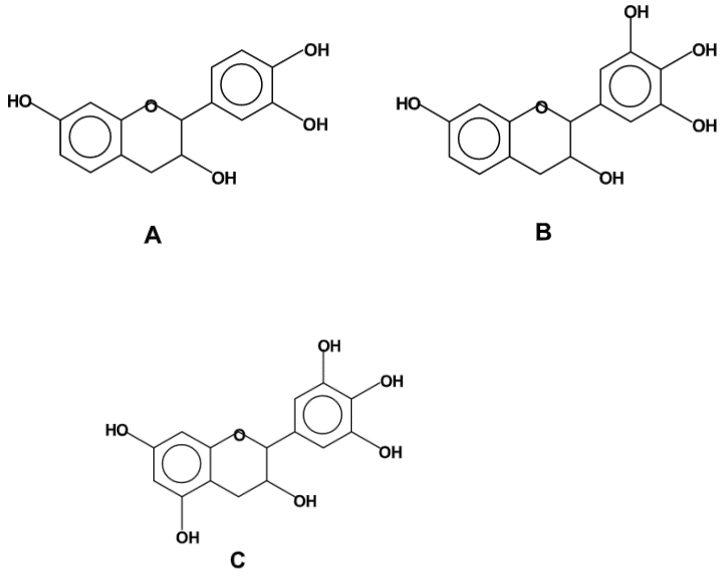

Figure 12. Structure of units of mass, 272m/z (A), 288 m/z (B) and 304 m/z (C)

	Unit Type		
Peak	**A**	**B**	**C**
Trimers			
889	1	1	1
889	-	3	-
905	-	2	1
905	1	-	2
921	-	1	2
Tetramers			
1161	1	3	-
1161	2	1	1
1193	-	3	1
1193	1	1	2
1209	-	2	2
1209	1	-	3
Pentamers			
1449	1	4	-
1449	2	2	1
1481	1	2	2
1481	-	3	1
Hexamers			
1737	1	5	-
1737	2	3	1
1769	1	3	2
1769	-	4	1

Table 3. Assignment of the peaks $[M+Na]^+$ in the MALDI - TOF/TOF spectra for mimosa tannin.

In mimosa the predominant repeating units of 288 m/z, that is type B unit. Furthermore, the presence of the trimer is more evident.

3.3 Preliminary characterization of polyphenolic compounds by LC-M/MS

Six samples of both vegetal and synthetic tannins were analyzed by LC-MS / MS. A semi quantitative approach was used to evaluate the content of polyphenols in the MRM method. The results of the analyses on the vegetable and synthetic tannins samples show the presence of different classes of compounds such as: anthocyanidin, flavonol-3-ol, flavonones, flavon and flavonol. The results obtained are reported in the Tables 4 and 5.

	Vegetable Tannins		
Molecule	**Chestnut**	**Mimosa**	**Soft Retan (Tara)**
Delphinidin diglucoside	735	425	1775
Delphinidin-3-O-glucoside	26605	5290	5085
Cyanidin-3-O-glucoside	560	2465	2480
Delphinidin-3-O-arabinoside	100	545	< 0.5
Petunidin-3-O-glucoside	600	265	< 0.5
Cyanidin-3-O-arabinoside	< 0.5	1870	20
Pelargonidin-3-O-glucoside	< 0.5	1995	1535
Petunidin-3-O-arabinoside	< 0.5	345	< 0.5
Peonidin-3-O-glucoside	735	11685	< 0.5
Malvidin-3-O-glucoside	1060	4585	< 0.5
Malvidin-3-O-arabinoside	640	< 0.5	< 0.5
Delphinidin rutinoside	360	< 0.5	1860
Naringin	630	4520	6900
Apigenin	870	< 0.5	385
Quercetin-3-glucoside	26060	4910	4695
Procyanidin B1	< 0.5	6600	265
Catechin	< 0.5	15425	< 0.5
Epicatechin	400	5020	330
Caffeine	2060	5615	4130
EGC 3-gallate	< 0.5	1505	2545
Gallocatechin	315	670	495
GC 3-gallate	< 0.5	1630	2180
Syringic acid	1035	< 0.5	< 0.5
Quercetin	12250	< 0.5	1575
Chlorogenic acid	575	1035	815
Quercetin-3-O-rhamnoside	1640	3115	615
Valoneic acid dilactone	47485	< 0.5	< 0.5
Phloretin	1630	2060	2910
Phloridzin	< 0.5	5020	< 0.5
Myricetin	1360	< 0.5	3440
Kaempferol	< 0.5	< 0.5	8315
Rutin	< 0.5	< 0.5	1830
Procyanidin C	< 0.5	3180	< 0.5

Table 4. Concentration in ng/g of different polyphenolic compounds in vegetable tannins by LC-MS/MS.

	Synthetic Tannins		
Molecule	Whitan RSD	Whitan White	Syncotan CBN
Delphinidin diglucoside	< 0.5	60	< 0.5
Cyanidin-3-O-glucoside	< 0.5	< 0.5	< 0.5
Delphinidin-3-O-arabinoside	60	2830	< 0.5
Petunidin-3-O-glucoside	100	< 0.5	< 0.5
Cyanidin-3-O-arabinoside	130	925	20
Pelargonidin-3-O-glucoside	< 0.5	495	< 0.5
Petunidin-3-O-arabinoside	< 0.5	27590	< 0.5
Malvidin-3-O-arabinoside	< 0.5	7630	< 0.5
Delphinidin rutinoside	< 0.5	< 0.5	< 0.5
Malvidin 3-O-p-coumaroylglucoside	< 0.5	< 0.5	< 0.5
Naringin	< 0.5	< 0.5	< 0.5
Flavone+Na	< 0.5	< 0.5	< 0.5
Apigenin	< 0.5	< 0.5	< 0.5
Quercetin-3-glucoside	< 0.5	225	< 0.5
Procyanidin B1	170	210	170
Epicatechin	535	100	1020
Caffeine	5860	4140	7225
EGC 3-gallate	830	< 0.5	765
Gallocatechin	680	385	1155
GC 3-gallate	860	< 0.5	440
Gallic acid	< 0.5	< 0.5	< 0.5
Syringic acid	< 0.5	< 0.5	< 0.5
6-Malonyldaidzin	< 0.5	< 0.5	< 0.5
Quercetin	1090	< 0.5	235
Chlorogenic acid	< 0.5	< 0.5	< 0.5
Quercetin-3-O-rhamnoside	980	10305	< 0.5
Valoneic acid dilactone	< 0.5	< 0.5	< 0.5
Myricetin	< 0.5	45	< 0.5
Procyanidin C	< 0.5	170	< 0.5

Table 5. Concentration in ng/g of different polyphenolic compounds in synthetic tannins by LC-MS/MS.

4. Conclusion

Synthetic and vegetal commercial tannins can be analysed by MALDI–TOF/TOF with DHB used as matrices. The MALDI spectrum shows the oligomer distribution and from each the oligomer masses, the degree of polymerization can be determined. The oligomer peaks appear as $[M+Na]^+$ molecular ions. The MALDI spectrum of synthetic tannins, for Whitan RSD and Whitan White Conc, showed the presence of dimer, trimer and tetramer of the polycondensation reaction of 4,4' dihydroxyphenylsulfone with formaldehyde. Syncotan CBN spectrum showed the presence of different condensation oligomers between phenol, urea and formaldehyde.

Tara and chestnut tannins are characterized by hydrolyzable tannins consisting mainly of units of gallic acid condensed with units of glucose. But the MALDI spectrum of chestnut tannins shows the presence also of ellagic acid units combined with glucose units. The MALDI spectrum of mimosa tannins are much more complex. Mimosa is mainly based on combination of three different type unit, at different masses, which we call A (272 m/z), B (288 m/z) and C (304 m/z), which combined give origin to different combinations of oligomers, with different degree of polymerization.

5. References

1. Sammarco, U.; Tecnologia conciaria, Milano, Editma casa editrice, **2007**.
2. Manzo, F.; Chimica e tecnologia del cuoio, Media Service Ed., 1999.
3. Giovando, S.; Pizzi, A.; Pasch, H.; Rode, K. Synthetic Tannins Structure by MALDI-TOF Mass Spectroscopy. Journal of Applied Polymer Science **2009**, 114, 1339–1347, doi:10.1002/app.30667.
4. Schrod, M.; Rode, K.; Braun, D.; Pasch, H. Matrix-Assisted Laser Desorption/Ionization Mass Spectrometry of Synthetic Polymers. VI. Analysis of Phenol–Urea–Formaldehyde Cocondensates. Journal of Applied Polymer Science **2003**, 90, 2540–2548, doi:10.1002/app.12989.
5. Du, G.; Lei, H.; Pizzi, A.; Pasch, H. Synthesis–Structure–Performance Relationship of Cocondensed Phenol–Urea–Formaldehyde Resins by MALDI-ToF and 13C NMR. Journal of Applied Polymer Science **2008**, 110, 1182–1194, doi:10.1002/app.28735.
6. Radebe, N.; Rode, K.; Pizzi, A.; Giovando, S.; Pasch, H. MALDI-TOF-CID for the Microstructure Elucidation of Polymeric Hydrolysable Tannins. Journal of Applied Polymer Science **2013**, 128, 97–107, doi:10.1002/app.38156.
7. Pizzi, A.; Pasch, H.; Rode, K.; Giovando, S. Polymer Structure of Commercial Hydrolyzable Tannins by Matrix-Assisted Laser Desorption/Ionization-Time-of-Flight Mass Spectrometry. Journal of Applied Polymer Science **2009**, 113, 3847–3859, doi:10.1002/app.30377.
8. Pasch, H.; Pizzi, A. Considerations on the Macromolecular Structure of Chestnut Ellagitannins by Matrix-Assisted Laser Desorption/Ionization-Time-of-Flight Mass Spectrometry. Journal of Applied Polymer Science 2002, 85, 429–437, doi:10.1002/app.10618.
9. Pasch, H.; Pizzi, A.; Rode, K. MALDI–TOF Mass Spectrometry of Polyflavonoid Tannins. Polymer **2001**, 42, 7531–7539, doi:10.1016/S0032-3861(01)00216-6.
10. Radebe, N.; Rode, K.; Pizzi, A.; Pasch, H. Microstructure Elucidation of Polyflavonoid Tannins by MALDI-TOF-CID. Journal of Applied Polymer Science **2013**, 127, 1937–1950, doi:10.1002/app.37568.

Part B – Treatments of wastewaters from the tanning industry

Chapter 4 – Advanced Oxidation Processes (APOs): Heterogeneous photodegradation for the abatement of recalcitrant COD

1. Introduction

The wastewater from the tanning industry represents a serious environmental problem for the high concentration of their organic and inorganic pollutants. In the numerous stages of tanning, many compounds are used such as acids, alkalis, chromium salts, tannins, solvents, dyes, oils, resins, synthetic tannins, but they aren't completely fixed on the leather, remaining in the water. The discharged wastewaters are characterized by high values of chemical oxygen (COD) and biochemical oxygen (BOD) , as well as the concentration of sulfate, chloride, heavy metals and different organic substances [1–3].

Conventional tanning process include the use of inorganic tannins, in particular chromium salt and they often generate substances which are dangerous for human health and the environment [4]. In the last few years alternative tanning processes have been developed, defined chrome-free, which replaces the chromium salts with vegetal and synthetic tannins. These tannins have some advantages and disadvantages: on one hand, they are defined as eco-friendly but, on the other hand, they are not degraded by conventional wastewater treatment processes [5,6]. The vegetal and synthetic tannins are also known to be poorly biodegradable, which result from the high values of COD from the tannery wastewater [7,8]. The increase of these compounds in wastewater and the concern about the unknown long-term effects of their accumulation in the environment brought researchers to a growing awareness about the need

to improve existing technologies, in order to develop new strategies for the removal of this new class of pollutants from wastewater. In the last years, studies on advanced oxidation processes (AOPs) have been increasing, in particular the photocatalytic oxidation process applied to the treatment of wastewater from the tanning industry [2,9].

The advanced oxidation processes (AOPs) have attracted great attention in recent years for the development of technologies which could allow the treatment of wastewater. AOP treatment uses strong oxidizing agents (O_3, H_2O_2) and/or catalysts (Fe, Mn,TiO_2) sometimes supported in activity by high-energy radiation, e.g., UV [9].

These processes are all based on the production and utilization of hydroxyl radicals, the most important of which is the hydroxyl radical (·OH). Free radicals are atoms or molecules that have one or more unpaired electrons, such as the superoxide radical ($O_2^{\cdot-}$), hydroperoxyl radical ($HO_2\cdot$) and hydroxyl radical. The latter is highly reactive and it can oxidize and decompose numerous pollutants to CO_2 and inorganic ions, in means of its high standard potential of 2.8 V. Advanced oxidation processes are sequences of chain reactions and they involve the propagation of the root cycle once the radical has been formed [10]. There are numerous methods that lead to the formation of the hydroxyl radical and one of these is photocatalysis and of particular interest is the titanium dioxide TiO_2, used as a semiconductor catalyst.

In reaction 1, irradiating suspensions of titanium dioxide with photons at an energy higher or equal to the band interval of titanium dioxide (3.2 eV), a pair of charge carriers (e^-/h^+) are generated, which in turn it leads to the formation of strongly oxidizing radical species. This happens because, photons lead to the promotion of electrons from the valence band to the conduction band, leaving a lack of electrons.

$$TiO_2 + h\nu \rightarrow e^- + h^+ \ (1)$$

Some couples (e^-/h^+) react with each other (reaction 2), while others reach the surface of the titanium dioxide, reacting with the hydroxyl groups present on the surface (reaction 3), forming adsorbed hydroxyl radicals $\cdot OH_{ads}$, which can leave the surface to form free radicals $\cdot OH_{free}$ (reaction 4).

$$h^+ + e^- \rightarrow \text{heat} \ (2)$$

$$h^+ + \cdot OH_{ads}^- \rightarrow \cdot OH_{ads} \ (3)$$

$$h^+ + H_2O \rightarrow H_2O^+ \rightarrow H^+ + \cdot OH_{free} \ (4)$$

In systems where air is present, oxidizing species are formed such as $O_2\cdot^-$ and H_2O_2 (reactions 5-6):

$$e^- + O_2 \rightarrow O_2\cdot^- \ (5)$$

$$O_2\cdot^- + e^- (+2H^+) \rightarrow H_2O_2 \ (6)$$

The degradation of pollutants can therefore occur directly on the surface of the catalyst or with the interaction with free hydroxyl radicals [11]. The use of titanium dioxide as a catalyst is widespread as it is the most effective in the photocatalytic degradation of organic pollutants in the presence of UV radiation. Its use is also and above all important because titanium dioxide is a non-dangerous, ecological compound and it does not require additional chemicals. In principle, it manages to complete the slaying of drugs and then it can be recovered and used again [12]. In this part of my thesis, I studied COD abatement processes, deriving from the use of vegetable and synthetic tannins in the tanning processes, using

heterogeneous photodegradation, catalyzed by inorganic nanocrystalline semiconductors (TiO_2 Aeroxide P-25).

2. Material and methods

The system used for photodegradation consists of a glass-lined reactor with a capacity of 1.5 L closed with a lid with three necks, in which they are inserted: in the center of reactor the UV lamp (Toshiba FL4BLB 15cm x 1.5cm, with a power of 4W and emission at the wavelength of 365 nm, 220 V), in the other the thermocouple for reading the reaction temperature and in the third a digital flow-meter regulator is added (supplied by Bronkhorst), connected also to a sintered filter, used as gas diffuser to warrant a good gas-liquid interface in the mass transfer of air to the liquid phase. The synthetic wastewater containing tannins were prepared, using the vegetable extracts of chestnut, mimosa and synthetic tannin based on hydroxyphenylsulphone, at a different concentration of COD. The different prepared solutions were inserted inside the reactor which was closed and connected to the thermostat at the desired reaction temperature, the air flow was adjusted to the pressure of 1 bar, the UV lamp was turned on and finally the catalyst was added. During this experiment, lasting a total of 5 hours, aliquots of sample were taken from the reactor every 30 minutes, and they were centrifuged at 3300 rpm for 15 minutes. The photodegradation efficiency was evaluated by determining the parameters pH, COD and TOC. To determine the pH, potentiometric methods were used (Mod 856/867, Metrohm, Switzerland). While COD and TOC were determined respectively; oxidative acid digestion followed by colorimetric methods (Hach, DR

3900, Germany) and sample combustion coupled with NDIR detector (TOC-V – Shimadzu, Japan). The quantification of COD and TOC was performed using an external calibration curve. The experiment was conducted in different temperature conditions, also at different catalyst and COD concentration. The scheme of the different conditions was reported in Table 1.

Experiment n°	Temperature (K)	p_B (g/L)	COD (mg/L)
1	298	0	200
2	298	0.5	200
3	298	0.5	100
4	298	0.5	50
5	298	1.0	200
6	298	1.5	200
7	313	0.5	200
8	323	0.5	200

Table 1. Different conditions of temperature and concentration of the catalyst used for the experiments, at fixed values of, Q_{air} = $1.0 \cdot 10^{-6} m^3/s$ and v = 500rpm.

3. Results and discussion

Different experiment was conducted to verify the influence of the temperature, the quantity of catalyst and finally the varying the initial concentration of COD. The results are shown in tables 2 to 9 in APPENDIX II. In figure 1 was represented the influence of the different quantities of catalyst. A first experiment was conducted in the absence of the catalyst, to verify eventual photodegradation due to the UV irradiation (Figure 1), but no substantial decrease in COD concentration was observed. Figure 2 shows that, by increasing the catalyst concentration, an increase of COD photodegradation was measured, suggesting a dependency of the photodegradation rate with the catalyst load. A reduction of the COD concentration of about 60% was observed at $\rho_{B=}$ 1.5 g/L

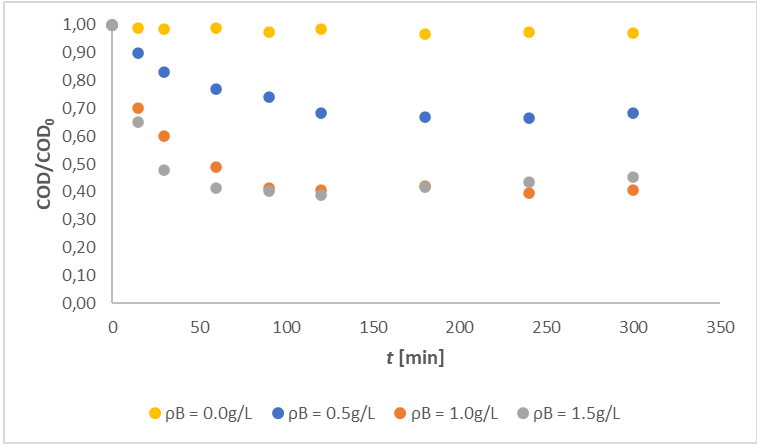

Figure 1. Effect of the catalyst loading on the photodegradation of tanning. The experiments were carried out fixing the following operation conditions: COD_0 = 200 mg/L, T = 298 K, Q_{air} = $1.0 \cdot 10^{-6} m^3/s$ and v = 500rpm.

Therefore, no significant differences were observed when using $\rho_{B=}$ 1.0 g/L or 1.5 g/L, probably due to the shield effect of the solid phase, allowing not to properly penetrate the liquid solution [13]. Moreover, also in this circumstance, after about 100 minutes from the beginning of the reaction the COD concentration reaches a stable *plateau* value. In Figure 2 the influence of the reaction temperature was investigated. It was observed that as the temperature increases, a reduction in COD is observed up to a maximum value of 40% at 323 K.

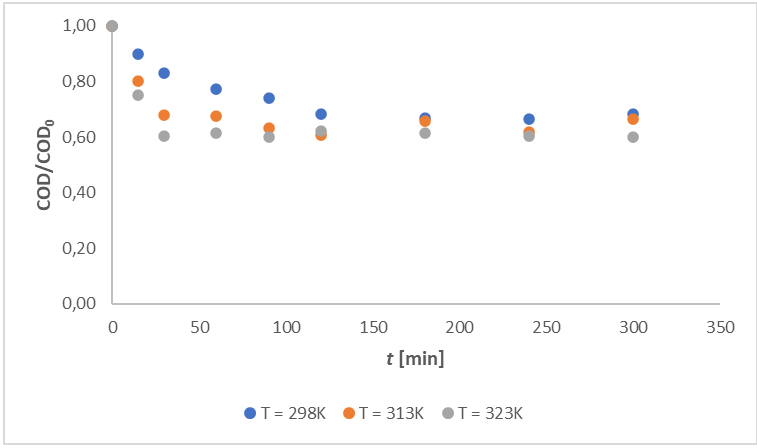

Figure 2. COD/COD_0 profile *vs.* reaction times for experiments conducted at different temperatures. The tests were conducted fixing the following operation conditions: COD_0 = 200 mg/L, ρ_B = 0.5 g/L, Q_{air} = $1.0 \cdot 10^{-6} m^3/s$ and v = 500rpm.

Furthermore, it is also observed that after 100 minutes from the beginning of the reaction the COD concentration reaches a stable plateau value. This effect was already observed in the literature, where Jouali *et al.* attributed the phenomenon to the shield effect due to the tanning residual content [14]. The assumption is indeed valid, considering the chemical complexity of the molecules and their by-products which could

undergo a more difficult photodegradation at a certain level of decomposition and which in turn can shield the catalyst, blocking the photodegradation process. The experiments carried out in different values of COD_0 are represented in Figure 3. The effect of this parameter was evaluated by varying its value from 50 mg/L to 200 mg/L. The results showed a degradation efficiency of about 54% for COD concentrations of 50 mg/L, while for concentrations above 100 mg/L, the efficiency decreases up to a maximum value of 40%.The effect of the high concentrations could probably be due to the absorption of the tannin molecules and their by-products on the surface of the catalyst and inhibiting the catalytic activity [13–16]. The results showed that the higher initial content of the COD, the faster is the reaction rate, suggesting a reaction order different than one.

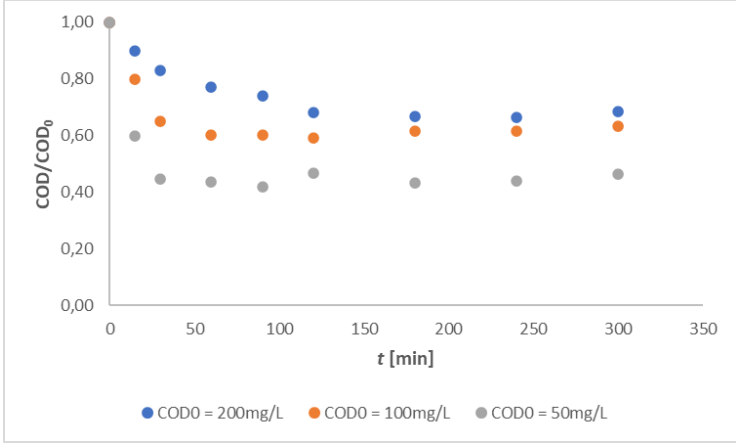

Figure 3. COD/COD_0 profile *vs.* reaction times for experiments carried out at different COD_0 values. The experiments were conducted fixing, ρ_B = 0.5 g/L, T = 298 K, $Q_{air} = 1.0 \cdot 10^{-6} m^3/s$ and v = 500rpm.

The experimental data collected, varying the reaction temperature, were interpreted to obtain the activation energy value. The Arrhenius law is applied (1):

$$ln\,(k) = ln\,ln\,(k_0) - \frac{E_a}{RT} \qquad (1)$$

k is the rate constant of the reaction, k_0 is the frequency factor, E_a is the activation energy, R is the ideal gas constant and T is the temperature. The kinetic parameters calculated are shown in the Table 10.

Temperature	***k* [1/s]**	***ln*(*k*) [-]**	***1/T* (1/K)**
298	0,00564	-5,18	0,00335
313	0,0107	-4,54	0,00319
323	0,0133	-4,32	0,00309

Table 10. Kinetic parameters calculated at different temperatures.

In Figure 4 Arrhenius plot are reported and from the slope it was calculate an activation energy value of E_a = 28 ± 2 kJ/mol, value of the order of magnitude for the photodegradation of complex organic molecules [17,18].

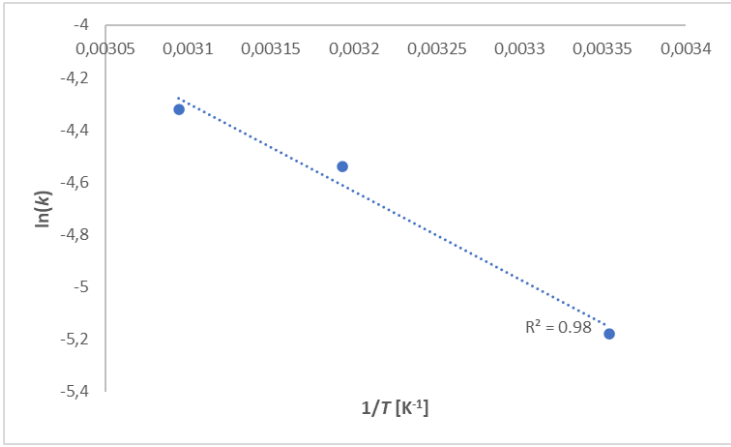

Figure 4. Arrhenius plot obtained from the data of experiments conducted at different temperatures.

As revealed, the R^2 value is more than acceptable and the confidence interval associated with the activation energy value is low, showing high reliability and statistical significance of the obtained parameter. These experiments lead all to the same *COD* final plateau value, that is dependent only on the catalyst loading and on the initial *COD* value as it will be seen below.

The effect of catalyst loading was understood both on the initial slope of the kinetic curves, proportional to the observed reaction rate (*r*) and the final plateau value of *COD*. The results are reported in Table 11 and Figure 5 A,B.

ϱB (g/L)	*ln*(*r*)	*ln*(*k*) [-]	*1/T* (1/K)
0.5	0,199	-5,18	0,00335
1.0	0,810	-4,32	0,00335
1.5	1,138	-4,05	0,00335

Table 11. Kinetic parameters calculated at different catalyst concentration

It is evident that the reaction rate is promoted by the amount of catalyst, showing a linearity coefficient near the unity (0.9), Figure 5A. Moreover, the final COD value, linearly decreases till 1g/L of catalyst, becoming then invariant with the catalyst loading, Figure 5B.

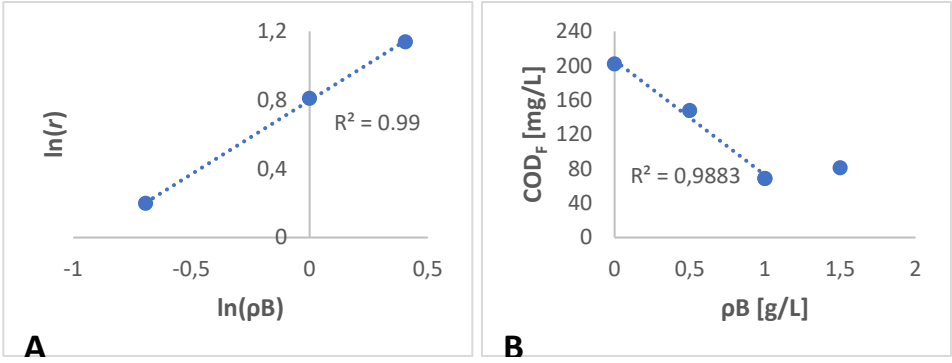

Figure 5. Effect of the catalyst loading on: A. the observed reaction rate, *r*; B. the COD *plateau* value, COD_F.

This fact could be always explained by the shield effect obtained when a high catalyst concentration is adopted. Finally, the effect of the initial *COD* value on the photodegradation kinetics was interpreted, concerning both the observed reaction rate and the final plateau value (Figure 6 A, B). As revealed, an increase in the COD_0 value corresponds to a non-linear increase of the reaction rate value, suggesting the occurrence of a more complex mechanism involving also superficial adsorption phenomena (Figure 6A). Figure 6B shows an important result, as the final COD value linearly depends on the initial one, with a linearity

coefficient of 0.7. This clearly indicates that higher is the contaminant quantity, higher is the residual, thus, its value is a matter of optimization.

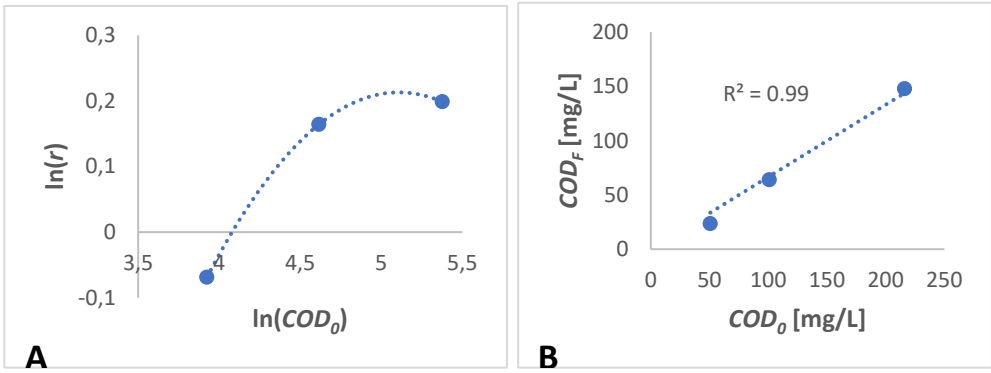

Figure 6. Effect of the initial COD value on: A. the observed reaction rate, *r*; B. the COD plateau value, COD_F.

4. Conclusion

An initial investigation of the photodegradation vegetal tannins of chestnut, mimosa, and synthetic tannins, mostly used in the tanning industry, was executed. The experiments were conducted simulating an industrial wastewater in different concentration of COD in the range of 50…200 mg/L. TiO_2 Areoxide P-25 was used as catalyst and it was also demonstrated to be an effective catalyst for COD abatement with a maximum value of 60%. From the collected evidence, an activation energy of Ea = 28 KJ/mol was obtained, comparable with the literature values obtained for persistent organic molecules. In every experiment, COD reached a plateau value, independent with the temperature value but linearly dependent with both the catalyst loading and the initial COD value. Higher is the catalyst load, more efficient is the photodegradation process, while using high values of COD_0 could lead to non-optimal

reaction conditions as it inhibits the reaction itself, suggesting a superficial mechanism.

5. References

1. Bharagava, R.N.; Saxena, G.; Mulla, S.I.; Patel, D.K. Characterization and Identification of Recalcitrant Organic Pollutants (ROPs) in Tannery Wastewater and Its Phytotoxicity Evaluation for Environmental Safety. *Arch Environ Contam Toxicol* **2018**, *75*, 259–272, doi:10.1007/s00244-017-0490-x.
2. Lofrano, G.; Meriç, S.; Zengin, G.E.; Orhon, D. Chemical and Biological Treatment Technologies for Leather Tannery Chemicals and Wastewaters: A Review. *Science of The Total Environment* **2013**, *461–462*, 265–281, doi:10.1016/j.scitotenv.2013.05.004.
3. Tünay, O.; Kabdasli, I.; Orhon, D.; Ates, E. Characterization and Pollution Profile of Leather Tanning Industry in Turkey. *Water Science and Technology* **1995**, *32*, 1–9, doi:10.1016/0273-1223(96)00132-1.
4. Kolomaznik, K.; Adamek, M.; Andel, I.; Uhlirova, M. Leather Waste—Potential Threat to Human Health, and a New Technology of Its Treatment. *Journal of Hazardous Materials* **2008**, *160*, 514–520, doi:10.1016/j.jhazmat.2008.03.070.
5. Mavlyanov, S.M.; Islambekov, Sh.Yu.; Ismailov, A.I.; Dalimov, D.N.; Abdulladzhanova, N.G. Vegetable Tanning Agents. *Chemistry of Natural Compounds* **2001**, *37*, 1–24, doi:10.1023/A:1017605223089.
6. Krishnamoorthy, G.; Sadulla, S.; Sehgal, P.K.; Mandal, A.B. Green Chemistry Approaches to Leather Tanning Process for Making Chrome-Free Leather by Unnatural Amino Acids. *Journal of Hazardous Materials* **2012**, *215–216*, 173–182, doi:10.1016/j.jhazmat.2012.02.046.
7. Hansen, É.; Monteiro de Aquim, P.; Hansen, A.W.; Cardoso, J.K.; Ziulkoski, A.L.; Gutterres, M. Impact of Post-Tanning Chemicals on the Pollution Load of Tannery Wastewater. *Journal of Environmental Management* **2020**, *269*, 110787, doi:10.1016/j.jenvman.2020.110787.
8. Di Iaconi, C.; Lopez, A.; Ramadori, R.; Di Pinto, A.C.; Passino, R. Combined Chemical and Biological Degradation of Tannery Wastewater by a Periodic Submerged Filter (SBBR). *Water Research* **2002**, *36*, 2205–2214, doi:10.1016/S0043-1354(01)00445-6.
9. Schrank, S.G.; José, H.J.; Moreira, R.F.P.M.; Schröder, H.Fr. Elucidation of the Behavior of Tannery Wastewater under Advanced Oxidation Conditions. *Chemosphere* **2004**, *56*, 411–423, doi:10.1016/j.chemosphere.2004.04.012.
10. WANG, J.L.; XU, L.J. Advanced Oxidation Processes for Wastewater Treatment: Formation of Hydroxyl Radical and Application. *Critical Reviews in Environmental Science and Technology* **2012**, *42*, 251–325, doi:10.1080/10643389.2010.507698.

11. Oturan, M.A.; Aaron, J.-J. Advanced Oxidation Processes in Water/Wastewater Treatment: Principles and Applications. A Review. *Critical Reviews in Environmental Science and Technology* **2014**, *44*, 2577–2641, doi:10.1080/10643389.2013.829765.
12. Choina, J.; Kosslick, H.; Fischer, Ch.; Flechsig, G.-U.; Frunza, L.; Schulz, A. Photocatalytic Decomposition of Pharmaceutical Ibuprofen Pollutions in Water over Titania Catalyst. *Applied Catalysis B: Environmental* **2013**, *129*, 589–598, doi:10.1016/j.apcatb.2012.09.053.
13. Naraginti, S.; Thejaswini, T.V.L.; Prabhakaran, D.; Sivakumar, A.; Satyanarayana, V.S.V.; Arun Prasad, A.S. Enhanced Photo-Catalytic Activity of Sr and Ag Co-Doped TiO2 Nanoparticles for the Degradation of Direct Green-6 and Reactive Blue-160 under UV & Visible Light. *Spectrochimica Acta Part A: Molecular and Biomolecular Spectroscopy* **2015**, *149*, 571–579, doi:10.1016/j.saa.2015.04.101.
14. Jouali, A.; Salhi, A.; Aguedach, A.; Lhadi, E.K.; El Krati, M.; Tahiri, S. Photo-Catalytic Degradation of Polyphenolic Tannins in Continuous-Flow Reactor Using Titanium Dioxide Immobilized on a Cellulosic Material. *Water Science and Technology* **2020**, *82*, 1454–1466, doi:10.2166/wst.2020.420.
15. Gnanaprakasam, A.; Sivakumar, V.M.; Thirumarimurugan, M. Influencing Parameters in the Photocatalytic Degradation of Organic Effluent via Nanometal Oxide Catalyst: A Review. *Indian Journal of Materials Science* **2015**, *2015*, e601827, doi:10.1155/2015/601827.
16. Ali, M.H.H.; Al-Afify, A.D.; Goher, M.E. Preparation and Characterization of Graphene – TiO2 Nanocomposite for Enhanced Photodegradation of Rhodamine-B Dye. *The Egyptian Journal of Aquatic Research* **2018**, *44*, 263–270, doi:10.1016/j.ejar.2018.11.009.
17. Lair, A.; Ferronato, C.; Chovelon, J.-M.; Herrmann, J.-M. Naphthalene Degradation in Water by Heterogeneous Photocatalysis: An Investigation of the Influence of Inorganic Anions. *Journal of Photochemistry and Photobiology A: Chemistry* **2008**, *193*, 193–203, doi:10.1016/j.jphotochem.2007.06.025.
18. Chen, D.; Ray, A.K. Photodegradation Kinetics of 4-Nitrophenol in TiO2 Suspension. *Water Research* **1998**, *32*, 3223–3234, doi:10.1016/S0043-1354(98)00118-3.

Chapter 5 – Remediation of wastewaters containing vegetable and synthetic tannins by adsorption with TiO_2

1. Introduction

Adsorption can be defined as a mass transfer event when one or several constituents (present in the liquid or gaseous phase) are fixed onto one porous solid surface [1]. The process is classified among the advanced treatments, suitable for the removal of pollutants in suspended, dissolved and colloidal form present in wastewater. Due to the increasingly restrictive limits imposed on wastewater treatment plants, during recent years, the use of advanced treatments is demanded, either in terms of efficiency in reducing pollutant concentrations or in terms of reducing the global toxicity of the final effluent. Furthermore, the use of this type of treatment is compulsory when reducing the concentrations of pollutants, organic and of different nature is needed.

Adsorption is the event when a transfer of one or more components takes place from a fluid mixture (liquid or gaseous) to a solid surface where they form physical or chemical interactions, causing a variation in interfacial concentration with respect to the phases adjacent. Referring to the second factor, relating to the affinity between the solute and the solid, three different types of forces of attraction must be considered: electrostatic forces, Van der Waals forces and chemical forces.

In the first case, adsorption occurs because of the presence of electrostatic forces that allow the bond between the ions of the adsorbate and the charges present on the surface of the adsorbent.

The absorption that occurs because of Van der Waals forces is generally called physical adsorption; it occurs at low temperatures and is not "Site-specific", this means that the adsorbed molecules do not attach onto a specific site, but they are quite free to undergo translational movements on the interface. Van der Waals forces are weak intermolecular forces and for this reason the process is considered reversible. If the adsorbate goes through chemical interactions with the adsorbent, then we can talk about chemical adsorption. The "chemically adsorbed" molecules, unlike the previous case, are not free to move on the surface since the adsorbate forms very strong localized bonds with the sites of the adsorbent. Most of the adsorption phenomena occurs because of the interaction of the three mechanisms. It is therefore not easy to distinguish between physical and chemical adsorption [1–6].

In the papers and books about the argument of adsorption, the writers generally agree in affirming that the first and most important information to obtain during the characterization of an adsorbent/adsorbate system is related to the equilibrium of the single component with a solid material.

In order for an adsorption process in a liquid / solid system to be successful, the solute or solutes must be removed from the solution and their consequent adsorption on the surface of the adsorbent material. When the concentration of the solute in solution is in dynamic equilibrium with the concentration of the solute on the surface, it is said

that equilibrium has been reached. In different words, when the adsorption rate is equal to the desorption rate, then the thermodynamic equilibrium condition has been reached, which means that the adsorbing capacity of the material is exhausted. The achievement of equilibrium, therefore, allows us to evaluate the adsorption capacity of a material against a certain contaminant. The theoretical adsorption capacity is expressed through adsorption isotherms.

The isotherm adsorption typically shows the adsorbate amount retained by the solid versus remaining in fluid phase (depending on the nature of this last one, this quantity can be expressed as pressure or concentration). The adjective isotherm indicates that the set of experiments conducted for the construction of this curve must be performed at the same temperature (this parameter influences the process). In 1888, a first mathematical approach to represent this concept was proposed by van Bemmelen [3]. It is described by following equation:

$$q = \frac{V(C_0 - C_{eq})}{m}$$

Where:

q = capture capacity, mg_{solute}/g_{solid}

V = volume of solution, L

C_0 = initial concentration of adsorbate, mg/L

Ceq = equilibrium concentration of adsorbate, mg/L

m = solid mass, g

In different words, considering a certain volume V of solution with initial concentration C_0 of a compound to remove and a certain mass m of adsorbent material, at a fixed temperature and after that the system reaches the equilibrium condition, the quantity of adsorbed compound per solid mass unit is computable by the written equation. When using this equation to represent the equilibrium conditions of an adsorbate/adsorbent system it would be necessary to fix two parameters among m, V and C_0 and to vary the third one measuring step by step the reached equilibrium concentration.

Moreover, this equation is derived by a simple mass balance on the adsorption system and it does not consider the mechanism where the solute retention occurs; in fact, some writers suggest to use much more generic definitions such retention curve or solute disappearance curve [3]. For practical purposes, an equation that allows to associate a value of capture capacity of the solid to a value of equilibrium concentration, independently by the operative parameters of the experiment, it is more convenient and versatile. For this reason, several models have been developed. The most used isotherms are those of Freundlich and Langmuir.

Langmuir isotherm

The Langmuir equation is based on four important hypotheses. It is assumed that:

- The active sites on the surface are energetically homogeneous,
- Each site can hold only one atom or molecule.
- The phenomenon runs until the complete formation of the monolayer.

- Adsorption is localized and the energy needed for the process doesn't depend on the coverage degree.

Since the number of specific sites per unit weight of adsorbent is fixed, adsorption will take place until all sites are completely occupied. This generally corresponds to the assumption of the presence of a single layer of molecules adsorbed on the surface. The mathematical form of the Langmuir isotherm is:

$$C_S = C_S^* \frac{bC_L}{1 + bC_L}$$

Where:

b = affinity parameter, m^3_{liq}/mol

b expresses the dependence of the isotherm by the temperature; mathematically, this parameter is described by a typical Arrhenius-like function as in following equation:

$$b = b_0 e^{\frac{-\Delta H}{RT}}$$

With:

b_0 = pre-exponential constant, $m^3_{LIQ} \cdot mol^{-1}$

ΔH = enthalpy variation due to the adsorption process, $J \cdot mol^{-1}$

R = ideal gas universal constant, $J \cdot mol^{-1} \cdot K^{-1}$

T = temperature, K

Varying the experiment temperature, the value of b changes influencing the isotherm shape that will reach its plateau for lower or higher solute

concentration, depending on the case. Although the range of validity defined by the Langmuir conditions appears particularly limited, the equation well interprets a wide set of experimental data [5].

Freundlich isotherm

The Freundlich isotherm is based on the hypothesis that the adsorbent has a heterogeneous surface consisting of points where the heat of adsorption is reduced exponentially with the degree of coverage. The Freundlich isotherm is expressed by the following relationship:

$$C_S = K_F C_L^{1/n}$$

Where:
K_F = Freundlich adsorption constant, $(mol \cdot m_{SOL}^{-3}) \cdot (mol \cdot m_{LIQ}^{-3})^{-n}$
n = adsorption intensity, -

The values of these parameters are generally computed by an optimization process on experimental data. As the value of n grows, the isotherm assumes the form of the so-called square function so approximating to the irreversible isotherm, which mathematical form is represented by a constant (in this specific case by the value of KF). The versatility where the function changes its shape by varying the value of the exponent n makes it particularly suitable for the interpretation of systems characterized by a distribution of adsorption heats (that is due by an energetic heterogeneity of the active sites).

The Freundlich isotherm doesn't conceive a limitation in the quantity of adsorbed compounds which thus are able to grow indiscriminately when solute concentration increases [2].

In this part of my thesis, I studied the event of adsorption, using TiO_2 Aeroxide P-25 as an adsorbent material, used to treat wastewater deriving from the tanning industry and its potential use to decrease the high concentrations of COD due to the presence of poorly biodegradable organic contaminants, such as synthetic tannins and natural.

2. Material and methods

The system used for adsorption tests consists of a glass-lined reactor with a capacity of 1.5 L closed with a lid with three necks, in which they are loaded: thermocouple for reading the reaction temperature and in the other a digital flowmeter regulator added (supplied by Bronkhorst), connected to a sintered filter used as gas sparger, to warrant a good gas-liquid interface in the mass transfer of air to the liquid phase. The synthetic wastewater containing tannins were prepared, using the vegetable extracts of chestnut, mimosa and synthetic tannin based on hydroxyphenyl sulfone, at a different concentration of COD. The experiment lasted a total of 5 hours and, every 5 minutes, aliquots of sample were taken from the reactor and centrifuged at 3300 rpm for 15 minutes. The adsorption efficiency was evaluated by determining the parameters pH, COD and TOC. For determination of pH, potentiometric method was performed (Mod 856/867, Metrohm, Switzerland). COD and TOC were determined respectively; oxidative acid digestion followed by colorimetric methods (Hach, DR 3900, Germany) and

sample combustion coupled with NDIR detector (TOC-V – Shimadzu, Japan). The quantification of COD and TOC was performed using an external calibration curve. The experiments were conducted at different conditions of temperatures, adsorbent material concentrations and COD concentration; the scheme of the different conditions was reported in Table 1.

Experiment n°	Temperature (K)	p_B (g/L)	COD (mg/L)
1	293	0.5	200
2	293	0.5	100
3	293	0.5	50
4	293	1.0	200
5	293	1.5	200
6	313	0.5	50
7	323	0.5	50

Table 1. Different conditions of temperature and concentration of the catalyst used for the experiments, at fixed values of, $Q_{air} = 1.0 \cdot 10^{-6} m^3/s$ and $v = 500$rpm.

3. Results and discussion

Different experiment was conducted to verify the influence of the temperature, the quantity of adsorbent material and finally by varying the initial concentration of COD. The results are shown in Tables 2 to 8 in APPENDIX III.

In Figure 1 the variation of the COD concentration ratio are reported, with respect to the initial concentration (COD_0) utilizing different initial COD concentration (200, 100 and 50 mg/L), versus the adsorption time.

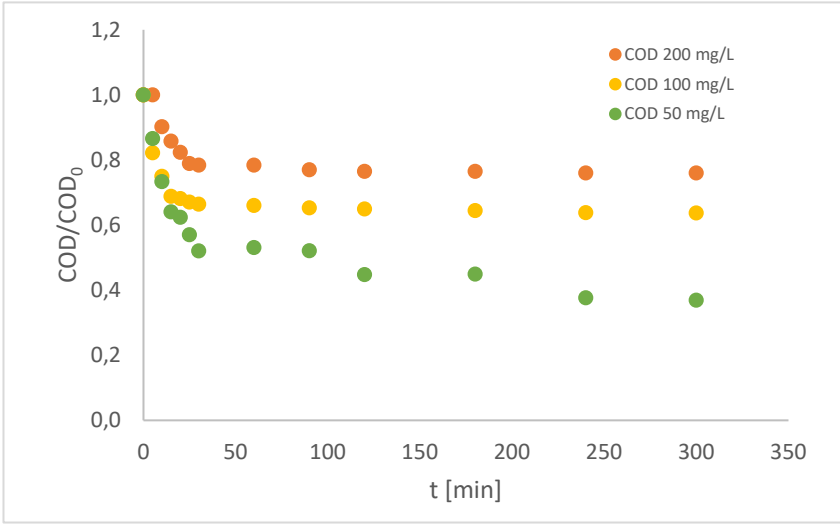

Figure 1. COD/COD_0 profile vs reaction times for experiments carried out at different COD_0 values. The experiments were conducted fixing, ρ_B = 0.5 g/L, T = 298 K, $Q_{air} = 1.0 \cdot 10^{-6} m^3/s$ and v = 500rpm.

It is observed that an increase in the initial COD amount decreases the amount of COD adsorbed on the TiO_2 surface. The maximum observed value is 65% when the COD concentration is 50 mg/L. Furthermore, the COD concentration ratio demonstrated an initial drop at a high rate then slows down as it goes toward equilibrium after it remained constant.

Effects of concentration of TiO_2 utilized in the adsorption process was investigated using three different concentration (0.5, 1.0 and 1.5 g/L), while the initial COD concentration was kept the same, at 200 mg/L.

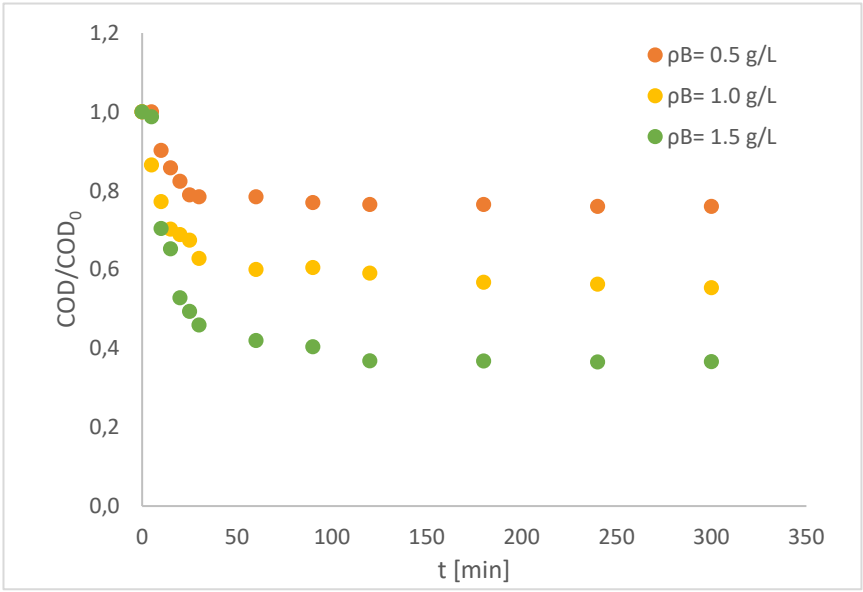

Figure 2. Effect of the catalyst loading. The experiments were carried out fixing the following operation conditions: COD_0 = 200 mg/L, T = 298 K, Q_{air} = $1.0 \cdot 10^{-6} m^3/s$ and v = 500rpm.

In figure 2, the effect of the adsorbent content on the kinetic curves is reported. The simulations performed at different solid contents show good agreement. As can been appreciated, using greater amounts of solid, an increase of the adsorption kinetics can be observed. In fact, the initial slope of the kinetic curves increases when loading a bigger

amount of TiO_2 in the adsorber. This aspect is in line with the typical experimental evidence reported in the literature.

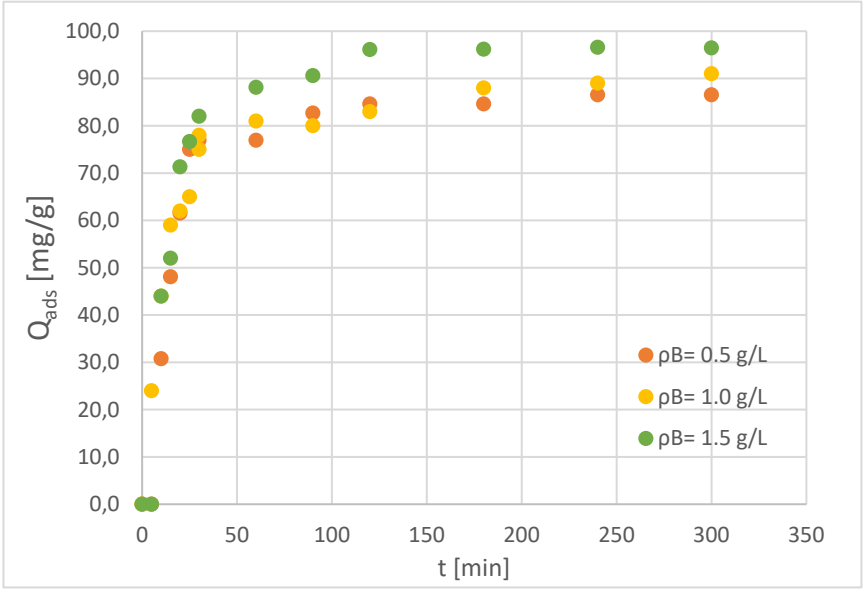

Figure 3. Effect of the catalyst concentration on the COD uptake.

In figure 3, it was observed that the COD uptake at equilibrium was the highest for the case of a TiO_2 concentration of 1.5 g/L, followed by a concentration of 1 g/L.

The variation of COD absorption with adsorption time, using a TiO_2 of 0.5 g/L and a different initial COD concentration, is illustrated in Fig. 4. The COD removal or absorption rate showed a high rate increase for the initial concentration of three different COD value up to a certain value then the curves flatten; the COD removal rate stopped when equilibrium was reached.

The curves also clearly demonstrate that initial COD concentrations of 50 and 100 mg/L exhibited similar uptake behavior, whereas it was much higher for an initial COD concentration of 200 mg/L as can be

clearly shown by the upper curve. This result is in a good agreement with what was previously reported in literature [7,8].

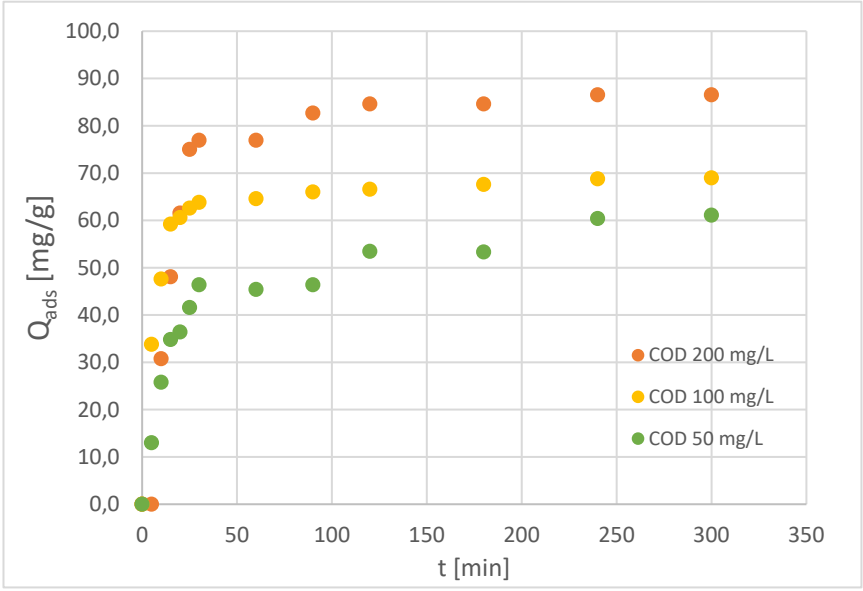

Figure. 4. Variation of COD removal efficiency with time during the adsorption treatment of wastewater with titanium dioxide for different initial COD concentrations. The experiments were carried out fixing the following operation conditions: ρ_B = 0.5 g/L, T = 298 K, Qair = $1.0 \cdot 10^{-6} m^3/s$ and v = 500rpm.

Temperature plays an important role as a variable in adsorption. To investigate the effect of temperature on the COD uptake by the TiO_2 in this research, three different temperatures were used. The initial COD concentrations was kept the same at 50 mg/L.

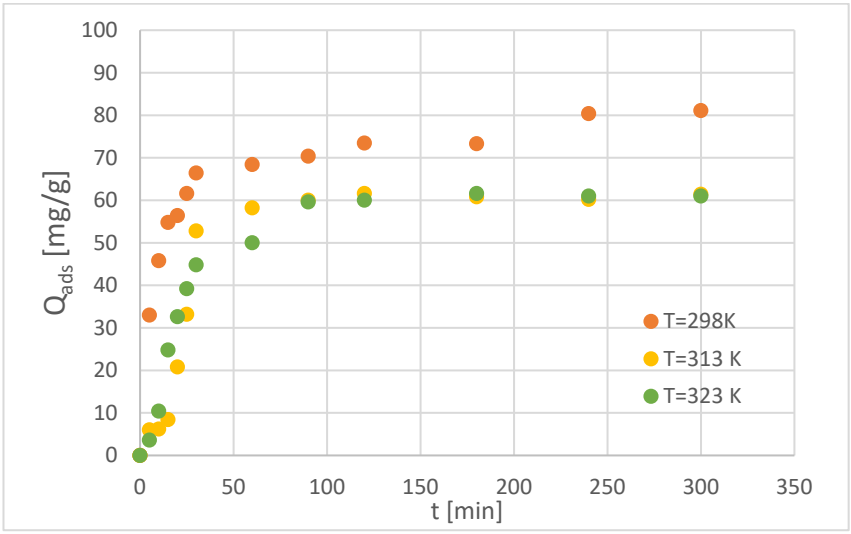

Figure. 5. Variation of COD removal efficiency with time during the adsorption treatment of wastewater with titanium dioxide for different temperature. The experiments were carried out fixing the following operation conditions: ρ_B = 0.5 g/L, COD = 50 mg/L, $Q_{air} = 1.0 \cdot 10^{-6} m^3/s$ and v = 500rpm.

The influence of the reaction temperature was reported in Figure 5. An increase in the amount of COD adsorbed at low temperatures is observed. No significant difference was observed between the temperature of 313 and 323 K. This indicates that the temperature has demonstrated a negative effect on the COD adsorption, and subsequently, it manifests the exothermic nature of the process. The experimental data collected varying the reaction condition were interpreted to obtain the adsorption isotherms. The adsorption isotherm experiments have been performed at 298 K, by preparing different solutions of COD and different TiO_2 amount. The collected experimental

data have been fitted with classical isotherm. The analysis of the R2 value of 0.99 for Freundlich isotherm suggested the use of this equation.

In Figure 6, the fitting curves are shown. Optimized Freundlich's parameters are Kf = 42±1 and n=7.4 ±0.2.

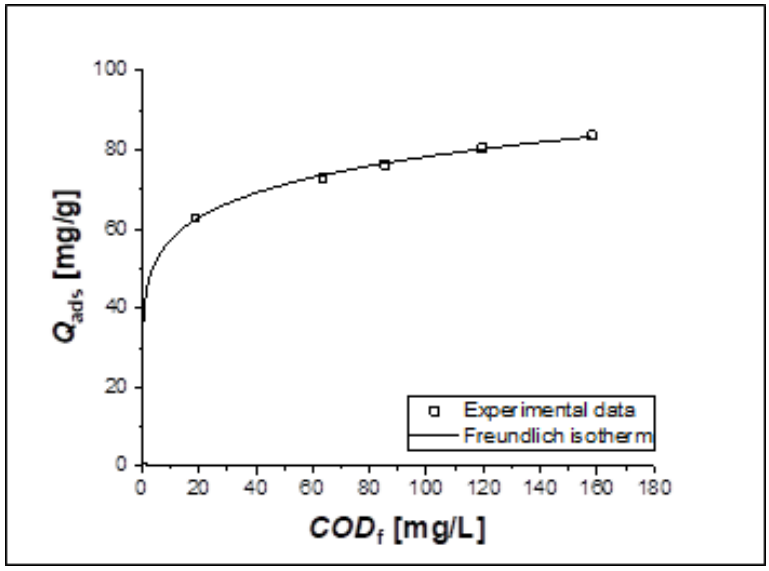

Figure. 6. Adsorption isotherm analysis.

4. Conclusion

A preliminary investigation of adsorption process with TiO_2 Aeroxide P-25 for abatement of recalcitrant COD was performed. The effect of temperature, catalyst loading, and different initial concentrations of COD were studied.

It is observed that an increase in the initial COD amount decreases the amount of COD adsorbed on the TiO2 surface. The maximum observed value is 65% when the COD concentration is 50 mg/L. It was observed also that the COD uptake at equilibrium was the highest for the case of a TiO_2 concentration of 1.5 g/L. The effect on the COD removing rate has shown that increasing the temperature had a negative effect on the COD uptake, which is an indication of the exothermic nature of the current adsorption process. The obtained data indicates that the TiO_2 was efficient in removing the recalcitrant COD, due to the presence of local and vegetal tannins commonly used in the tanning industry and it perfectly fitted the Freundlich isotherm model. Furthermore, the n values of the Freundlich model are >1, indicating a favorable adsorption. The magnitude of the exponent n gives an indication on the favorability of adsorption. It is generally stated that values of n in the range 2…10 represent good, 1…2 moderately difficult, and < 1 poor adsorption characteristics [9].

5. References

1. Dabrowski, A. Adsorption--from Theory to Practice. Adv Colloid Interface Sci **2001**, 93, 135–224, doi:10.1016/s0001-8686(00)00082-8.
2. Insights into the Modeling of Adsorption Isotherm Systems. Chemical Engineering Journal, **2010**, 156, 2-10 doi.org/10.1016/j.cej.2009.09.013.
3. Limousin, G.; Gaudet, J.-P.; Charlet, L.; Szenknect, S.; Barthès, V.; Krimissa, M. Sorption Isotherms: A Review on Physical Bases, Modeling and measurement. Applied Geochemistry **2007**, 22, 249–275, doi:10.1016/j.apgeochem.2006.09.010.
4. Giles, C.H.; Smith, D.; Huitson, A. A General Treatment and Classification of the Solute Adsorption Isotherm. I. Theoretical. Journal of Colloid and Interface Science **1974**, 47, 755–765, doi:10.1016/0021-9797(74)90252-5.
5. Brunauer, S.; Emmett, P.H.; Teller, E. Adsorption of Gases in Multimolecular Layers. J. Am. Chem. Soc. 1938, 60, 309–319, doi:10.1021/ja01269a023.
6. Rudzinski, W.; Lee, S.; S, C.; Yan, E.; Panczyk, T. A Fractal Approach to Adsorption on Heterogeneous Solid Surfaces. 1. The Relationship Between Geometric and Energetic Surface Heterogeneity. J. Phys. Chem. B 10847.
7. Al Bsoul, A. The Use of Eucalyptus Leaves as Adsorbent for Copper Ion Removal. Desalination and Water Treatment **2014**, 52, 7838–7844, doi:10.1080/19443994.2013.832637.
8. Al Bsoul, A.; Hailat, M.; Abdelhay, A.; Tawalbeh, M.; Jum'h, I.; Bani-Melhem, K. Treatment of Olive Mill Effluent by Adsorption on Titanium Oxide Nanoparticles. Science of The Total Environment 2019, 688, 1327–1334, doi:10.1016/j.scitotenv.**2019**.06.381.
9. Treybal, R.E. Mass-Transfer Operations; McGraw-Hill chemical engineering series; 3d ed.; McGraw-Hill: New York, 1980; ISBN 978-0-07-065176-0.

CONCLUSION

The results acquired from this project indicate in general that the water disposed by numerous companies after the purification plants have showed limit values to be higher than the legal parameters, such as chlorides and sulphates. All the above samples demonstrate a high organic matter content, as shown by the high COD and TOC. These parameters were compared using Pearson's correlation at the $p < 0.05$ significance level. The results indicated that the COD and TOC have very strong correlation with $r = 0.98$ and $p < 0.05$; this suggests that the high values of COD depend only on the presence of organic compounds. Furthermore, the ratio between BOD_5 and COD (always less than 0.5) suggests that these compounds are not biodegradable. The analysis of developing organic contaminants, such as phenols, chlorophenols, alkylphenols and ethoxylated alkyl-phenols showed the presence in low concentrations (between 5...10 ug/L) of phenol in most of the samples and the presence of only 4-nonylphenol diethoxylate was just above the limit of quantification of 0.5 ug/L. These concentrations cannot justify the high COD values. From the reconstruction of a real matrix containing polyphenols, the results indicated that the COD and total polyphenols concentration were correlated to $r \simeq 1.00$ and $p < 0.05$, therefore these values are probably to be attributed to the presence of polyphenolic substances. A first preliminary study of 5 samples by MALDI TOF/TOF analysis showed the presence of some peaks which could be correlated to the use of synthetic tannins based on phenol, formaldehyde and urea. Further analyses are needed, using different techniques, in order to receive more insights. The

chemical characterization of vegetal and synthetic tannins, commonly used in the tanning industry, was carried out. Synthetic and vegetable commercial tannins can be analyzed by MALDI–TOF/TOF with DHB used as matrices. The MALDI spectrum shows the oligomer distribution. The oligomer peaks appear as $[M+Na]^+$ molecular ions. From each of the oligomer masses, the degree of polymerization can be determined. The MALDI spectrum of synthetic tannins, in particular for Whitan RSD and Whitan White Conc, showed the presence of dimer, trimer and tetramer of the polycondensation reaction of 4,4' dihydroxyphenylsulfone with formaldehyde. Syncotan CBN spectrum showed the presence of different condensation oligomers between phenol, urea and formaldehyde. Tara and chestnut tannins are characterized by hydrolyzable tannins consisting mainly of units of gallic acid condensed with units of glucose. The MALDI spectrum of chestnut tannins showed instead the presence also of ellagic acid units combined with glucose units. Much more complex are the MALDI spectrum of mimosa tannins. Mimosa is mainly based on combination of three different type unit, with different masses, so-called A (272 m/z), B (288 m/z) and C (304 m/z), which combined give origin to different combinations of oligomers with different degree of polymerization. In the second part of my research project, I focused on the techniques in order to drop recalcitrant COD, photodegradation and adsorption. An initial investigation of the photodegradation vegetal tannins of chestnut, mimosa, and synthetic tannins, mostly used in the tanning industry was completed. The experiments were conducted simulating an

industrial wastewater at different concentration of COD in the range of 50…200 mg/L. TiO_2 Aeroxide P-25 was used as catalyst, and it demonstrated to be an effective catalyst for COD reducer with a maximum value of 54%. From the collected proof, an activation energy of Ea = 28 KJ/mol was obtained equivalent to the literature values obtained for persistent organic molecules. In every experiment, COD reached a plateau value, independent on the temperature value but linearly dependent with both the catalyst loading and the initial COD value. Higher is the catalyst load, more efficient is the photodegradation process, whilst using high values of COD_0 could lead to non-optimal reaction conditions as it inhibits the reaction itself, suggesting a superficial mechanism. A preliminary investigation of adsorption process with TiO_2 Aeroxide P-25 for reducing the recalcitrant COD was carried out. It is observed that an increase in the initial COD amount decreases the amount of COD adsorbed on the TiO_2 Aeroxide P-25 surface. The maximum value observed is 65% when the COD concentration is 50 mg/L. By comparing the results obtained from the photodegradation and adsorption process in terms of COD removal%, under the same experimental conditions, it is observed that when the COD concentration is less than or equal to 50 mg / L the adsorption process is favored compared to that of photodegradation or the reaction kinetics is slowed down. It was also detected that the COD uptake at its equilibrium was the highest for the case of a TiO_2 concentration of 1.5 g/L. The effect on the COD removing rate has shown that increasing the temperature had a negative effect on the COD uptake, which is an indication of the

exothermic nature of the current adsorption process. The obtained data indicates that the TiO_2 was efficient in removing the recalcitrant COD, due to the presence of local and vegetal tannins commonly used in the tanning industry and it did perfectly suit the Freundlich isotherm model. Furthermore, the n values of Freundlich model are >1, indicating a more favorable adsorption.

APPENDIX I

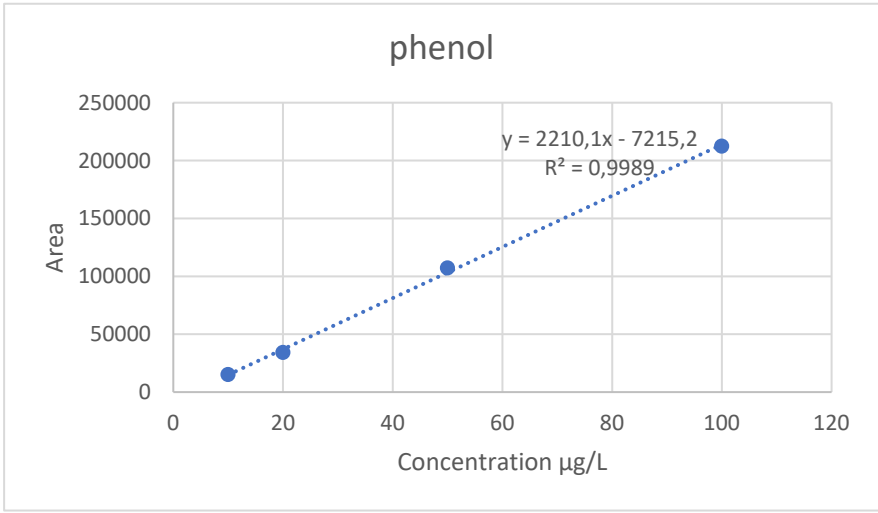

Figure 10. Calibration curve of phenol.

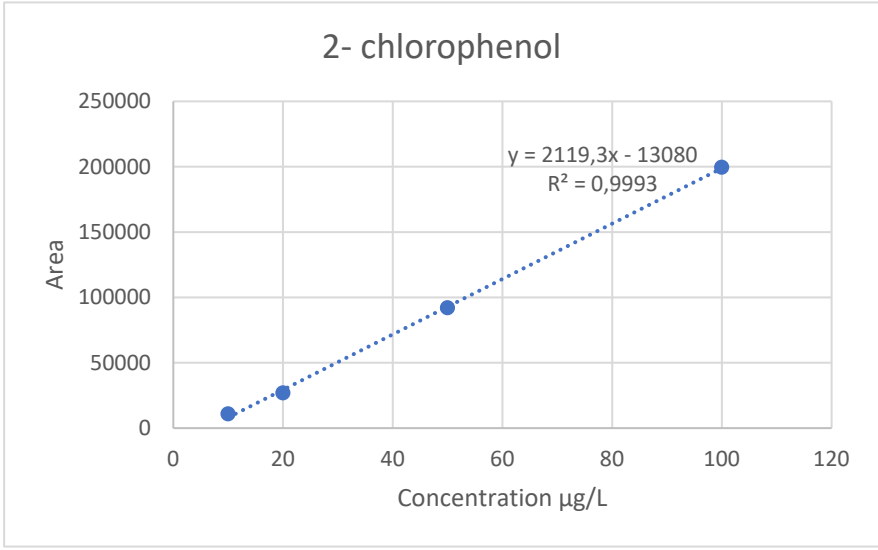

Figure 11. Calibration curve of 2-chlorophenol.

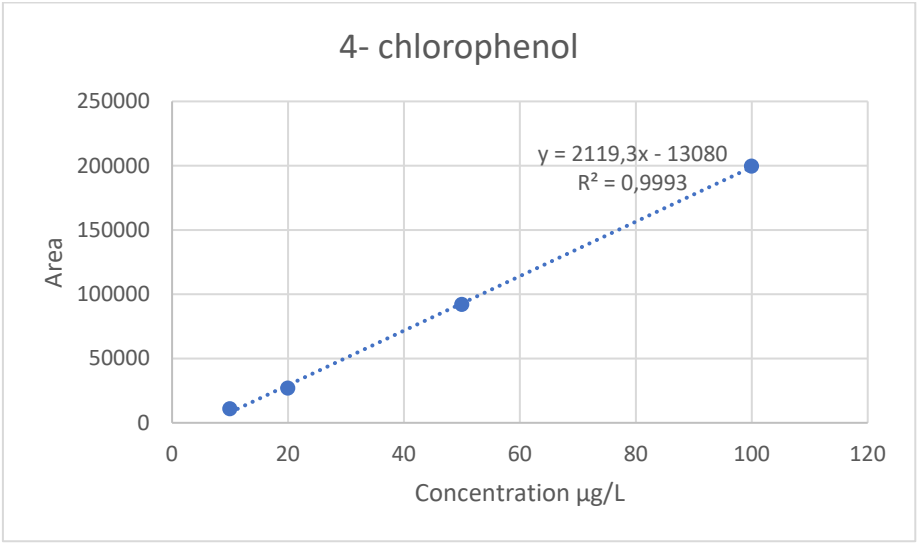

Figure 12. Calibration curve of 4-chlorophenol.

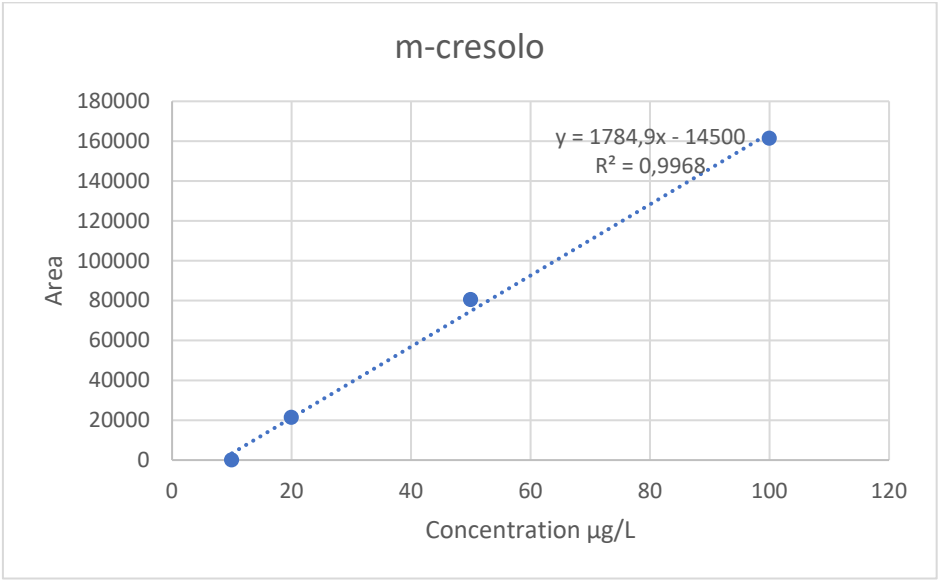

Figure 13. Calibration curve of m-cresol.

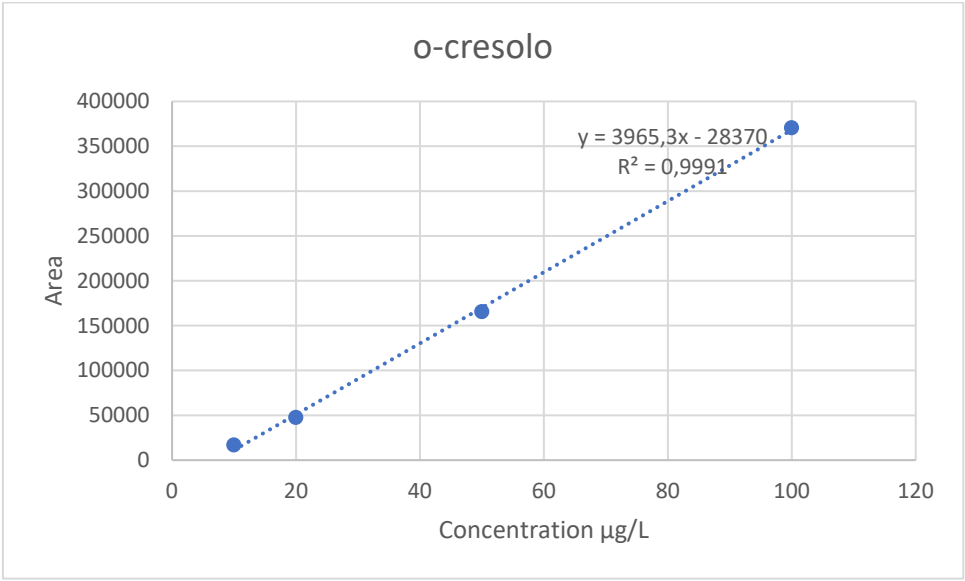

Figure 14. Calibration curve of o-cresol.

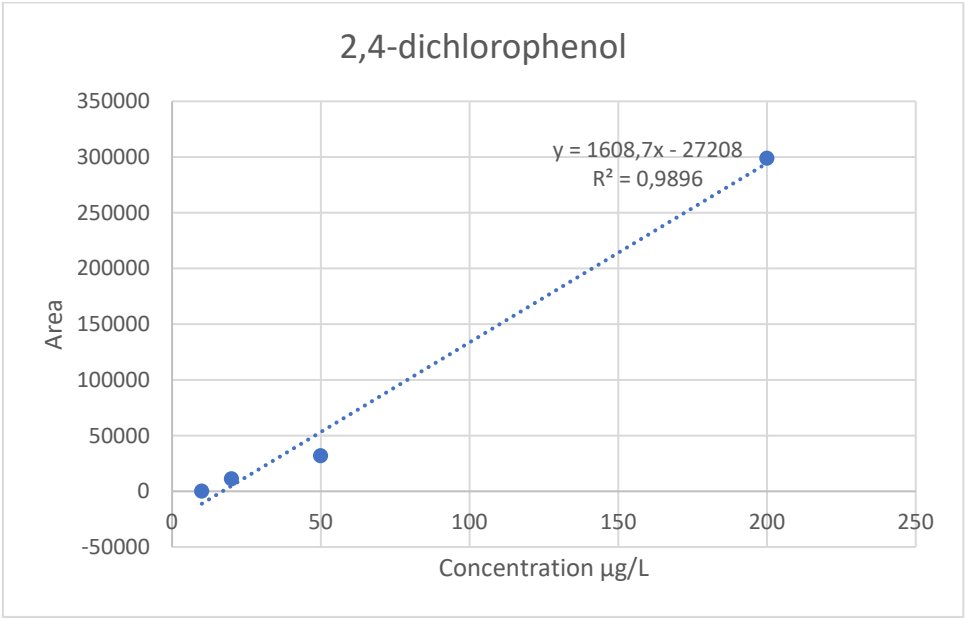

Figure 15. Calibration curve of 2,4-dichlorophenol.

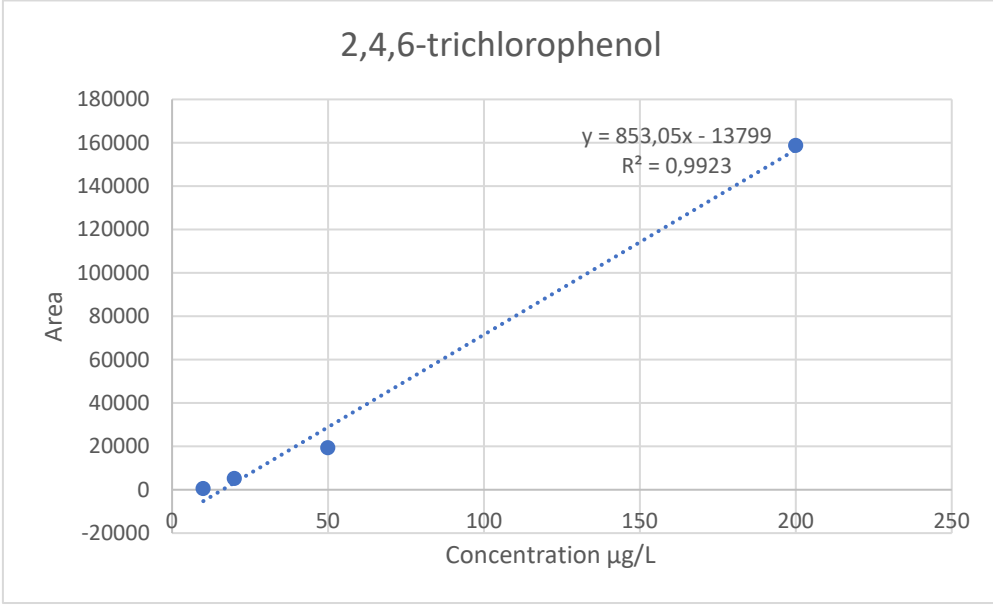

Figure 16. Calibration curve of 2,4,6-trichlorophenol.

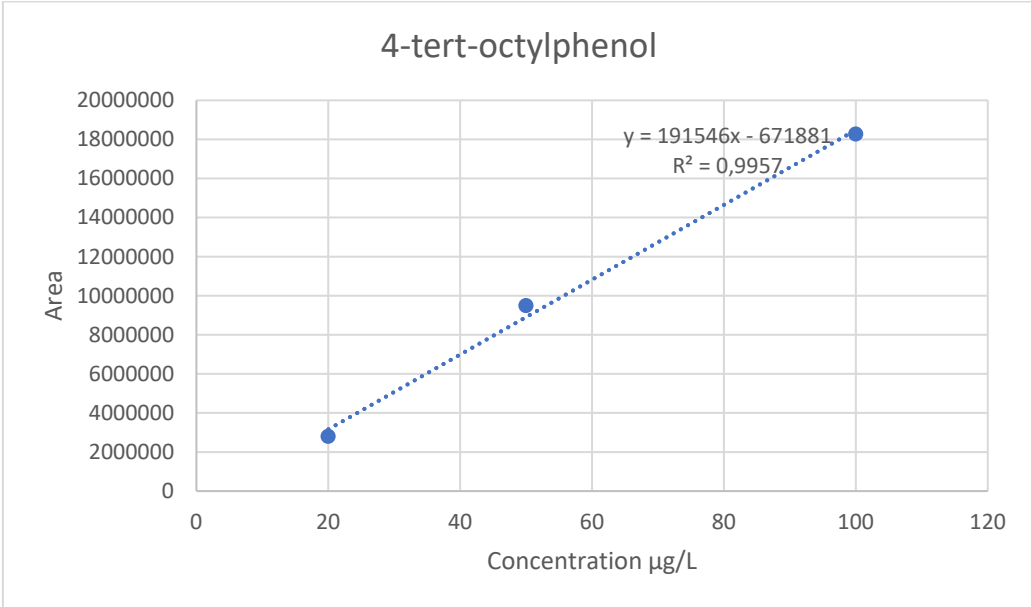

Figure 17. Calibration curve of 4-tert-octylphenol.

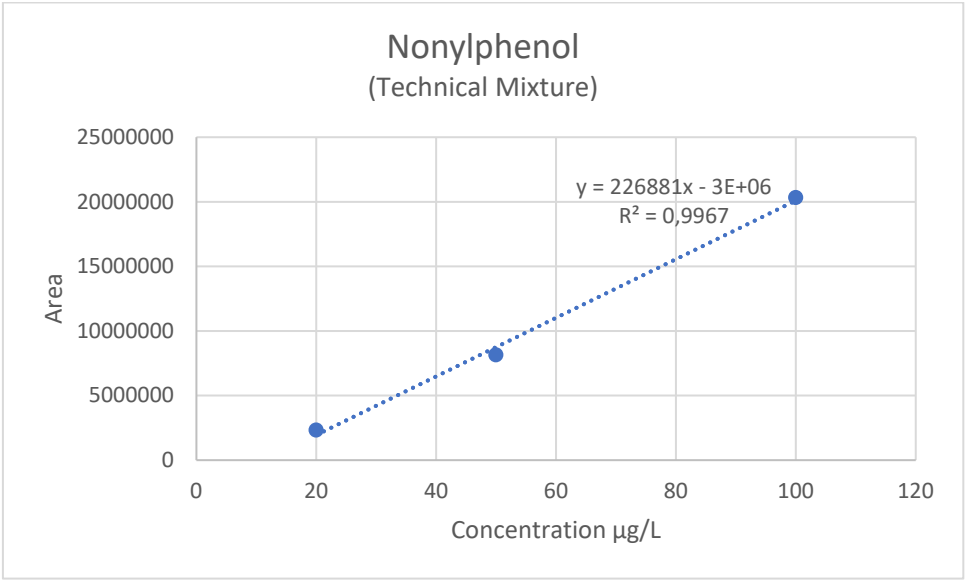

Figure 18. Calibration curve of nonylphenol.

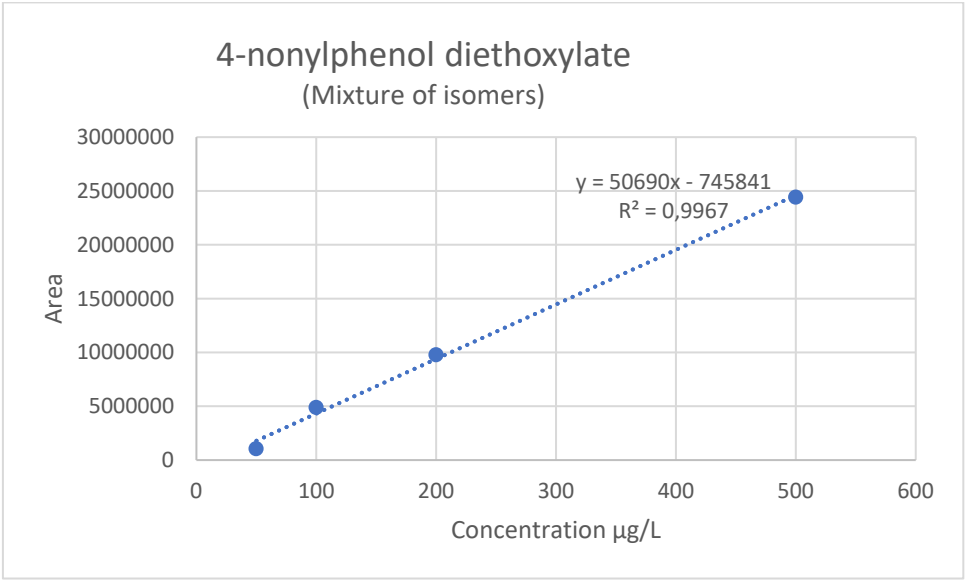

Figure 19. Calibration curve of 4-nonylphenol diethoxylate.

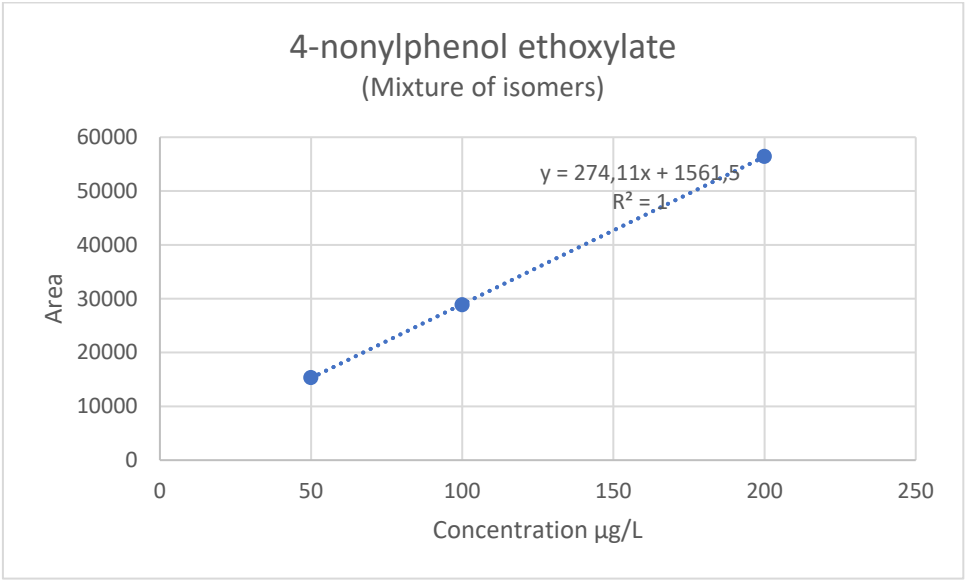

Figure 20. Calibration curve of 4-nonylphenol ethoxylate.

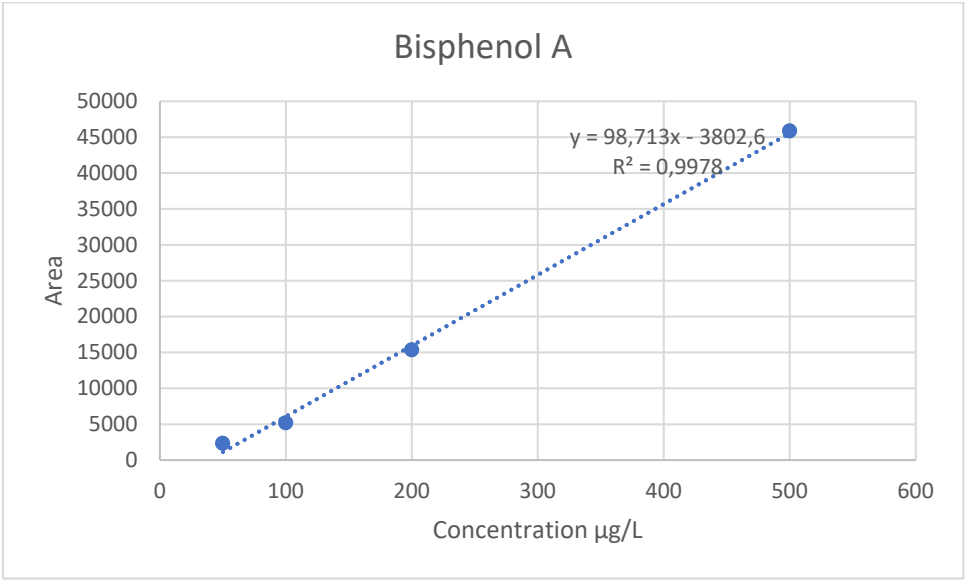

Figure 21. Calibration curve of bisphenol A.

	Instrumental		Sample
Compounds	**LOD**	**LOQ**	**LOQ**
4-tert-octylphenol	6.6	20	0.5
Nonylphenol (Technical Mixture)	7.7	23	0.5
4-Nonylphenol	6.2	19	0.5
4-nonylphenol ethoxylate (Mixture of isomers)	17	50	0.5
4-nonylphenol diethoxylate (Mixture of isomers)	11	34	0.5
Bisphenol A	15	45	0.5

Table 12. Values of instrumental LOD and LOQ and LOQ in the sample, of alkylphenols and alkylphenols ethoxylate expressed in µg/L.

	Instrumental		Sample
Compounds	**LOD**	**LOQ**	**LOQ**
Phenol	1.7	5.0	0.1
2-Chlorophenol	1.9	5.6	0.1
m-Cresol	1.9	5.6	0.1
o,p-Cresol	1.6	4.7	0.1
2,4-Dichlorophenol	2.2	6.7	0.1
4-Chlorophenol	2.3	7.0	0.1

Table 13. Values of instrumental LOD and LOQ and LOQ in the sample, of phenols and chlorophenols expressed in µg/L.

Compounds	u_{rip}	u_{tar}	U	Recovery %
4-tert-octylphenol	0.19	0.08	0.23	71
Nonylphenol (Technical Mixture)	0.21	0.10	0.26	65
4-Nonylphenol	0.23	0.07	0.27	76
4-nonylphenol ethoxylate (Mixture of isomers)	0.26	0.11	0.30	81
4-nonylphenol diethoxylate (Mixture of isomers)	0.24	0.15	0.28	86
Bisphenol A	0.30	0.13	0.30	90
Min	0.19	0.07	0.23	71
Max	0.30	0.15	0.30	90
Mean	0.24	0.11	0.27	78

Table 14. Relative values of uncertainty of repeatability (u_{rip}), uncertainty of calibration (u_{tar}), expanded uncertainty (U) of alkylphenols and alkylphenols.

Compounds	u_{rip}	u_{tar}	U	Recovery %
Phenol	0.17	0.05	0.25	68
2-Chlorophenol	0.15	0.06	0.21	75
m-Cresol	0.19	0.11	0.28	78
o,p-Cresol	0.16	0.14	0.27	81
2,4-Dichlorophenol	0.12	0.08	0.20	86
4-Chlorophenol	0.21	0.10	0.30	77
Min	0.15	0.05	0.20	68
Max	0.21	0.14	0.30	86
Mean	0.17	0.09	0.25	78

Table 15. Relative values of uncertainty of repeatability (u_{rip}), uncertainty of calibration (u_{tar}), expanded uncertainty (U) of of phenols and chlorophenols.

Parameter	LOQ	Parameter	LOQ
Total Phosphorus	< 1	**Cd**	< 0.0006
Ammonium	< 1	**Hg**	<0.0001
Chromium (VI)	< 0.02	**Pb**	< 0.02
Fluoride	<1	**Sn**	< 0.001
Nitrate	< 1	**Ba**	< 0.005

Table 16. Values of limit of quantification (LOQ) expressed in mg/L.

Parameter	LOQ
Animal and vegetable fats and olis	< 1
Hydrocarbon	< 0.5
Aromatic Solvent	< 0.02
Chlorinated solvents	< 0.1
T. Pesticides	< 0.005
aldrin	< 0.001
dieldrin	< 0.001
endrin	<0.0002
isodrin	<0.0002
NAP	<0.0001
ACE	<0.0001
ACY	<0.0001
FLR	<0.0001
PHE	<0.0001
ANT	<0.0001
FLT	<0.0001
PYR	<0.0001
BaA	<0.0001
CHR	<0.0001
BkF	<0.0001
BbF	<0.0001
BaP	<0.0001
DhA	<0.0001
IND	<0.0001
BgP	<0.0001

Table 17. Values of limit of quantification (LOQ) expressed in mg/L.

APPENDIX II

Time [min]	pH	COD (mg/L)	TOC (mg/L)
0	5.21	208	88.6
15	5.15	207	88.2
30	5.10	205	87.3
60	5.05	206	85.5
90	5.01	203	52.4
120	4.90	205	84.5
180	4.87	201	83.7
240	4.85	203	83.5
300	4.76	202	83.1

Table 2. Experimental results of tests conducted at COD concentrations of 200 mg/L, T = 298K, ρ_B = 0 g/L, Q_{air} = 1.0·10-6m^3/s and v = 500rpm.

Time [min]	pH	COD (mg/L)	TOC (mg/L)
0	4.59	216	74.1
15	4.63	195	65.3
30	4.66	180	52.4
60	4.67	167	54.0
90	4.70	160	56.9
120	4.72	148	55.4
180	4.68	145	55.7
240	4.72	144	55.9
300	4.93	148	56.0

Table 3. Experimental results of tests conducted at COD concentrations of 200 mg/L, T = 298K, ρ_B = 0.5 g/L, Q_{air} = 1.0·10-6m^3/s and v = 500rpm.

Time [min]	pH	COD (mg/L)	TOC (mg/L)
0	5.48	101	44.9
15	5.36	80.8	38.7
30	5.10	58.5	31.6
60	5.15	60.7	31.5
90	5.22	60.8	31.7
120	5.10	59.8	31.7
180	5.04	62.1	32.4
240	4.95	62.3	31.4
300	4.90	63.9	32.2

Table 4. Experimental results of tests conducted at COD concentrations of 100 mg/L, T = 298K, ρ_B = 0.5 g/L, Q_{air} = 1.0·10-6m^3/s and v = 500rpm.

Time [min]	pH	COD (mg/L)	TOC (mg/L)
0	5.52	50.6	27.8
15	5.26	30.4	22.6
30	4.49	22.6	18.5
60	4.50	22.1	18.9
90	4.53	21.2	18.7
120	4.56	23.6	18.7
180	4.58	21.9	19.2
240	4.60	22.3	18.7
300	4.61	23.4	22.3

Table 5. Experimental results of tests conducted at COD concentrations of 50 mg/L, T = 298K, ρ_B = 0.5 g/L, Q_{air} = 1.0·10-6m^3/s and v = 500rpm.

Time [min]	pH	COD (mg/L)	TOC (mg/L)
0	4.94	169	71.2
15	4.96	118	52.9
30	4.90	80.0	43.4
60	4.93	82.2	41.6
90	5.02	70.0	40.7
120	5.00	68.8	40.8
180	5.07	71.1	41.2
240	5.12	66.9	40.5
300	6.38	68.5	40.3

Table 6. Experimental results of tests conducted at COD concentrations of 200 mg/L, T = 298K, ρ_B = 1.0 g/L, Q_{air} = 1.0·10-6m^3/s and v = 500rpm.

Time [min]	pH	COD (mg/L)	TOC (mg/L)
0	4.86	179	75.3
15	4.95	116	63.4
30	5.10	85.5	46.1
60	5.10	74.2	42.3
90	5.09	72.2	41.7
120	5.03	69.7	40.3
180	5.08	74.9	50.6
240	5.38	78.0	47.8
300	5.35	81.1	48.9

Table 7. Experimental results of tests conducted at COD concentrations of 200 mg/L, T = 298K, ρ_B = 1.5 g/L, Q_{air} = 1.0·10-6m^3/s and v = 500rpm.

Time [min]	pH	COD (mg/L)	TOC (mg/L)
0	4.83	156	73.7
15	4.82	124	65.4
30	4.82	105	56.1
60	4.82	105	55.7
90	4.77	98.0	55.3
120	4.78	94.1	54.3
180	4.78	102	53.2
240	4.83	95.7	54.2
300	4.81	103	53.6

Table 8. Experimental results of tests conducted at COD concentrations of 200 mg/L, T = 313K, ρ_B = 0.5 g/L, Q_{air} = 1.0·10-6m^3/s and v = 500rpm.

Time [min]	pH	COD (mg/L)	TOC (mg/L)
0	4.55	165	66.6
15	4.58	124	61.6
30	4.68	99.2	50.7
60	4.63	102	50.6
90	4.64	98.8	50.0
120	4.67	102	50.8
180	4.61	101	51.4
240	4.59	99.2	50.6
300	4.78	98.7	49.6

Table 9. Experimental results of tests conducted at COD concentrations of 200 mg/L, T = 323K, ρ_B = 0.5 g/L, Q_{air} = 1.0·10-6m^3/s and v = 500rpm**.**

APPENDIX III

Time [min]	pH	COD (mg/L)	TOC (mg/L)
0	5.33	204	81.2
5	5.30	204	81.1
10	5.26	184	80.6
15	5.25	175	78.9
20	5.20	168	68.7
25	5.17	161	67.1
30	5.23	160	66.2
60	5.30	160	66.2
90	5.24	157	66.2
120	5.26	156	65.2
180	5.22	156	67.4
240	5.16	155	67.8
300	5.10	155	66.9

Table 2. Experimental results of tests conducted at COD concentrations of 200 mg/L, T = 298K, ρ_B = 0.5 g/L, Q_{air} = 1.0·10-6m^3/s and v = 500rpm.

Time [min]	pH	COD (mg/L)	TOC (mg/L)
0	5.48	95.0	56.7
5	5.47	78.1	54.3
10	5.42	71.2	51.6
15	5.42	65.4	48.7
20	5.40	64.7	47.2
25	5.36	63.7	45.7
30	5.10	63.1	44.7
60	5.15	62.7	42.4
90	5.22	62.0	43.1
120	5.10	61.7	40.9
180	5.04	61.2	40.7
240	4.95	60.6	39.6
300	4.90	60.5	39.5

Table 3. Experimental results of tests conducted at COD concentrations of 100 mg/L, T = 298K, ρ_B = 0.5 g/L, Q_{air} = 1.0·10-6m^3/s and v = 500rpm.

Time [min]	pH	COD (mg/L)	TOC (mg/L)
0	5.52	58.4	29.8
5	5.50	41.9	27.6
10	5.48	35.5	26.4
15	5.35	31.0	24.3
20	5.32	30.2	23.6
25	5.26	27.6	23.4
30	4.49	25.2	22.2
60	4.50	24.2	22.7
90	4.53	23.2	23.6
120	4.56	21.7	22.9
180	4.58	21.7	23.8
240	4.60	18.2	23.6
300	4.61	17.8	24.9

Table 4. Experimental results of tests conducted at COD concentrations of 50 mg/L, T = 298K, ρ_B = 0.5 g/L, Q_{air} = 1.0·10-6m^3/s and v = 500rpm.

Time [min]	pH	COD (mg/L)	TOC (mg/L)
0	5.33	215	79.5
5	5.27	186	75.6
10	5.26	166	74.8
15	5.27	151	67.6
20	5.28	148	64.3
25	5.26	145	61.7
30	5.27	135	55.6
60	5.13	129	55.0
90	5.10	130	55.7
120	5.16	127	56.3
180	5.13	122	55.6
240	5.07	121	57.0
300	5.05	119	59.1

Table 5. Experimental results of tests conducted at COD concentrations of 200 mg/L, T = 298K, ρ_B = 1.0 g/L, Q_{air} = 1.0·10-6m^3/s and v = 500rpm.

Time [min]	pH	COD (mg/L)	TOC (mg/L)
0	5.07	233	80.6
5	5.06	230	80.1
10	5.03	164	78.4
15	5.05	152	76.7
20	5.10	123	75.7
25	4.95	115	65.4
30	5.10	107	60.7
60	5.10	97.8	56.7
90	5.09	94.1	48.9
120	5.03	85.8	41.5
180	5.08	85.7	41.2
240	5.38	85.1	40.6
300	5.35	85.3	39.7

Table 6. Experimental results of tests conducted at COD concentrations of 200 mg/L, T = 298K, ρ_B = 1.5 g/L, Q_{air} = 1.0·10-6m^3/s and v = 500rpm.

Time [min]	pH	COD (mg/L)	TOC (mg/L)
0	5.21	51.7	31.5
5	5.15	49.0	29.0
10	5.17	48.9	28.7
15	5.10	47.8	26.4
20	5.05	41.6	24.6
25	4.82	35.4	22.4
30	4.81	25.6	19.7
60	4.82	22.9	19.3
90	4.76	22.0	19.7
120	4.78	21.2	19.1
180	4.75	21.6	18.9
240	4.80	21.9	18.2
300	4.81	21.3	18.2

Table 7. Experimental results of tests conducted at COD concentrations of 50 mg/L, T = 313K, ρ_B = 0.5 g/L, Q_{air} = 1.0·10-6m^3/s and v = 500rpm.

Time [min]	pH	COD (mg/L)	TOC (mg/L)
0	4.55	51.9	30.6
5	4.54	50.2	29.7
10	4.56	46.8	27.6
15	4.58	39.6	22.6
20	4.57	35.7	21.4
25	4.58	32.4	20.6
30	4.68	29.6	18.2
60	4.63	27.0	18.2
90	4.64	22.2	18.4
120	4.67	22.0	18.0
180	4.61	21.2	17.9
240	4.59	21.5	17.8
300	4.78	21.5	17.6

Table 8. Experimental results of tests conducted at COD concentrations of 50 mg/L, T = 323K, ρ_B = 0.5 g/L, Q_{air} = 1.0·10-6m^3/s and v = 500rpm**.**

PUBLICATIONS

Toscanesi, M., Russo, V., Medici, A., Giarra, A., Di Serio, M., Trifuoggi, M. Remediation of wastewater from the tanning industry by adsorption with TiO_2. ChemEngineering 2022 (*Manuscript submitted*)

Toscanesi, M., Russo, V., Medici, A., Giarra, A., Di Serio, M., Trifuoggi, M. Heterogeneous photodegradation for abatement of recalcitrant COD in the wastewater derived from the tanning industry. ChemEngineering 2022 (*Manuscript submitted*)

Elia, V., Napoli, E., Germano, R., Roviello, V., Oliva, R., Niccoli, M., Amoresano, A., **Toscanesi, M**., Trifuoggi, M., Fabozzi, A., Yinnon, T.A. Water perturbed by cellophane: comparison of its physicochemical properties with those of water perturbed with cotton wool or Nafion (2021) Journal of Thermal Analysis and Calorimetry, 146 (5), pp. 2073-2088.
DOI: 10.1007/s10973-020-10185-0
https://link.springer.com/content/pdf/10.1007/s10973-020-10185-0.pdf

Tommasi, F., Thomas, P.J., Pagano, G., Perono, G.A., Oral, R., Lyons, D.M., **Toscanesi, M.**, Trifuoggi, M. Review of Rare Earth Elements as Fertilizers and Feed Additives: A Knowledge Gap Analysis (2021) Archives of Environmental Contamination and Toxicology, 81 (4), pp. 531-540.
DOI: 10.1007/s00244-020-00773-4
https://link.springer.com/article/10.1007/s00244-020-00773-4

Carraturo, F., Carmela, C., Compagnone, M., Libralato, G., **Toscanesi, M**., Trifuoggi, M., Galdiero, E., Guida, M. Evaluation of microbial communities of bottled mineral waters and preliminary traceability analysis using ngs microbial fingerprints (2021) Water (Switzerland), 13 (20), art. no. 2824.
DOI: 10.3390/w13202824
https://www.mdpi.com/2073-4441/13/20/2824/htm

Aiello, G., Barra, D., Parisi, R., Arienzo, M., Donadio, C., Ferrara, L., **Toscanesi, M**., Trifuoggi, M.Infralittoral ostracoda and benthic foraminifera of the Gulf of Pozzuoli (Tyrrhenian Sea, Italy)(2021) Aquatic Ecology, 55 (3), pp. 955-998.

DOI: 10.1007/s10452-021-09874-1
https://link.springer.com/article/10.1007/s10452-021-09874-1

Nastro, R.A., Leccisi, E., **Toscanesi, M.**, Liu, G., Trifuoggi, M., Ulgiati, S.
Exploring avoided environmental impacts aswell as energy and resource recovery from microbial desalination cell treatment of brine (2021) Energies, 14 (15), art. no. 4453.
DOI: 10.3390/en14154453
https://www.mdpi.com/1996-1073/14/15/4453

Thomas, P.J., Perono, G., Tommasi, F., Pagano, G., Oral, R., Burić, P., Kovačić, I., **Toscanesi, M.**, Trifuoggi, M., Lyons, D.M. Resolving the effects of environmental micro- and nanoplastics exposure in biota: A knowledge gap analysis (2021) Science of the Total Environment, 780, art. no. 146534.
DOI: 10.1016/j.scitotenv.2021.146534
https://www.sciencedirect.com/science/article/pii/S0048969721016028?via%3Dihub

Albarano, L., Zupo, V., Caramiello, D., **Toscanesi, M**., Trifuoggi, M., Guida, M., Libralato, G., Costantini, M. Sub-chronic effects of slight pah- and pcb-contaminated mesocosms in paracentrotus lividus lmk: A multi-endpoint approach and de novo transcriptomic (2021) International Journal of Molecular Sciences, 22 (13), art. no. 6674.
DOI: 10.3390/ijms22136674
https://www.mdpi.com/1422-0067/22/13/6674

Trifuoggi, M., Ferrara, L., **Toscanesi, M.**, Mondal, P., Ponniah, J.M., Sarkar, S.K., Arienzo, M.
Spatial distribution of trace elements in surface sediments of Hooghly (Ganges) river estuary in West Bengal, India (2021) Environmental Science and Pollution Research.
DOI: 10.1007/s11356-021-15918-8
https://link.springer.com/content/pdf/10.1007/s11356-021-15918-8.pdf

Corniello, A., Guida, M., Stellato, L., Trifuoggi, M., Carraturo, F., Del Gaudio, E., Del Giudice, C., Forte, G., Giarra, A., Iorio, M., Marzaioli, F., **Toscanesi, M.** Hydrochemical, isotopic and microbiota characterization of telese mineral waters (Southern Italy) (2021) Environmental Geochemistry and Health.
DOI: 10.1007/s10653-021-00806-4

https://link.springer.com/article/10.1007%2Fs10653-021-00806-4

Oral, R., Pagano, G., Ferrara, L., **Toscanesi, M.**, Mozzillo, M., Gravina, M., Natalc, G.D., Thomas, P.J., Tcz, S., Siciliano, A., Guida, M., Trifuoggi, M. Sediment pollution and toxicity in a formerly industrialized bay in central mediterranean (POZZUOLI, Italy) (2020) Fresenius Environmental Bulletin, 29 (10), pp. 9498-9510.
https://www.scopus.com/record/display.uri?eid=2-s2.0-85099966846&origin=resultslist

Pagano, G., Pallardó, F.V., Lyakhovich, A., Tiano, L., Fittipaldi, M.R., **Toscanesi, M.**, Trifuoggi, M. Aging-related disorders and mitochondrial dysfunction: A critical review for prospect mitoprotective strategies based on mitochondrial nutrient mixtures
(2020) International Journal of Molecular Sciences, 21 (19), art. no. 7060, pp. 1-16.
DOI: 10.3390/ijms21197060
https://www.mdpi.com/1422-0067/21/19/7060

Thomas, P.J., Oral, R., Pagano, G., Tez, S., **Toscanesi, M.**, Ranieri, P., Trifuoggi, M., Lyons, D.M. Mild toxicity of polystyrene and polymethylmethacrylate microplastics in Paracentrotus lividus early life stages (2020) Marine Environmental Research, 161, art. no. 105132.
DOI: 10.1016/j.marenvres.2020.105132
https://www.sciencedirect.com/science/article/pii/S0141113620300234?via%3Dihub

Arienzo, M., Bolinesi, F., Aiello, G., Barra, D., Donadio, C., Stanislao, C., Ferrara, L., Mangoni, O., **Toscanesi, M.**, Giarra, A., Trifuoggi, M. The environmental assessment of an estuarine transitional environment, Southern Italy (2020) Journal of Marine Science and Engineering, 8 (9), art. no. 628.
DOI: 10.3390/JMSE8090628
https://www.mdpi.com/2077-1312/8/9/628

Memoli, V., Panico, S.C., Santorufo, L., Barile, R., Di Natale, G., Di Nunzio, A., **Toscanesi, M.**, Trifuoggi, M., De Marco, A., Maisto, G. Do wildfires cause changes in soil quality in the short term? (2020)

International Journal of Environmental Research and Public Health, 17 (15), art. no. 5343, pp. 1-14.
DOI: 10.3390/ijerph17155343
https://www.mdpi.com/1660-4601/17/15/5343

Arienzo, M., Ferrara, L., **Toscanesi, M.**, Giarra, A., Donadio, C., Trifuoggi, M.
Sediment contamination by heavy metals and ecological risk assessment: The case of Gulf of Pozzuoli, Naples, Italy (2020) Marine Pollution Bulletin, 155, art. no. 111149.
DOI: 10.1016/j.marpolbul.2020.111149
https://www.sciencedirect.com/science/article/pii/S0025326X20302678

Nasta, P., Palladino, M., Sica, B., Pizzolante, A., Trifuoggi, M., **Toscanesi, M.**, Giarra, A., D'Auria, J., Nicodemo, F., Mazzitelli, C., Lazzaro, U., Di Fiore, P., Romano, N.
Evaluating pedotransfer functions for predicting soil bulk density using hierarchical mapping information in Campania, Italy (2020) Geoderma Regional, 21, art. no. e00267.
DOI: 10.1016/j.geodrs.2020.e00267
https://www.sciencedirect.com/science/article/pii/S235200942030016X

Ferrara, L., Trifuoggi, M., **Toscanesi, M.**, Donadio, C., Barra, D., Aiello, G., Arienzo, M.
Source identification and eco-risk assessment of polycyclic aromatic hydrocarbons in the sediments of seawaters facing the former steel plant ILVA, Naples, Italy (2020) Regional Studies in Marine Science, 35, art. no. 101097.
DOI: 10.1016/j.rsma.2020.101097
https://www.sciencedirect.com/science/article/pii/S2352485519307972

Carotenuto, Y., Vitiello, V., Gallo, A., Libralato, G., Trifuoggi, M., **Toscanesi, M.**, Lofrano, G., Esposito, F., Buttino, I. Assessment of the relative sensitivity of the copepods Acartia tonsa and Acartia clausi exposed to sediment-derived elutriates from the Bagnoli-Coroglio industrial area: Sensitivity of Acartia tonsa and Acartia clausi to sediment elutriates (2020) Marine Environmental Research, 155, art. no. 104878.
DOI: 10.1016/j.marenvres.2020.104878
https://www.sciencedirect.com/science/article/pii/S0141113619307111?via%3Dihub

Fattoruso, G., Agresta, A., Guarnieri, G., **Toscanesi, M.**, De Vito, S., Fabbricino, M., Trifuoggi, M., Di Francia, G. A Software System for Predicting Trihalomethanes Species in Water Distribution Networks Using Online Networked Water Sensors (2020) Lecture Notes in Electrical Engineering, 629, pp. 417-423.
DOI: 10.1007/978-3-030-37558-4_62

Trifuoggi, M., Pagano, G., Oral, R., Pavičić-Hamer, D., Burić, P., Kovačić, I., Siciliano, A., **Toscanesi, M.**, Thomas, P.J., Paduano, L., Guida, M., Lyons, D.M.
Microplastic-induced damage in early embryonal development of sea urchin Sphaerechinus granularis (2019) Environmental Research, 179, art. no. 108815.
DOI: 10.1016/j.envres.2019.108815
https://www.sciencedirect.com/science/article/pii/S0013935119306127?via%3Dihub

Nastro, R.A., Gambino, E., **Toscanesi, M**., Arienzo, M., Ferrara, L., Trifuoggi, M.
Microbial Fuel Cells (MFCs) remediation activity of marine sediments sampled at a dismissed industrial site: What opportunities?
(2019) Journal of Cleaner Production, 235, pp. 1559-1566.
DOI: 10.1016/j.jclepro.2019.07.019
https://www.sciencedirect.com/science/article/pii/S0959652619323583

Oral, R., Pagano, G., Siciliano, A., **Toscanesi, M.**, Gravina, M., Di Nunzio, A., Palumbo, A., Thomas, P.J., Tommasi, F., Burić, P., Lyons, D.M., Guida, M., Trifuoggi, M.
Soil pollution and toxicity in an area affected by emissions from a bauxite processing plant and a power plant in Gardanne (southern France) (2019) Ecotoxicology and Environmental Safety, 170, pp. 55-61.
DOI: 10.1016/j.ecoenv.2018.11.122
https://www.sciencedirect.com/science/article/pii/S0147651318312673?via%3Dihub

Panzella, L., Moccia, F., **Toscanesi, M.**, Trifuoggi, M., Giovando, S., Napolitano, A.
Exhausted woods from tannin extraction as an unexplored waste biomass: Evaluation of the antioxidant and pollutant adsorption properties and activating e ects of hydrolytic treatments
(2019) Antioxidants, 8 (4), art. no. 84.
DOI: 10.3390/antiox8040084
https://www.mdpi.com/2076-3921/8/4/84

Arienzo, M., **Toscanesi, M.,** Trifuoggi, M., Ferrara, L., Stanislao, C., Donadio, C., Grazia, V., Gionata, D.V., Carella, F. Contaminants bioaccumulation and pathological assessment in Mytilus galloprovincialis in coastal waters facing the brownfield site of Bagnoli, Italy. (2019) Marine Pollution Bulletin, 140, pp. 341-352.
DOI: 10.1016/j.marpolbul.2019.01.064
https://linkinghub.elsevier.com/retrieve/pii/S0025-326X(19)30084-0

Trifuoggi, M., Pagano, G., Oral, R., Gravina, M., **Toscanesi, M.**, Mozzillo, M., Siciliano, A., Burić, P., Lyons, D.M., Palumbo, A., Thomas, P.J., D'Ambra, L., Crisci, A., Guida, M., Tommasi, F. Topsoil and urban dust pollution and toxicity in Taranto (southern Italy) industrial area and in a residential district (2019) Environmental Monitoring and Assessment, 191 (1), art. no. 43, .DOI: 10.1007/s10661-018-7164-7
https://link.springer.com/article/10.1007/s10661-018-7164-7

Carella, A., Centore, R., Borbone, F., **Toscanesi, M.**, Trifuoggi, M., Bella, F., Gerbaldi, C., Galliano, S., Schiavo, E., Massaro, A., Muñoz-García, A.B., Pavone, M.
Tuning optical and electronic properties in novel carbazole photosensitizers for p-type dye-sensitized solar cells (2018) Electrochimica Acta, 292, pp. 805-816.
DOI: 10.1016/j.electacta.2018.09.204
https://www.sciencedirect.com/science/article/pii/S001346861832214X

Trifuoggi, M., Donadio, C., Ferrara, L., Stanislao, C., **Toscanesi, M.**, Arienzo, M.
Levels of pollution of rare earth elements in the surface sediments from the Gulf of Pozzuoli (Campania, Italy) (2018) Marine Pollution Bulletin, 136, pp. 374-384.
DOI: 10.1016/j.marpolbul.2018.09.034

https://www.sciencedirect.com/science/article/pii/S0025326X1830674X?via%3Dihub

ATTENDED CONGRESSES/WORKSHOPS/SUMMERS SCHOOL/CONTRIBUTION

Toscanesi et al. Distribution and enrichment of trace metals in surface marine sediments in the Gulf of Pozzuoli and off the coast of the brownfield metallurgical site of Ilva of Bagnoli. **Convegno nazionale sugli ambienti marino costieri. 19-20 June 2019 Naples. Oral Communication**

Toscanesi et al., "Speciazione e origine di idrocarburi policiclici aromatici mediante GC-MS in diverse matrici ambientali". **Incontro di Scienza delle Separazioni della società Chimica Italiana. 28-29 November 2019, Napoli - Poster session.**

Toscanesi et al., "Heterogeneous photodegradation for abatement of recalcitrant COD in the wastewater derived from the tanning industry". **XXVII Congresso Nazionale della società Chimica Italiana 14-23 September 2021– Poster Session**